BIOACTIVITY MODIFICATION OF CEMENT-TYPE BIOMATERIALS

（セメント型生体材料への生体活性化処理）

GRADUATE SCHOOL OF LIFE SCIENCE AND SYSTEMS ENGINEERING

KYUSHU INSTITUTE OF TECHNOLOGY

LIU Jinkun

2015

Ph.D. SUPERVISOR

Associate Professor, Toshiki Miyazaki

CONTENTS

Chapter 1

GENERAL INTRODUCTION

Cement-type biomaterials own intrinsic characteristics of conventional cements used in industry: transformation from the pastes into hardened masses. The coherent structure and deformable capacity during this curing process make them become perfect option in adapting to the complex inner construction of human body, therefore cement-type biomaterials are widely used as the filler and binder in the field of implantation and reconstructive procedures. As the filler, the mechanical properties need to be paid attention to ensure the biomaterials satisfy basic requirements of the implant regions; as the binder, now available mechanical interlocking between biocements and bone is unable to maintain a long-term stabilization, the fixation must be improved by modification.

1. Glass ionomer cement

1.1. Definition of Glass ionomer cement (GIC)

The first generation of glass ionomer cement (GIC) products, ASPA (alumino-silicate-poly-acrylate), introduced in the 1970s by Wilson and Kent [1], was applied as a tooth colored material. Over 3 decades of development, its application is not only limited on dentistry, but also extended to the implant and reconstructive surgical procedures [2]. The definition of glass ionomer cement can be summarized as follows: one kind of cement that consists of acid decomposable glass powders and a water soluble acidic polymer, which can be set by the neutralization reaction between both components, the final structure is partly degraded glass particles surrounded by a siliceous hydrogel bound together with a polyanions matrix [3]. Compared with other dental water-based cements, GIC presents ease of molding, no obvious shrinkage, no significant increase in temperature, better biocompatibility without inflammatory response in mouth [4].

1.2. Chemical composition of GIC

GIC is generally divided into powder and liquid system. The powder system used in GIC formulation is aluminosilicate glasses containing calcium compounds or fluorides. The composition of original glasses with ion release ability is based on SiO_2-Al_2O_3 or SiO_2-Al_2O_3-CaO (CaF_2) to which other components such as Na_2O, Na_3AlF_6, $AlPO_4$, AlF_3 or P_2O_5 can be added. One representative composition in commercial product is 41.9 SiO_2, 28.6 Al_2O_3, 1.6 AlF_3, 15.7 CaF_2, 9.3 NaF, 3.8 $AlPO_4$, in mass% [5]. There are two synthetic methods in processing of glass powders: melt quench route and sol–gel process. The mixture of Al_2O_3, SiO_2, metal oxides, metal fluorides and phosphates is melted at higher temperature in the range of 1100 to 1500 °C. After fusion, the molten glass is quenched into water, the generated coarse fit is further ground by dry milling, until the particles can pass through a 45 μm or 15 μm mesh sieves for the application of restorative and luting cements, respectively [6]. Although melt quench route is well established for producing glass fillers, there are problems exposed in respects of the feasibility of melting, variation in the final glass composition especially the loss of fluorine during melting and cooling [7]. The sol–gel process enables to produce glass powders at low temperature with high homogeneity and purity. Bertolini *et al.* [8-10] synthesized powder of niobium fluoride silicate by sol–gel method. The method allowed sintering temperature down to 600~700 °C. And the obtained glass powders with a crystalline phase still could react with the solution of poly(acrylate acid) (PAA). Cestari *et al.* [11,12] employed nonhydrolytic sol–gel method to prepare calcium and sodium fluoroaluminosilicate glasses, these synthesized powders exhibited a potential required for the acid-base reaction with PAA solution. The liquid component of GIC is the aqueous solution of acidic polymer with carboxylic groups. The most common acidic polymers are homopolymer of acrylic acid, derivative copolymers of acrylic and itaconic acids (poly(AA–co–IA)) [13], or acrylic and maleic acid (poly(AA–co–MA)) [14]. The addition of itaconic acid or maleic acid is for lowering the gelation tendency of polymer solutions [15]. The liquid also contains about 5 to

15% m/m (mass per mass) (+) tartaric acid effective for control in setting reaction [16]. Its role has been proved in improving handling characteristics and sharpening set [17].

1.3. Chemistry of setting

General formula in setting reaction of cement may be written as follows:

$$H_2A + MO_x \cdot SiO_2 \Rightarrow x\ SiO_2 + MA + H_2O \quad (1\text{-}1)$$

In the above equation, M represents the forming cation in cement and $MO_x \cdot SiO_2$ acts as the proton accepter, while A represents the forming anion and H_2A acts as the proton donor. $xSiO_2$ + MA is viewed as formed salt-gel matrix. The setting reaction can be divided into 3 overlapping stages:

(1) dissolution, Al^{3+}, Ca^{2+}, Na^{+} and F^{+} ions are released from the surface of glass particles by acid attack then leached into the aqueous medium, siliceous hydrogel layers surrounded on the unreacted particles are also formed.

(2) gelation, initially Ca^{2+}, and later, Al^{3+} ions bind with the polyanion chains via carboxyl groups to precipitate a hard polycarboxylic salts gel [18]. The initial set is achieved by cross linking of Ca^{2+} ions, the polycarboxylic salts of Al form the dominate component with respect to mechanical strength.

(3) hydration, the maturation phase is a progressive hydration of the matrix salts, leading to sharp improvement in physical properties [19], and the reaction step is depicted in **Figure 1-1**.

1.4. Challenges in clinical application

Glass ionomer cement still faces some challenges in clinical application. Because water plays an important role as the medium of setting reaction and the hydrates of reaction procedure, initial setting stage needs the relative humidity (R. H.) of operating environment being kept at a high level (above 90%), the condition which failed to match this condition caused a decline in physical strength of set cements [20]. In addition, there are too many factors of affecting the

mechanical strength of GIC over timing. Variations are derived from the variability in composition, size and distribution of glass powders [21], molecular weight of acidic polymer and its concentration in liquid [22], P/L ratio [23] as well as testing conditions such as specimen dimension, storage media [24, 25]. Biocompatibility of GIC depends on the applied position: in tooth, the chemical bonding is accomplished by developing an ion enriched layer due to the reaction occur between carboxyl group (-COOH) of PAA and calcium from the dentine or enamel [3]. When implanted into body, the bonding between cement and bone is attributed to the mechanical interlocking rather than a bioactive mineralized layer. Kamitakahara *et al.* [26] revealed that the existence of PAA even in ppm grade inhibited the apatite formation on GIC surface, which meant that any PAA-containing GIC would lose bioactivity in body environment. But a novel GIC based on calcium zinc silicate glasses (0.14 CaO, 0.29 ZnO, 0.57 SiO_2, in mol%) prepared by Boyd *et al.* [27] owned a potential to induce the nucleation of amorphous calcium phosphate after soaking in simulated body fluid (SBF), which indicated that PAA might not be the main reason responsible for bioactivity loss. Deeper reason need to be studied.

1.5. Modification to improve the properties of GIC

Due to the drawbacks mentioned above, it is necessary to enhance the properties of GIC to satisfy new application requirements in the craniofacial reconstruction and orthopaedic use. Modification strategies are listed as: (1) choosing an alternative polymer, for example: poly(vinyl phosphonic acid) (PVPA), stronger acid than PAA, is more reactive and hydrolytically more stable in cement formation. The PVPA-based cement with excellent initial water resistance owned a low fluoride release and increased flexural strength over 90 days [28]; Poly(γ-glutamic acid) (γ-PGA), a water soluble biodegradable polymer, shows nontoxicity to humans and environmentally benign. FT-IR spectra and elemental analyses proved its feasibility in cement formation, the maximum compressive strength of 130 MPa was

comparable to that of PAA-based product [29]. (2) adding functional powder, powder selection is determined by the purpose of reinforcement: the addition of silver-tin alloy [30] or stainless steel [31] to glass-ionomer system was succeed to sharpen the mechanical strength of set cement; bioglass S53P4 [32], TiO_2 nanoparticles [33] incorporated in GIC improved the antimicrobial effects. Choi *et al.* [34] added a sol–gel derived bioactive glass (25 CaO, 5 P_2O_5, 70 SiO_2, in mol%) into commercial GIC product (GC, Fuji I). The complex induced the apatite deposition, showing *in vitro* bone bioactivity. (3) upgrading to resin-modified cement, the conventional acid-base components are modified with monomers and photopolymerization initiators. In this system, parts of the carboxylic groups in PAA are replaced with cross-linkable bifunctional compounds containing vinyl groups [35]. The addition of 2-hydroxyethyl methacrylate (HEMA) is necessary to retain all the components in a single phase. This resin-modified cement showed longer working and setting time but lower compressive strength compared to glass ionomer only [36]. Xie *et al.* [37] developed a novel bioactive glass-ionomer cement modified with resin, which exhibited biomedical function of dentin capping mineralization. In the system, the synthesized star-shape PAA was used as a liquid, while Fuji II LC filler and bioactive glass S53P4 as a filler. As a result, the cement system not only showed mechanical strength similar to original Fuji II LC cement clinically utilized but also induced the apatite precipitation in SBF environment.

2. Polymethylmethacrylate (PMMA) cement

2.1. Development of polymethylmethacrylate (PMMA) cement

Thesis about the polymerization of methyl methyacrylate (MMA) published by Otto Röhm in 1901 created available and basic sources for bone cement [38]. Afterwards, the commercial manufactures brought a rapid development on this new polymer. Namely, the first cold-curing cement developed by the company Degussa was used to fill the defects of the skeleton and to produce cranial plates in 1943 [39]. In 1960, Sir John Charnley first succeeded

fixation of artificial hip joints in the femur by using self-setting cement [40], both established the feasibility of PMMA cement in orthopaedics. The function of PMMA cement is filling space between the artificial joints and bone, serving as the medium to bond both. Due to its intrinsic strength, PMMA cement can share the elastic impact and transfer the load on the prosthesis to bone as possible, which is beneficial to the long-term stability after implantation. Besides that, PMMA bone cement acts as the carriers of antibiotics [41].

2.2. Compositions of polymethylmethacrylate (PMMA) cement

PMMA bone cement is normally composed of PMMA powder and MMA liquid. Its powder: liquid mass ratio is usually 2: 1. The powder component comprises microspheres of ground PMMA or copolymer which contribute 83 to 99% in the proportion of powder, the remaining components include benzoyl peroxide (BPO) for initiating the cement curing, barium sulfate ($BaSO_4$) or zirconium dioxide (ZrO_2) as the radiopacifier for the cement visibility in radiographs. Optionally an antibiotic or a dye for coloring of the powder are also present. Basic ingredients of the liquid are monomer MMA and N,N-dimethyl-p-toluidine (DmpT) at a weight ratio of 0.4 to 2.8%. PPM-grade hydroquinone is added to stabilize MMA in preventing premature polymerization during storage.

2.3. Reaction mechanism

It shall be noted that the radiopacifier, antibiotics and dye do not involve in the polymerization reaction. The transformation from MMA to PMMA relies on the initiator (BPO)/accelerator (DmpT) system. The reaction process is depicted in **Figure 1-2**. After mixing, DmpT leads to the decomposition of BPO under a reduction/oxidation reaction based on electron transfer, which generates benzoyl radicals and benzoate anions. The free radicals can initiate the polymerization via inducing an immediate formation of chains by adding themselves to the C=C double bond of MMA, and a high number of radicals bring rapid

formation of polymer chains. When two reactive radical-chain ends meet, they react to form non-reactive completed polymer chains. As a result of this termination in chains, the polymerization comes to a standstill and no radicals remain. The whole polymerization of MMA is an exothermic reaction and the heating release causes an increase in temperature during the curing stage [42].

2.4. Viscosity and handling properties in curing

The chemical composition and powder/liquid ratio determines the viscosity of PMMA cement. Viscosity affects handling characteristics of PMMA cement, and an appropriate viscosity helps cement penetrate the bone for good attachment in quality and longevity. Two basic requirements for the cement viscosity are listed as: (1) it should be sufficiently low to make sure that the cement dough can be delivered from the syringe to the defect sites, (2) the penetration should reach to the interstices of bone [43]. The type (low, medium and high) of PMMA bone cement is categorized with regards to its viscosity. Low viscosity cement owns a long lasting liquid to low viscosity wetting phase and remains sticky state longer than medium or high viscosity cement. Medium viscosity cement is considered to be dual phase between low and high in viscosity, the mixing of powder and liquid is easy and homogeneous due to the low viscosity state in prime. High viscosity cement has shortest wetting phase and loses the stickiness very fast, therefore it is hard to determine the end of working phase because the viscosity in this type remains almost unchanged.

The increase in viscosity over time changes the low-viscosity mass into the dough further converts into the solid matrix. The polymerization process can be divided into four phases [44]: (1) mixing; mixing phase (up to 1 minute) starts immediately after the addition of liquid to the powder, and this state ends when the dough becomes homogenous and hard to be stirred. The liquid can wet the surface of prepolymerized beads even make them dissolve completely, which consequently leads to increase in viscosity of the mixture.

(2) waiting; a period allows further swelling of the beads and permits persistent polymerization which leads to an increase in viscosity, and it ends when the sticky dough reaches a non-sticky state.

(3) working; sufficiently low viscosity enables the dough can be reshaped in operation. The viscosity continues to increase by continuous polymerization, and heat generation in the cement occurs by the exothermic reaction, meanwhile, volume shrinkage is occurred as the monomer converts into the polymer with higher density.

(4) hardening; in the last period the temperature reaches its peak that represents the termination of polymerization, the cement finally becomes a hard consistency.

2.5. Limitations on clinical application

The polymerization of MMA is an exothermic reaction, one mole MMA can release heating of 57 kJ, which leads to an increase in temperature over curing process. The maximum temperature measured *in vitro* is approximately 60 to 80 ºC. This can be also affected by cement composition, powder/liquid ratio, and the radiopacifier [45]. This short-term temperature rising is regarded as the main reason for aseptic loosening of the prostheses caused by heat necrosis [39]. Expect that, PMMA cement is considerably more brittle than bone [46] and its tensile stress is comparatively low [47]. The weakness can be ascribed to the replacement of radiopacifier $BaSO_4$ or ZrO_2, which increases the risk of loosening [48]. Stabilization of PMMA matrix can improve the transfer of load across the interface between cement and prosthesis, and reduce the possibility of crack formation in cement. One more limitation on PMMA bone cement is that the connection to bone relies on an intrinsic mechanical interlocking rather than directly chemical bonding due to the cement itself is a bioinert material [49]. The low biological affinity may induce a fibrous tissue capsule surrounding on cement further leads to the loosening of implant after a long period. Consequently micromotion is

occurred by the loosening at the interface between cement and bone to cause fixation failure of the implant [50].

2.6. Modification to improve the properties of PMMA cement

Various additives such as carbon fibers [51], titanium fibers [52] and glass fibers [53] have been developed to improve the mechanical strength. Vallo *et al.* [54] used cross-linked PMMA beads to replace 30 mass% of the PMMA powder, the flexural strength increased by 22.4%. Hydroxyapatite ($Ca_{10}(PO_4)_6(OH)_2$) modified PMMA bone cement exhibited a linear increase in compression strength (98 to 111 MPa) and a linear decrease in tensile strength (27 to 21 MPa) [55]. Jin *et al.* [56] developed composite cements based on multi-walled carbon nanotubes and PMMA fabricated by melting blending, and revealed that the incorporated nanotubes were well dispersed in the polymer matrix and the storage moduli of all composite cements were increased.

It is essential to develop biocompatible and bone-bonding PMMA bone cement to prevent the loosening of implant. The modification to achieve this aim can be divided into two directions. One is mixing of bioactive ceramic fillers to the cement. It has been previously reported that bioactive ceramics such as hydroxyapatite [57], glass-ceramics A-W [58] and titanium dioxide [59] which were added to the powder of PMMA cement succeed in inducing the apatite precipitation on sample surface in simulated body environment. Tan *et al.* [60] developed a new PMMA cement loaded with a derivative chitosan named as quaternized hydroxypropyltrimethyl ammonium chloride chitosan (HACC). The results showed that HACC modification can lower polymerization temperature, prolong setting time, and induce enhanced apatite formation on the surface after soaking in SBF compared to other PMMA cements. The obtained novel type of anti-infective bone cement improved physical properties and activity of bone formation, leading to enhanced osteointegration of the cement in clinical use. Lopes *et al.* [61] processed a new poly(methylmethacrylate)-co-(ethylhexylacrylate)

(PMMA-co-EHA) composites filled with 0, 30, 40 and 50 mass% of $Ca_3(PO_4)_2$-MgO-SiO_2 glasses. The obtained results showed that: a hydroxyapatite (HA)-like layer was found on the surface of prepared composites, the formation of HA-like layer was accelerated by increasing the content of glasses. When the cement contained 40 or 50 mass% of glasses, it only took 7 days immersion in SBF to make apatite completely cover on their surfaces.

Another direction is inspired by the studies [62] focusing on the formation mechanism of apatite on bioactive materials in simulated body environment: some functional groups such as Si-OH [63], -COOH [64] or PO_4H_2 [65] owns the potential to attract apatite nucleation and Ca^{2+} ions released from biomaterials will accelerate the growth of apatite. The findings suggest the combinations of functional groups and Ca^{2+} ions can provide PMMA bone cement with apatite-forming ability. Methacryloxypropyltrimethoxysilane (MPS) containing Si-OH groups added in liquid and various calcium salts added in powder were first proposed by Mori *et al.* [66], the results showed that MPS combined with calcium chloride, calcium acetate, calcium hydroxide or calcium methacrylate successfully induced the formation of apatite on cement surface, and the cement modified with calcium acetate owned appropriate setting time and compressive strength. Based on the same functional groups (Si-OH), Sugino *et al.* [67] found that the decreasing in bending strength of modified cements was ascribed to the generation of pores in the matrix through the release of Ca^{2+} ions after soaking in SBF, and the pores filled with the newly formed apatite was able to prevent deeper deterioration of mechanical strength. Miyazaki *et al.* [68] optimized the contents of both additives in balancing the apatite-forming ability and other physical properties required by ISO 5833, the hardened cement containing 20 mass% of $CaCl_2$ in powder and 20 mass% of MPS in liquid was more osteoconductive to living bone after implantation in rabbit tibia than the unmodified cement.

3. Apatite formation in body environment

Ca^{2+}, Na^{+}, or K^{+} ions released from representative bioactive ceramics, such as Bioglass®, HA, and glass-ceramic A-W are capable of forming Si-OH or Ti-OH groups on ceramics surface via an ion exchange with H_3O^{+} ions [69]. The Si-OH and Ti-OH groups own the potential to induce the nucleation of apatite, and the released ions mentioned above boost the ionic activity product of apatite [70], which leads to an acceleration in apatite nucleation [71]. The growth of apatite nuclei counts on the continuous consumption of Ca^{2+} ions and PO_4^{3-} ions in the surrounding fluid [72].

Except Si-OH and Ti-OH groups, the catalytic effect of Zr-OH and Ta-OH groups for apatite nucleation have been proved [73, 74]. Self-assembled monolayers (SAMs) on Au substrate indicated that -COOH and PO_4H_2 groups are also helpful for apatite nucleation [65, 66]. The functional groups own the ability to attract Ca^{2+} ions to the surfaces, the accumulation of the positively charged Ca^{2+} ions creates a positively charged surface, then the surface will combine with PO_4^{3-} ions (negatively charged) to form amorphous calcium phosphate. This calcium phosphate spontaneously transforms into the apatite due to its stability in body environment. In addition, the formation period can be accelerated by releasing Ca^{2+} ions from biomaterials themselves into the surrounding fluid to increase the degree of supersaturation of apatite, the nucleation process is described in **Figure 1-3**.

4. Purpose of this research

The main research purpose in this thesis is that: utilizing various modifications to provide cement-type materials with forming ability of bioactive minerals after soaking in simulated body fluid, and optimizing physical properties to insure these biocements own potential clinical applications.

In chapter 2, a microbial acidic polymer poly(γ-glutamic acid) (γ-PGA) was adopted to develop new-type glass ionomer cement with bioactivity and satisfied mechanical property.

The feasibility of cement forming based on glass compositions and γ-PGA was explored and discussed. Besides the bioactivity evaluation, the preparation parameters including the powder/liquid ratio and the concentration of γ-PGA in improving the diametral tensile strength of cements were also optimized.

In chapter 3, incorporation of phosphate (PO_4H_2) groups containing monomer phosphoric acid 2-hydroxyethyl methacrylate ester (Pa2hme) and calcium acetate into PMMA bone cement was attempted to induce apatite deposition on modified cement surface in simulated body environment. Efforts of the combinations of different contents of calcium acetate and Pa2hme on apatite-forming period, setting time and compressive strength were investigated. According to the pH tendencies and the concentrations of Ca and P in SBF over designed soaking intervals, the influences of both additives on apatite formation were also discussed.

In chapter 4, another phosphate-containing monomer Bis [2-(methacryloyloxy) ethyl] phosphate (BisP) combined with calcium acetate was employed to further improve the apatite forming and physical properties of PMMA bone cement based on the experiences from chapter 3. The same investigation and discussion mentioned in chapter 3 were also conducted. Besides that, the role of each additive on apatite formation was examined, the optimization related to the contents of both additives was explored by taking apatite-forming ability and practical standard ISO 5833 into consideration. The performances of BisP and Pa2hme on apatite formation, setting and mechanical strength were compared.

References

[1] A. D. Wilson and B. E. Kent, “A new translucent cement for dentistry. The glass ionomer cement,” *Br. Dent. J.*, 1972, 132(4): 133–135.

[2] R. T. Ramsden, R. C. Herdman and R. H. Lye, “Ionomeric bone cement in neuro-otological surgery,” *J. Laryngol. Otol.*, 1992, 106(11): 949–953.

[3] M. J. Tyas and M. F. Burrow, "Adhesive restorative materials: a review," *Aust. Dent. J.*, 2004, 49(3): 112–121.

[4] J. W. Nicholson, "Chemistry of glass-ionomer cements: a review," *Biomaterials*, 1998, 19(6): 485–494.

[5] A. D. Wilson and J. W. McLean, Glass ionomer cement, (Quintessence Publishing Co., 1988).

[6] M. Braden, R. L. Clarke, J. Nicholson and S. Parker, Polymeric Dental Materials, (Springer, 1997).

[7] S. G. Griffin and H. G. Hill, "Glass composition influence on glass polyalkenoate cement mechanical properties," *J. Non-Cryst. Solids*, 1996, 196(2): 255–259.

[8] M. J. Bertolini, G. P. D. Regina, M. A. Zaghete and R. Gimenes, "Evaluation of glass ionomer cements properties obtained from niobium silicate glasses prepared by chemical process," *J. Non-Cryst. Solids*, 2005, 351(6-7): 466–471.

[9] M. J. Bertolini, M. A. Zaghete, R. Gimenes, G. C. Padovani and C. A. S. Cruz, "Preparation and evaluation of an experimental luting glass ionomer cement to be used in dentistry," *J. Mater. Sci. Mater. Med.*, 2009, 20(9): 1781–1785.

[10] M. J. Bertolini, M. A. Zaghete, R. Gimenes and G. C. Padovani, "Determination of the properties of an experimental glass polyalkenoate cement prepared from niobium silicate powder containing fluoride," *Dent. Mater.*, 2008, 24(1): 124–128.

[11] A. Cestari, L. R. Avila, E. C. O. Nassor, S. P. P. Fabiana, P. S. Calefi, K. J. Ciuffi, N. Shirley, A. C. P. Gomes and E. J. Nassar, "Characterization of the calcium-fluoroaluminosilicate glass prepared by a non-hydrolytic sol-gel route for future dental application as glass ionomer cement," *Mater. Res.*, 2009, 12(2): 139–143.

[12] A. Cestari, L. C. Bandeira, P. S. Calefi, E. J. Nassar and K. J. Ciuffi, "Preparation of calcium fluoroaluminosilicate glasses containing sodium and phosphorus by the nonhydrolytic sol-gel method," *J. Alloys Compd.*, 2009, 472(1-2): 299–306.

[13] A. W. G. Walls, “Glass polyalkenoate (glass-ionomer) cements: a review,” *J. Dent.*, 1986, 14(6): 231–246.

[14] S. Saito, S. Tosaki and K. Hirota, “Advances in Glass Ionomer cements,” *J. Appl. Oral. Sci.*, 2006, 14(spe): 3–9.

[15] S. Crisp, B. G. Lewis and A. D. Wilson, “Characterization of glass ionomer cements. I. Long term hardness and compressive strength,” *J. Dent.*, 1976, 4(4): 162–166.

[16] J. W. Nicholson, P. J. Brookman, O. M. Lacy and A. D. Wilson, “Fourier transform infrared spectroscopic study of the role of tartaric acid in glass-ionomer dental cements,” *J. Dent. Res.*, 1988, 67(12): 1451–1454.

[17] H. J. Prosser, C. P. Richards and A. D. Wilson, “NMR spectroscopy of dental cements. II. The role of tartaric acid in glass ionomer cements,” *J. Biomed. Mater. Res.*, 1982, 16(4): 431–445.

[18] A. D. Wilson, “The chemistry of dental cements,” *Chem. Soc. Rev.*, 1978, 7(2): 265–296.

[19] A. D. Wilson and J. W. Nicholson, Acid-Base cements: their biomedical and industrial applications. (Cambridge Press, 1993).

[20] S. Crisp, B. G. Lewis and A. D. Wilson, “Glass ionomer cements: Chemistry of erosion,” *J. Dent. Res.*, 1976, 55(6): 1032–1041.

[21] A. D. Wilson, S. Crisp, H. J. Prosser, B. G. Lewis and S. A. Merson, “Aluminosilicate glasses for polyelectrolyte cements,” *Ind. Eng. Chem. Res.*, 1980, 19(2): 263–270.

[22] A. D. Wilson, R. G. Hill, C. P. Warrens and B. G. Lewis, “The influence of polyacid molecular weight on some properties of glass-ionomer cements,” *J. Dent. Res.*, 1989, 68(2): 89–94.

[23] A. Mônica, C. P. Antônio, C. S. Lourenço, A. C. S. Mário and C. Simonides, “Compressive strength of resin-modified glass ionomer restorative material: Effect of P/L ratio and storage time,” *J. Appl. Oral Sci.*, 2005, 13(4): 356–359.

[24] A. Mallmann, J. C. O. Ataíde, A. Rosa, P. V. Rocha and L. B. Jacques, "Compressive strength of glass ionomer cements using different specimen Dimensions," *Braz. Oral. Res.*, 2007, 21(3): 204–208.

[25] M. Behr, M. Rosentritt, H. Loher, C. Kolbeck, C. Trempler, B. Stemplinger, V. Kopzon and G. Handel, "Changes of cement properties caused by mixing errors: The therapeutic range of different cement types," *Dent. Mater.*, 2008, 24(9): 1187–1193.

[26] M. Kamitakahara, M. Kawashita, T. Kokubo and T. Nakamura, "Effect of polyacrylic acid on the apatite formation of a bioactive ceramic in a simulated body fluid: fundamental examination of the possibility of obtaining bioactive glass-ionomer cements for orthopaedic use," *Biomaterials*, 2001, 22(13): 3191–3196.

[27] D. Boyd and M. R. Towler, "The processing, mechanical properties and bioactivity of zinc based glass ionomer cements," *J. Mater. Sci. Mater. Med.*, 2005, 16(9): 843–850.

[28] V. H. W. Khouw-Liu, H. M. Anstice and G. J. Pearson, "An in vitro investigation of a poly(vinyl phosphonic acid) based cement with four conventional glass-ionomer cements. Part 1: flexural strength and fluoride release," *J. Dent.*, 1999, 27(5): 351–357.

[29] A. S. Ledezma-Pérez, J. Romero-García, G. Vargas-Gutiérrez, and E. Arias-Marín, "Cement formation by microbial poly(γ-glutamic acid) and fluoroalumino-silicate glass," *Mater. Lett.*, 2005, 59(24–25): 3188–3191.

[30] J. J. Simmons, "The miracle mixture: glass ionomer and amalgam alloy powder," *Tex. Dent. J.*, 1983, 10(3): 6–12.

[31] J. A. Williams, R. W. Billington and G. J. Pearson, "The comparative strengths of commercial glass-ionomer cements with and without metal additions," *Br. Dent. J.*, 1992, 172(7): 279–282.

[32] H. Y. Urpo, T. Närhi and E. Söderling, "Antimicrobial effects of glass ionomer cements containing bioactive glass (S53P4) on oral micro-organisms in vitro," *Acta Odontol. Scand.*, 2003, 61(4): 241–246.

[33] S. E. Elsaka, I. M. Hamouda and M. V. Swain, “Titanium dioxide nanoparticles addition to a conventional glass-ionomer restorative: Influence on physical and antibacterial properties,” *J. Dent.*, 2011, 39(9): 589–598.

[34] J. Y. Choi, H. H. Lee and H. W. Kim, “Bioactive sol–gel glass added ionomer cement for the regeneration of tooth structure,” *J. Mater. Sci. Mater. Med.*, 2008, 19(10): 3287–3294.

[35] S. B. Mitra, “Adhesion to Dentin and Physical Properties of a Light-cured Glass-ionomer Liner/Base,” *J. Dent. Res.*, 1991, 70(1): 72–74.

[36] H. M. Anstice and J. W. Nicholson, “Studies in the setting of polyelectrolyte materials,” *J. Mater. Sci. Mater. Med.*, 1994, 5(5): 299–302.

[37] D. Xie, J. Zhao, Y. M. Weng, J. G. Park, H. Jiang and J. A. Platt, “Bioactive glass-ionomer cement with potential therapeutic function to dentin capping mineralization,” *Eur. J. Oral Sci.*, 2008, 116(5): 479–487.

[38] T. J. DO, “Polymethylmethacrylate: Properties and Contemporary Uses in Orthopaedics,” *J. Am. Acad. Orthop. Surg.*, 2010, 18(5): 297–305.

[39] K. D. Kühn, W. Ege and U. Gopp, “Acrylic bone cements: Composition and properties,” *Orthop. Clin. North Am.*, 2005, 36(1): 17–28.

[40] J. Charnley, “Anchorage of the femoral head prosthesis of the shaft of the femur,” *J. Bone Joint Surg.*, 1960, 42: 28–30.

[41] H. W. Buchholz, R. A. Elson, E. Engelbrecht, H. Lodenkämper, J. Röttger and A. Siegel, “Management of deep infection of total hip replacement,” *J. Bone Joint Surg.*, 1980, 63(3): 342–353.

[42] K. D. Kühn, Bone cements (Springer, Berlin 2000).

[43] S. Goodman, “Wear particulate and osteolysis,” *Orthop. Clin. North Am.*, 2005, 36(1): 41–48.

[44] S. S. Haas, G. M. Brauer and G. Dickson, “A characterization of polymethylmethacrylate bone cement,” *J. Bone Joint Surg.*, 1975, 57(3): 380–391.

[45] J. C. Webb and R. F. Spencer, “The role of polymethylmethacrylate bone cement in modern orthopaedic surgery,” *J. Bone Joint Surg.*, 2007, 89(7): 851–857.

[46] S. Saha and S. Pal, “Mechanical properties of bone cement: a review,” *J. Biomed. Mater. Res.*, 1984, 18(4): 435–462.

[47] S. Saha and S. Pal, “Mechanical characterization of commercially made carbon-fiber reinforced polymethylmethacrylate,” *J. Biomed. Mater. Res.*, 1986, 20(6): 817–826.

[48] G. M. Sylvain, S. Kassab, R. Coutts and R. Santore, “Early failure of a roughened surface, precoated femoral component in total hip arthroplasty,” *J. Arthroplasty*, 2001, 16(2): 141–148.

[49] R. Skripitz and P. Aspenberg, “Attachment of PMMA cement to bone: force measurements in rats,” *Biomaterials*, 1999, 20(4): 351–356.

[50] A. Race, M. A. Miller, M. T. Clarke, K. A. Mann and P. A. Higham, “The effect of low viscosity cement on mantle morphology and femoral stem micromotion: A cadaver model with simulated blood flow,” *Acta Orthop.*, 2006, 77(4): 607–616.

[51] A. J. Bowman and T. R. Manley, “The elimination of breakages in upper dentures by reinforcement with carbon fibre,” *Br. Dent. J.*, 1984, 156(3): 87–89.

[52] S. M. Khaled, P. A. Charpentier and A. S. Rizkalla, “Physical and mechanical properties of PMMA bone cement reinforced with nano-sized titania fibers,” *J. Biomater. Appl.*, 2011, 25(6): 515–537.

[53] H. D. Stipho, “Effect of glass fiber reinforcement on some mechanical properties of autopolymerizing polymethyl methacrylate,” *J. Prosthet. Dent.*, 1998, 79(5): 580–584.

[54] C. I. Vallo, G. A. Abraham, T. R. Cuadrado and J. S. Roman, “Influence of cross-linked PMMA beads on the mechanical behavior of self-curing acrylic cements,” *J. Biomed. Mater. Res. B*, 2004, 70(2): 407–416.

[55] B. Basgorenay, K. Ulubayram, K. Serbetci, E. Onurhan and N. Hasirci, “Preparation, modification, and characterization of acrylic cements,” *J. Appl. Polym. Sci.*, 2006, 99(6): 3631–3637.

[56] Z. Jin, K. P. Pramoda, G. Xu and S. H. Goh, "Dynamic mechanical behavior of melt-processed multi-walled carbon nanotube/poly(methyl methacrylate) composites," *Chem. Phys. Lett.*, 2001, 337(1-3): 43–47.

[57] J. T. Heikkilä, A. J. Aho, I. Kangasniemi and A. Yli-Urpo, "Polymethylmethacrylate composites: disturbed bone formation at the surface of bioactive glass and hydroxyapatite," *Biomaterials*, 1996, 17(18): 1755–1760.

[58] S. Shinzato, M. Kobayashi, W. F. Mousa, M. Kaminuma, M. Neo, Y. Kitamura, T. Kokubo and T. Nakamura, "Bioactive polymethyl methacrylate-based bone cement: Comparison of glass beads, apatite- and wollastonite-containing glass-ceramic, and hydroxyapatite fillers on mechanical and biological properties," *J. Biomed. Mater. Res. A*, 2000, 51(2): 258–272.

[59] K. Goto, J. Tamura, S. Shinzato, S. Fujibayashi, M. Hashimoto, M. Kawashita, T. Kokubo and T. Nakamura, "Bioactive bone cements containing nano-sized titania particles for use as bone substitutes," *Biomaterials*, 2005, 26(33): 6496–6505.

[60] H. L. Tan, S. G. Guo, S. B. Yang, X. F. Xu, and T. T. Tang, "Physical characterization and osteogenic activity of the quaternized chitosan-loaded PMMA bone cement," *Acta Biomater.*, 2012, 8(6): 2166–2174.

[61] P. P. Lopes, B. J. M. Leite Ferreirab, N. A. F. Almeida, M. C. Fredel, M. H. V. Fernandes, and R. N. Correia, "Preparation and study of in vitro bioactivity of PMMA-co-EHA composites filled with a $Ca_3(PO_4)_2$-SiO_2-MgO glass," *Mater. Sci. Eng. C*, 2008, 28(4): 572–577.

[62] T. Kokubo, H. M. Kim and M. Kawashita, "Novel bioactive materials with different mechanical properties," *Biomaterials*, 2003, 24(13): 2161–2175.

[63] P. Li, C. Ohtsuki, T. Kokubo, K. Nakanishi, N. Soga and K. Groot, "The role of hydrated silica, titania, and alumina in inducing apatite on implants," *J. Biomed. Mater. Res. A*, 1994, 24(1): 7–15.

[64] T. Miyazaki, C. Ohtsuki, Y. Akioka, M. Tanihara, J. Nakao, Y. Sakaguchi and S. Konagaya, "Apatite Deposition on Polyamide Films Containing Carboxyl Group in a Biomimetic Solution," *J. Mater. Sci. Mater. Med.*, 2003, 14(7): 569–574.

[65] M. Tanahashi and T. Matsuda, "Surface functional group dependence on apatite formation on self-assembled monolayers in a simulated body fluid," *J. Biomed. Mater. Res.*, 1997, 34(3): 305–315.

[66] A. Mori, C. Ohtsuki, A. Sugino, K. Kuramoto, T. Miyazaki, M. Tanihara and A. Osaka, "Bioactive PMMA-Based Bone Cement Modified with Methacryloxypropyltrimethoxysilane and Calcium Salts --Effects of Calcium Salts on Apatite-Forming Ability--," *J. Ceram. Soc. Jpn.*, 2003, 111(10): 739–742.

[67] A. Sugino, T. Miyazaki, G. Kawachi, K. Kikuta and C. Ohtsuki, "Relationship between apatite-forming ability and mechanical properties of bioactive PMMA-based bone cement modified with calcium salts and alkoxysilane," *J. Mater. Sci. Mater. Med.*, 2008, 19(3):1399–1405.

[68] T. Miyazaki, C. Ohtsuki, M. Kyomoto, M. Tanihara, A. Mori and K. Kuramoto, "Bioactive PMMA bone cement prepared by modification with methacryloxypropyltrimethoxysilane and calcium chloride," *J. Biomed. Mater. Res. A.*, 67(4): 1417–1423.

[69] C. Ohtsuki, T. Kokubo, K. Takatsuka and T. Yamamuro, "Compositional dependence of bioactivity of glasses in the system CaO-SiO_2-P_2O_5: Its in vitro evaluation," *J. Ceram. Soc. Jpn.*, 1991, 99(1): 1–6.

[70] K. Ohura, T. Yamamuro, T. Nakamura, T. Kokubo, Y. Ebisawa, Y. Kotoura and M. Oka, "Bone-bonding ability of P_2O_5-free $CaO \cdot SiO_2$ glasses," *J. Biomed. Mater. Res. A*, 1991, 25(3): 357–365.

[71] H. M. Kim, T. Himeno, M. Kawashita, T. Kokubo and T. Nakamura, "The mechanism of biomineralization of bone-like apatite on synthetic hydroxyapatite: an in vitro assessment," *J. R. Soc. Interface*, 2002, 22(1):17–22.

[72] W. F. Neuman and M. W. neuman, The chemical dynamics of bone mineral. (University of Chicago Press, IL, 1958).

[73] P. Li, C. Ohtsuki, T. Kokubo, K. Nakanishi, N. Soga, T. Nakamura and T. Yamamuro, "Apatite formation induced on silica gel in a simulated body fluid," *J. Am. Ceram. Soc.*, 1992, 75(8): 2094–2097.

[74] P. Li, C. Ohtsuki, T. Kokubo, K. Nakanishi, N. Soga, T. Nakamura, T. Yamamuro and K. Groot, "The role of hydrated silica, titania and alumina in forming biologically active bone-like apatite on implant," *J. Biomed. Mater. Res. A*, 1994, 28(1): 7–15.

Tables and Figures

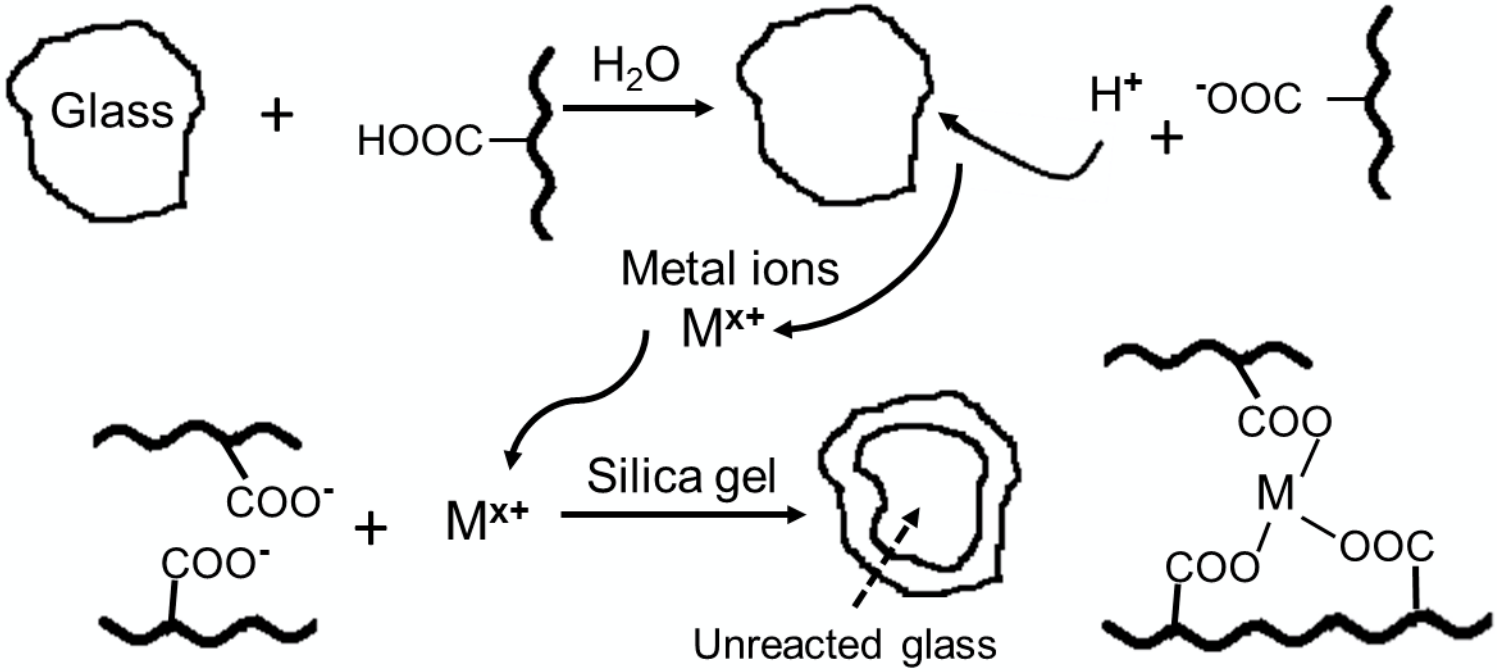

Figure 1-1. Setting reaction of glass ionomer cement.

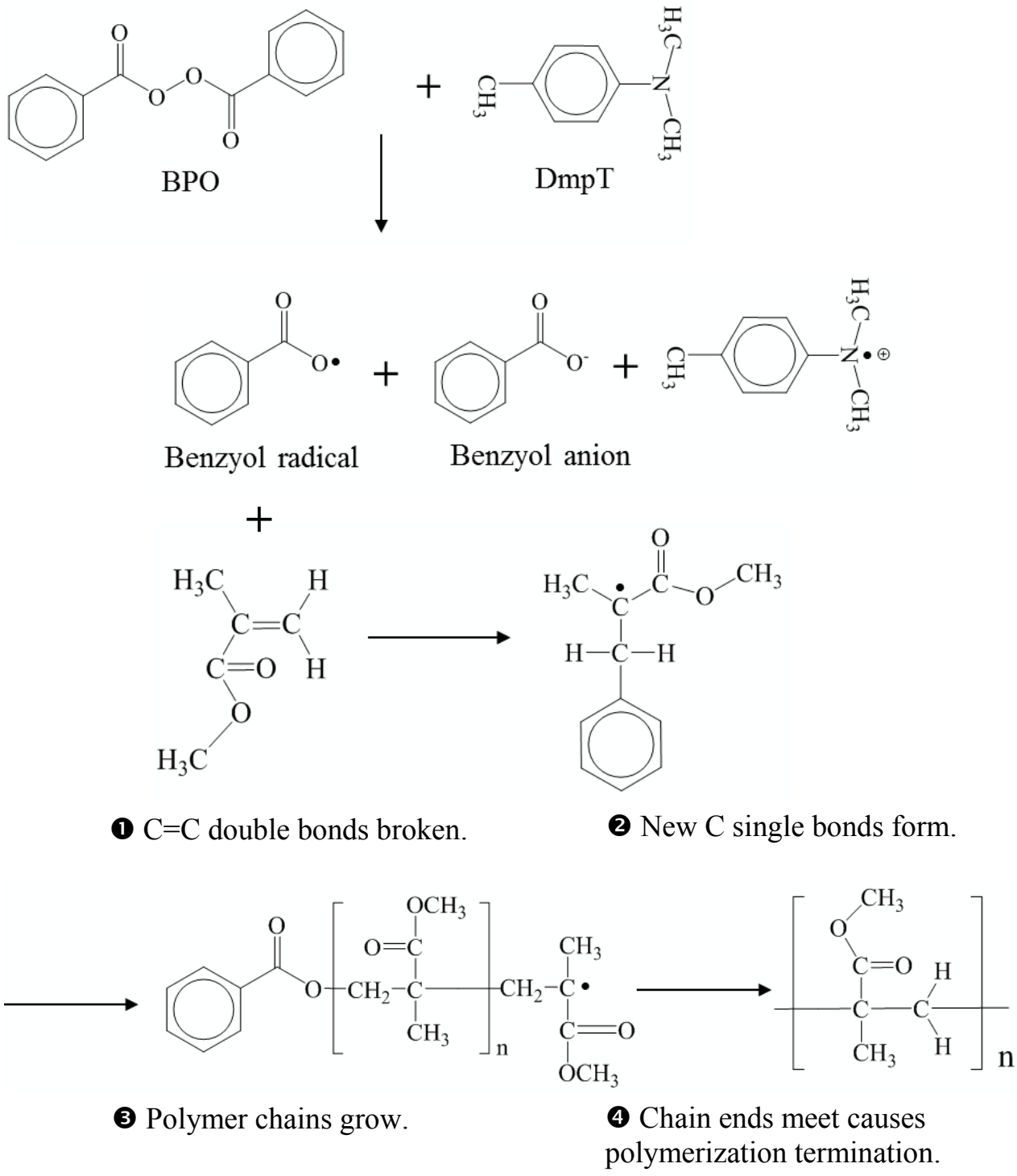

Figure 1-2. Steps in the polymerization of methyl methacrylate (MMA).

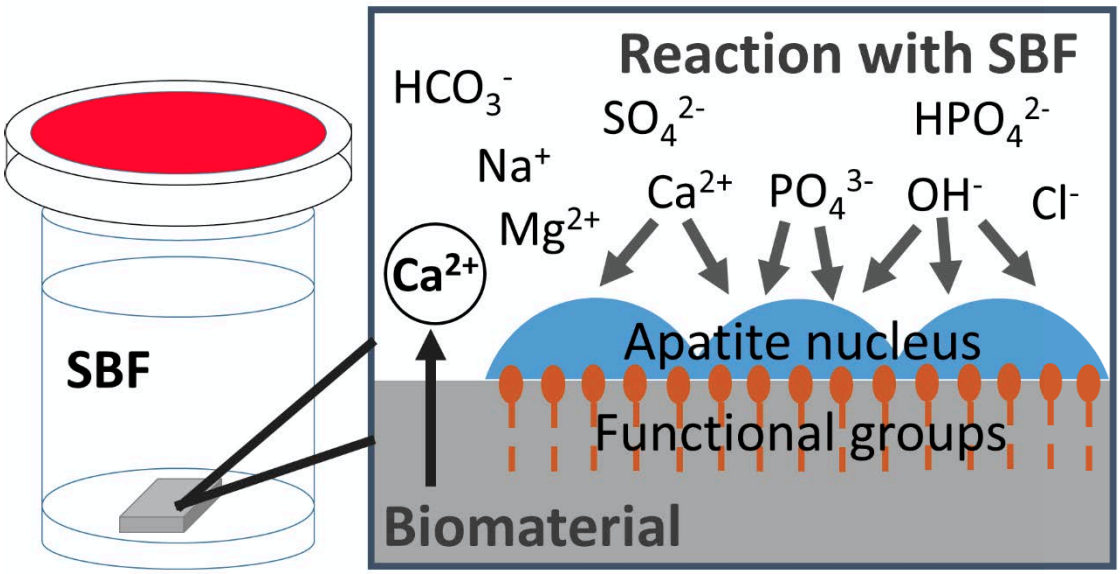

Figure 1-3. Nucleation mechanism of apatite on the surface of biomaterials incorporated with calcium source in simulated body environment.

Chapter 2

THE INVESTGATION OF BIOACTIVITY AND MECHANICAL PROPORTIES OF GLASS-IONOMER CEMENT PREPARED BY SIO_2-AL_2O_3-CAO SYSTEM AND POLY(γ-GLUTAMIC ACID)

1. Introduction

Glass ionomer cement (GIC) has been successfully used in dental restoration for more than thirty years [1]. Recently, the application is extended to implant fixation and reconstructive surgical procedures [2]. Their biological functions in dental role include direct adhesion to tooth mineral and release of fluoride ions to defend against dental caries [3]. In comparison with other restorative cements, GIC exhibits attractive features such as ease of molding, no obvious shrinkage, no significant increase in temperature, better biocompatibility without inflammatory response in mouth [4].

Commercial products for cement preparation consist of SiO_2-Al_2O_3-CaO (CaF_2) glass fillers and about 40~50% m/m poly(acrylic acid) (PAA) solution. GIC can bond chemically to the tooth structure by developing an ion enriched layer due to the reaction occur between carboxyl group (-COOH) of PAA and calcium from the dentine or enamel [5]. When implanted into the body, although their specific structures with negative charge of Si-OH groups on the surface of glass particles and -COOH groups from PAA can attract Ca^{2+} ions easily [6]. The bonding between cements and bone is attributed to mechanical interlocking rather than a bioactive mineralized layer. Kamitakahara *et al.* revealed that the existence of PAA even in ppm order inhibited the apatite formation on GIC surface in SBF, meaning that any PAA-containing GIC might lack bioactivity in body environment [7]. If such cements are intended for orthopaedic use, a new substitution of polyalkenoic acid must be developed.

In order to provide GIC with bioactivity, a microbial poly(γ-glutamic acid) (γ-PGA) will be adopted as an alternative acidic polymer to prepare cements. γ-PGA is a polypeptide in which the repetitive units of D- and L-glutamic acids are copolymerized through the chemical

bond between the amino and the carboxylic groups to give the chemical structure shown in **Figure 2-1**. The polymer comes from a natural component of Japanese soybean Natto, owns water solubility and non-toxicity to human beings and environment. Due to its rich –COOH groups, the γ-PGA hydrogels modified with Ca^{2+} ions to induce the formation of apatite in SBF has been reported [8]. And it has also been used in the preparation of GIC [9], but the information related to the bioactivity of cement is not reported yet.

In the present study, the aim was to build bioactive glass ionomer cement with satisfied mechanical strength. Besides the bioactivity testing, the preparation parameters in improving the mechanical properties of cements were also optimized.

2. Experimental

2.1. Poly(γ-glutamic acid)

Poly(γ-glutamic acid) used in this study was a food grade polymer supplied by Meiji Seika Kaisha, Japan. The range of molecular mass was from 800,000 to 1,200,000, and the concentrations (m/m) of γ-PGA solutions were set as 10%, 20%, 30% and 40%, respectively.

2.2. Glass powders synthesis

Glass G550 with the basic composition of 50 SiO_2, 50 Al_2O_3, in mass% and glass G532 with the basic composition of 50 SiO_2, 30 Al_2O_3, 20 CaO, in mass% were synthesized by sol–gel method [10]. The molar ratios of raw materials $Si(OC_2H_5)_4$ (Nacalai tesque, Inc., Kyoto, Japan), C_2H_5OH (Wako Pure Chemical Industries, Osaka, Japan), distilled water and hydrochloric acid (HCl, Nacalai tesque, Inc., Kyoto, Japan) as a catalyst were maintained at 1: 10: 50: 0.02. Addition amounts of $Al(NO_3)_3{\cdot}9H_2O$ and $Ca(NO_3)_2{\cdot}4H_2O$ (Wako Pure Chemical Industries, Osaka, Japan) was based on the glass compositions (seen in **Table 2-I**). The initial sol solutions were divided into two parts: Solution A was the mixture of 1M HCl solution, half of the C_2H_5OH, $Al(NO_3)_3{\cdot}9H_2O$ and $Ca(NO_3)_2{\cdot}4H_2O$ dissolved in the distilled water. Solution

B containing $Si(OC_2H_5)_4$ and the remaining C_2H_5OH was stirred for 1 h at ambient temperature. Then, solution A was added by dropwise to continuous stirring solution B, the totally mixed solution was stirred for another hour then moved into a 85 ºC drying oven standing for 3 days. The gel was grinded and sintered in an electrically heated furnace in an air atmosphere at 800 ºC for 2 h, where the heating rate was controlled at 5 ºC /min. The final powders passed through a 45 μm mesh sieve were voted as the filler of cement preparation.

2.3. Cement preparation

Cement pastes were obtained by homogeneous mixing of glass fillers and different concentrations of γ-PGA solutions containing 10% m/m (+) tartaric acid (Wako Pure Chemical Industries, Osaka, Japan) on a glass slab with a spatula. The mixing ratios of powder/liquid (P/L, g/g) were increased from l: l to 2: 1, 0.25 as an interval. The pastes packed into cylindrical poly(meth acrylic) molds were allowed to set and aged at 37 ºC in an incubator with a relative humidity (R.H.) of 98%.

2.4. pH measurement of glass powders and mixed pastes

The glass powders weighed at 1 g were dropped into 19 mL H_2O (concentration marked as 5, in mass%) and stirred for 1 h, the measured pH in aquatic medium was identified as the pH of glass powders. 1 g homogeneous mixed pastes were incubated for designed periods, then immersed in 5 mL pure water to measure the pH which was regarded as the pH of pastes.

2.5. Mechanical strength measurement

The mechanical strength of cements was assessed by the diametral tensile strength (DTS). Samples removed from the mold (8 mm in diameter, 4 mm in height) were applied to DTS measurement after 3 days of aging. Before DTS testing, the diameter and length of each specimen need to be re-measured with a micrometer. All samples were crushed in diametrical

direction at a crosshead speed of 1 mm/min using a computer-controlled Universal Testing Machine (Autograph AG-1, Shimadzu Co., Kyoto, Japan). DTS values can be calculated by an equation listed below:

$$DTS = 2P/\pi DL \quad (2\text{-}1)$$

where P is the maximum applied load recorded at the fracture, D and L is the diameter and length of sample, respectively. DTS shown in the figure were average values of 10 specimens, and the bars represented standard deviation (SD).

2.6. Incubation in simulated body fluid

Simulated body fluid (SBF) was prepared by dissolving reagents of NaCl, $NaHCO_3$, KCl, $K_2HPO_4{\cdot}3H_2O$, $MgCl_2{\cdot}6H_2O$, $CaCl_2$ and Na_2SO_4 in ultrapure water with constantly stirring and buffering at pH 7.40 with tris(hydroxymethyl)aminomethane ($(CH_2OH)_3CNH_2$) and an appropriate volume of 1M HCl solution, all reagents were supplied by Nacalai tesque, Inc., Kyoto, Japan and the details of SBF preparation were described in literature [11]. The constituents in SBF were 142.0 Na^+, 5.0 K^+, 1.5 Mg^{2+}, 2.5 Ca^{2+}, 147.8 Cl^-, 4.2 HCO_3^-, 1.0 HPO_4^{2-}, 0.5 SO_4^{2-}, in mM, which was nearly equal to those of human blood plasma [12].

Aged cements with highest mechanical strength prepared by each γ-PGA solution were chosen for SBF trial to evaluate bioactivity in terms of the changes on surface structure and morphology. The cylindrical specimens with dimensions of $\phi\ 8 \times 4\ mm^3$ stored in the plastic containers filled with 30 mL SBF were incubated at 37 ºC for 7 days. After that, the samples were removed, rinsed with distilled water, dried at room temperature.

2.7. Characterization

The phases and morphologies of glass G550 and G532 were surveyed by X-ray diffractometer (XRD; MXP3V, MAC Science Ltd., Yokohama, Japan) and scanning electron microscope (SEM; S-3500N, Hitachi High-Technologies, Tokyo, Japan). pH meter (F-23IIC,

Horiba Ltd., Kyoto, Japan) was employed to detect pH of glass powders and mixed pastes. Fourier-transformed-infrared spectrometer (FT-IR; FT/IR6100, Jasco Analytical Instruments, Tokyo, Japan) was introduced to investigate the interior components of cements. Surface changes in the structure and morphology of cements were performed by thin-film X-ray diffractometer and scanning electron microscope combined with the energy-dispersive X-ray microanalyzer (EDX; EMAX Energy, Horiba Ltd., Kyoto, Japan). Glass samples were scanned from 10 to 60º in 2θ (where θ is the Bragg angle), cement samples were scanned from 20 to 60º. SEM observation required sputter coating a thin film of gold on specimens. Wavenumber of FT-IR spectra was set from 500 to 4000 cm^{-1}.

3. Results

Figure 2-2 exhibits the XRD patterns and SEM images of glass powders G550 and G532. No Crystalline peaks except a broad band centered at 2θ = 22.8º were observed on the G550 pattern, once parts of Al_2O_3 was replaced by CaO, the center of broad band shifted to 26.3º, both broad bands were identified as the characteristic of amorphous SiO_2, meaning that glass fillers G550 and G532 maintained non-crystalline structure. There were no obvious differences in the morphology and size between G550 and G532. Most of the particles were irregular. Namely, larger ones just passed through the 45 μm mesh sieve, while smaller ones was down to 10 μm below.

It was important to note that the pastes mixed by G532 powders and γ-PGA solution could not turn into hardened cements after 3 days aging, even after adjusting P/L ratios or concentrations of γ-PGA. Other cements prepared by G550 powders stable in SBF were obtained from 10 to 30% of γ-PGA. When the concentration was increased up to 40%, a tendency to gelation was found in this γ-PGA solution, and high viscosity created difficulties in the stage of measuring the amount of liquid phase and mixing the cement paste.

Figure 2-3 displays the FT-IR spectra of G550 glass filler, pure γ-PGA and cements prepared by γ-PGA with the concentration (m/m) of 10 to 30% at P/L ratio of 1: 1. The peak at about 1050 cm^{-1} on the spectra of G550 glass filler was determined to the stretching of polarized Si-O band, which was also found on all cement samples. The peak at around 1560 cm^{-1} on pure γ-PGA spectra was identified as the stretching of C=O double bonding. On the spectra of cements, two peaks appearing at 1458 cm^{-1} and 1613 cm^{-1} regardless of the concentrations of γ-PGA, were assigned to the C-O symmetric/asymmetric stretching of the aluminum polysalts, respectively. Aluminum polysalts was one kind of polycarbonxylic salt precipitates formed by binding of Al^{3+} ions with the polyanion chains via carboxyl groups. Its existence indicated that the connection between glass powders and γ-PGA was successfully constructed by acid attack.

Figure 2-4 summaries the DTS values of cement specimens using P/L ratio from 1: 1 to 2: 1 and γ-PGA concentration (m/m) of 10 to 30% after aging for 3 days. The highest strength (11.88 ± 1.43 MPa) was obtained under the P/L ratio of 1: 1 and the 30% m/m γ-PGA solution. It was clearly found that these two preparation parameters produced significant variations on DTS. The deterioration of DTS was following the increase of P/L ratio, and this change trend was consistent at each concentration of γ-PGA solutions. In addition, the increase in concentration of γ-PGA brought about apparent increase in DTS even under the same P/L ratio. **Figure 2-5** shows 3 representative DTS-strain curves of glass ionomer cements prepared under various preparation parameters (P/L ratio = 1: 1 or 2: 1; the concentration (m/m) of γ-PGA solution was 30% or 10%), the dashed lines and equations were corresponding to the fitting results of each curves. The slopes of linear equations reflected the resistance ability of glass ionomer cements under being deformed elastically, thus increasing the concentrations of γ-PGA solution or decreasing P/L ratios made the cements sustain higher tension (produce larger strain) at the same strain (tension). In addition, the maximum strain (3.25%) at fracture was small, this G550 glass/γ-PGA type cement was assumed as brittle material.

Figure 2-6 shows SEM micrographs combined with EDX spectra of the SBF-unsoaked cement surface and the deposits precipitating on the surfaces of cements prepared by P/L ratio of 1: 1 under various concentration (m/m) of γ-PGA, after soaking in SBF for 7 days. Except the elements of cement itself, no other substances were detected on SBF-unsoaked cement surface based on EDX spectra. These deposits looked like spherical particles, the size range was beyond 0.5 μm, most of them agglomerated with each other into larger particles and precipitated on cement surface, which was more clearly shown on the cement prepared by 20% (m/m) γ-PGA solution. The Ca peaks were detected in EDX spectra, it was an evidence that the deposits were calcium-containing compound.

TF-XRD patterns of the surfaces of cements prepared by different concentration of γ-PGA solution using P/L ratio of 1: 1, before and after soaking in SBF for 7 days are depicted in **Figure 2-7**. No crystalline peaks were detected on the TF-XRD pattern of SBF-unsoaked cement, which indicated that no change in structure was created during the setting and aging process. The peaks appearing at about 23.1º, 29.5º, 36.0º, 39.4º, 43.1º, 47.7º and 48.6º in 2θ on the diffraction pattern of cements surfaces were assigned to a diffraction envelope of (102), (104), (110), (113), (202), (018) and (116) that resulted from the calcite ($CaCO_3$, JCPDS Card No. 05-0586). Besides the calcite as main phase, the peaks assigned to the low-crystalline silica (JCPDS Card No. 33-1161) were also detected. The rest peaks were still unknown. The patterns of cements have illustrated that: calcite was deposited on cement surfaces irrespective of the concentration of γ-PGA after 7 days soaking in SBF.

Table 2-II shows pH values of glass powders measured in aqueous medium with a calculated concentration of 5 mass% and the pH of γ-PGA aqueous solution under various concentrations. The pH of G550 was 5.43, with an increase of CaO proportion in SiO_2-Al_2O_3-CaO system, pH of the glasses rapidly increased, G532 owned the pH of 9.97. Increase in concentration of γ-PGA caused a slight increase in pH. **Figure 2-8** depicted two pH tendencies in the initial period of the pastes mixed by G532 powders and 10% m/m γ-PGA at P/L ratio 2:

1 and 1: 1 measured in 5 ml pure water. Initial pH of the pastes mixed at P/L ratios of 2: 1 and 1: 1 was 7.18 and 8.55, respectively, both increased over time. The initial pH environment was far beyond the precipitation condition in setting, led to the failure in bonding between the polyanion chains of γ-PGA and metal ions.

4. Discussions

In SiO_2-Al_2O_3-CaO system, it has been reported that glasses in the composition regions of gehlenite or anorthite owned cement forming possibility [13]. The composition regions of gehlenite and anorthite was limited on the atomic ratio: Ca: Al < 1:2, Al: Si > 1:1 and Ca: Al ≥ 1: 2, Al: Si ≤ 1: 1, respectively. In our study, the atomic ratio of Al: Si in glass G550 was 1.18, and glass G532 exhibited Ca: Al = 0.58 and Al: Si = 0.71, both glasses were considered as ion-leachable glass and suitable for cement preparation.

When glass powders were mixed with the liquid, metal ions Ca^{2+} first then Al^{3+} were released from the surface of glass particles by acid attack then leached into the aqueous medium. The leached ions bound with the polyanion chains via the carboxyl groups to precipitate a hard polycarboxylic salts [14-16]. In this acid-base reaction, pH environment determined by the combination of glass and acid solution was important for the precipitation of polycarboxylic salts. The pH ranges of γ-PGA solutions were comparable to glass G550, which made it possible to bound with Al^{3+} ions and precipitate the polycarboxylic salts although the precipitation took a long time. But the acidity (reflected on pH) of γ-PGA was not strong enough to neutralize glass G532, which resulted in high initial pH, and the polycarboxylic salts couldn't be precipitated under such condition. The pH tendency shown in **Figure 2-8** was accordance with the result published by Ho et al [17], meaning that the calcium in the γ-PGA solution was in ionized state. The failure in precipitation stage interrupted the progressive hydration of the matrix salts, so the pastes mixed by glass G532 and γ-PGA solution did not transform into the maturation phase.

The set cement consisted of unreacted glass particles with a surrounding siliceous hydrogel bound together by a matrix of polyanions cross-linked by ionic bridges (seen in **Figure 2-9**). In the cement components, the hydrated matrix composed of metal ions and polymer were the dominant phase in determining the mechanical strength. Enhancement of physical properties could be attributed to the increase in the amount of ionic cross-links between mental ions and polymer chains [18]. In G550 glass/γ-PGA cement, increasing the concentration of γ-PGA manifested an increase in the amount of polymer chains. In addition, boosting the acidity of liquid forced more Al^{3+} ions being released from particles. The increased polymer chains and Al^{3+} ions were sources of ionic cross-links, which implied more aluminum polymer salts could be formed to improve the mechanical properties. Similarly, in the case of a limited content of liquid, excessive powders did not produce more ionic cross-links. Consequently, they brought about a decline in the proportion of polymer salts which resulted in the deterioration of mechanical strength, as shown in the results of DTS. The discussion about DTS variation on preparation parameters could be used to explain the changes on DTS-strain curves. Except that, considering the intrinsic properties of two raw materials in preparing cements, increasing the contents of brittle glass eventually brought brittleness to the cements, this material was more prone to be fractured; while the soft polymer γ-PGA was attributed to increase the flexibility of cements, which enhanced the deforming resistance at the breakage.

Although measured maximum DTS of the present G550 glass/γ-PGA cements achieved about 70% of the commercially available GIC [19], it paid the expense of setting. Due to the absence of calcium oxides, glass G550 increased the resistance to acid attack; and strong bonding in Al-O-Si bridges delayed the generation of Al polysalts, both prolonged the setting. Even the cement prepared by the γ-PGA concentration (m/m) of 30% at P/L ratio (g/g) of 1: 1 spent more than 1 h to change into hard shape since timing started from the mixing.

The bioactive materials achieve the osteoconduction which is considered as a chemical attaching to bone by the formation of a biologically active apatite layer on their surfaces via

chemical reactions with the surrounding body fluid [20]. The nucleation of the apatite layer is initialed by specific functional groups [21] (Si-OH, Ti-OH, or -COOH) combined with Ca^{2+} ions. In this study, Si-OH groups were the main constituents of a siliceous hydrogel surrounded on the glass particles, carboxyl groups may come from the unreacted γ-PGA; both of them might induce the Ca^{2+} ions precipitating on the surface of the cements.

However, unlike the commercial bioactive ceramics, the precipitates were assigned as calcite instead of apatite. The possible reason was ascribed to the combination of glass with γ-PGA might produce preferable condition for the precipitation of calcite. It is known that γ-PGA has high potential to adsorb Ca^{2+}. It is therefore assumed that mixture of γ-PGA and other components in cements may adsorb a lot of Ca^{2+} to produce the surface able to favorably deposit calcite, unlike the pure γ-PGA able to deposit the calcium phosphate.

Calcite is also considered as bioresorbable material applied in drug delivery [22]. In addition, it has reported that not only apatite but also calcite can bond with rabbit tibia [23]. On the basis of this report, the prepared GIC may also exhibit bioactivity.

5. Conclusions

Glass ionomer cements have been successfully attempted by using glass powders with a composition of 50 SiO_2 50 Al_2O_3 in mass% mixed with γ-PGA solution. Increasing the concentration of γ-PGA or decreasing the P/L ratio can enhance the cross linking degree of acidic polymers and the proportion of aluminum polysalts in cements, both are key roles in determining the mechanical properties. The cement prepared by the P/L ratio (g/g) of 1: 1 and the γ-PGA concentration (m/m) of 30% exhibited the highest diametral tensile strength (11.88 ± 1.43 MPa) after aging for 3 days. Calcite phase was deposited on cement surface after 7 days soaking in SBF, meaning that this SiO_2-Al_2O_3 glass/γ-PGA cement may own the bioactivity. Based on the diametral tensile strength and bioactivity evaluation, γ-PGA can be chosen as another alternative polyalkenoic acid in the preparation of glass ionomer cement.

References

[1] A. D. Wilson and B. E. Kent, "A new translucent cement for dentistry. The glass ionomer cement," *Br. Dent. J.*, 1972, 132(4): 133–135.

[2] R. T. Ramsden, R. C. Herdman, and R. H. Lye, "Ionomeric bone cement in neuro-otological surgery," *J. Laryngol. Otol.*, 1992, 106(11): 949–953.

[3] J. W. McLean, "Glass-ionomer cements," *Br. Dent. J.*, 1988, 164(9): 293–300.

[4] J. W. Nicholson, "Chemistry of glass-ionomer cements: a review," *Biomaterials*, 1998, 19(6): 485–494.

[5] M. J. Tyas and M. F. Burrow, "Adhesive restorative materials: A review," *Aust. Dent. J.*, 2004, 3(4): 112–121.

[6] T. Kokubo, H. M. Kim, and M. Kawashita, "Novel bioactive materials with different mechanical properties," *Biomaterials*, 2003, 24(13): 2161–6175.

[7] M. Kamitakahara, M. Kawashita, T. Kokubo, and T. Nakamura, "Effect of polyacrylic acid on the apatite formation of a bioactive ceramic in a simulated body fluid: fundamental examination of the possibility of obtaining bioactive glass-ionomer cements for orthopaedic use," *Biomaterials*, 2001, 22(13): 3191–3196.

[8] A. Sugino, T. Miyazaki and C. Ohtsuki, "Apatite-forming ability of polyglutamic acid hydrogels in body environment," *J. Mater. Sci. Mater. Med.*, 2008, 19(6): 2269–2274.

[9] A. S. Ledezma-Pérez, J. Romero-García, G. Vargas-Gutiérrez, and E. Arias-Marín, "Cement formation by microbial poly(γ-glutamic acid) and fluoroalumino-silicate glass," *Mater. Lett.*, 2005, 59(24–25): 3188–3191.

[10] M. Taira and M. Yamaki, "Preparation of SiO_2-Al_2O_3 glass powders by the sol–gel process for dental applications," *J. Mater. Sci. Mater. Med.*, 1995, 6(4): 197–200.

[11] T. Kokubo and H. Takadama, "How useful is SBF in predicting in vivo bone bioactivity?," *Biomaterials*, 2006, 27(15): 2097–2915.

[12] T. Kokubo, S. Ito, Z. T. Huang, T. Hayashi, S. Sakka, T. Kitsugi, and T. Yamamuro, "Ca, P-rich layer formed on high-strength bioactive glass-ceramic A-W," *J. Biomed. Mater. Res. A*, 1990, 24(3): 331–343.

[13] U. Lohbauer, "Dental Glass Ionomer Cements as Permanent Filling Materials?—Properties, Limitations and Future Trends," *Materials,* 2010, 3(1): 76–96.

[14] S. Crisp and A. D. Wilson, "Reactions in Glass Ionomer Cements: I. Decomposition of the Powder," *J. Dent. Res.*, 1974, 53(6): 1408–1413.

[15] S. Crisp, M. A. Pringuer, D. Wardleworth, and A. D. Wilson, "Reactions in Glass Ionomer Cements: II. An Infrared Spectroscopic Study," *J. Dent. Res.*, 1974, 53(6): 1414–1419.

[16] S. Crisp, and A. D. Wilson, "Reactions in Glass Ionomer Cements: III. The Precipitation Reaction," *J. Dent. Res.*, 1974, 53(6): 1420–1424.

[17] G. H. Ho, T. I. Ho, K. H. Hsieh, Y. C. Su, P. Y. Lin, J. Yang, K. H. Yang and S. C. Yang, "γ-Polyglutamic Acid Produced by Bacillus Subtilis (Natto): Structural Characteristics, Chemical Properties and Biological Functionalities," *J. Chin. Chem. Soc.*, 2006, 53(6): 1363–1384.

[18] S. Crisp, B. G. Lewis, and A. D. Lewis, "Characterisation of glass-ionomer cements 1. Long term hardness and compressive strength," *J. Dent.*, 1976, 4(4): 162–166.

[19] D. Xie, W. A. Brantley, B. M. Culbertson and G. Wang, "Mechanical properties and microstructures of glass-ionomer cements," *Dent. Mater.*, 2011, 27(11): 1170–1179.

[20] D. Arcos, I. Izquierdo-Barba and M. Vallet-Regí, "Promising trends of bioceramics in the biomaterials field," *J. Mater. Sci. Mater. Med.*, 2009, 20(2): 447–455.

[21] P. Li, C. Ohtsuki, T. Kokubo, K. Nakanishi, N. Soga and K. Groot, "The role of hydrated silica, titania, and alumina in inducing apatite on implants," *J. Biomed. Mater. Res. A*, 1994, 24(1): 7–15.

[22] J. Wang, J. S. Chen, J. Y. Zong, D. Zhao, F Li, R. X. Zhuo and S. X. Cheng, "Calcium Carbonate/Carboxymethyl Chitosan Hybrid Microspheres and Nanospheres for Drug Delivery, " *J. Phys. Chem. C*, 2010, 114(44): 18940–18945.

[23] Y. Fujita, T. Yamamuro, T. Nakamura, S. Kotani, C. Ohtsuki and T. Kokubo, "The bonding behavior of calcite to bone," *J. Biomed. Mater. Res.*, 1991, 25(8): 991–1003.

[24] S. M. Kenny and M. Buggy. "Bone cements and fillers: A review," *J. Mater. Sci. Mater. Med.*, 2003, 14(11): 923–938.

Tables and Figures

Table 2-I. Mixing ratios of raw materials for sol–gel synthesis of SiO_2-Al_2O_3-CaO powders.

Raw materials (molar ratio)						Composition of target product
TEOS	$Al(NO_3)_3 \cdot 9H_2O$	$Ca(NO_3)_2 \cdot 4H_2O$	C_2H_5OH	H_2O	HCl	SiO_2: Al_2O_3: CaO (w/w/w)
1	1.178	0	10	50	0.02	G550, 5: 5: 0
1	0.707	0.429	10	50	0.02	G532, 5: 3: 2

Table 2-II. pH values of glass powders in aqueous solution and γ-PGA aqueous solutions under different concentrations.

SiO_2-Al_2O_3-CaO	5-5-0 system	5-4.5-0.5 system	5-3-2 system
pH value	5.43	8.28	9.97
γ-PGA solution	10% (m/m)	20% (m/m)	30% (m/m)
pH value	5.41	5.32	5.24

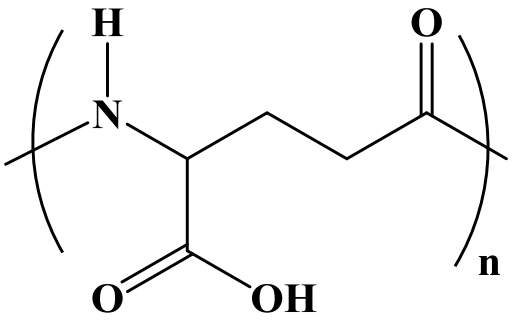

Figure 2-1. Chemical structure of poly(γ-glutamic acid) (γ-PGA)

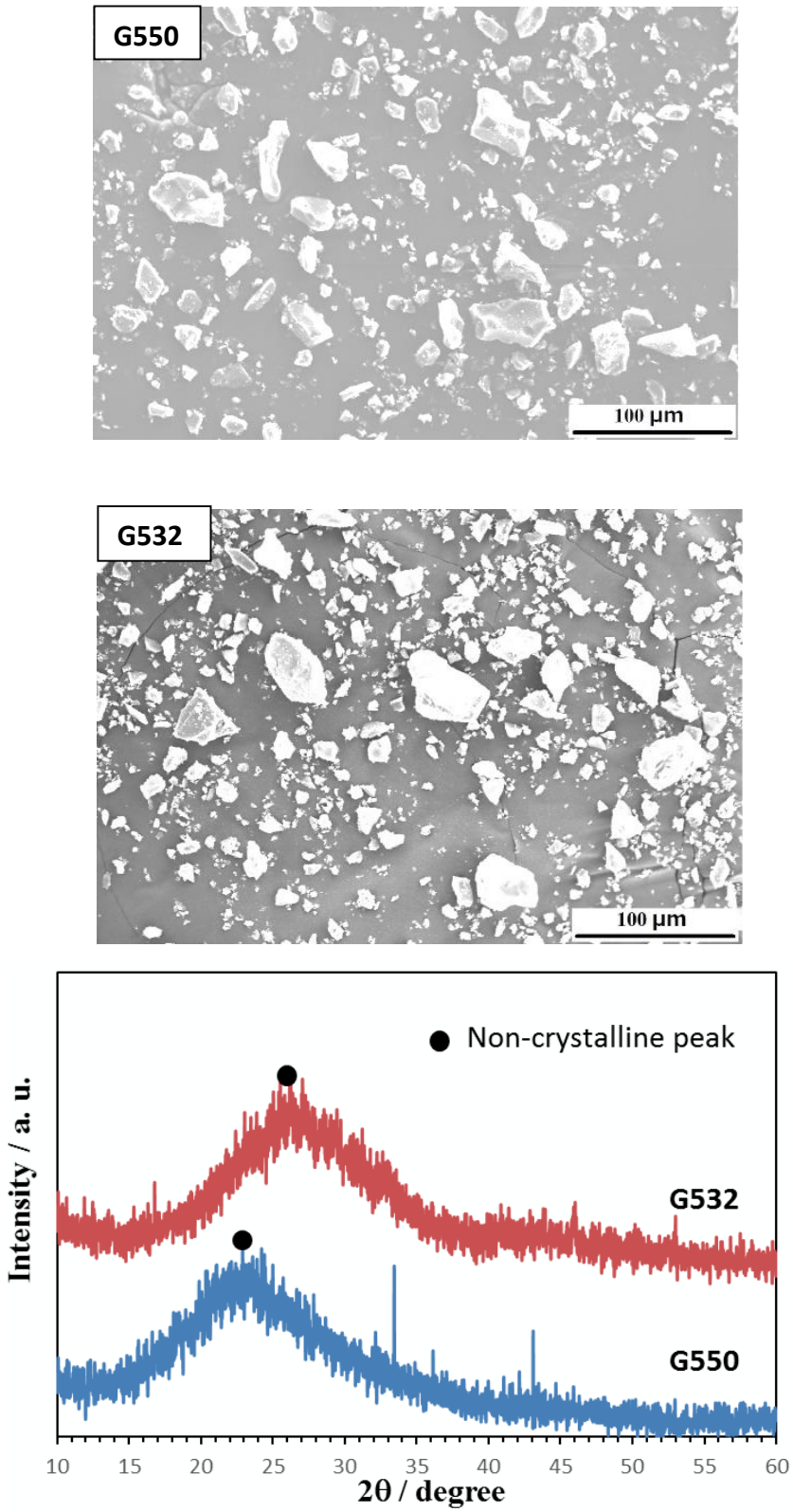

Figure 2-2. SEM micrographs (upper) and XRD patterns (lower) of glass powders G532 and G550.

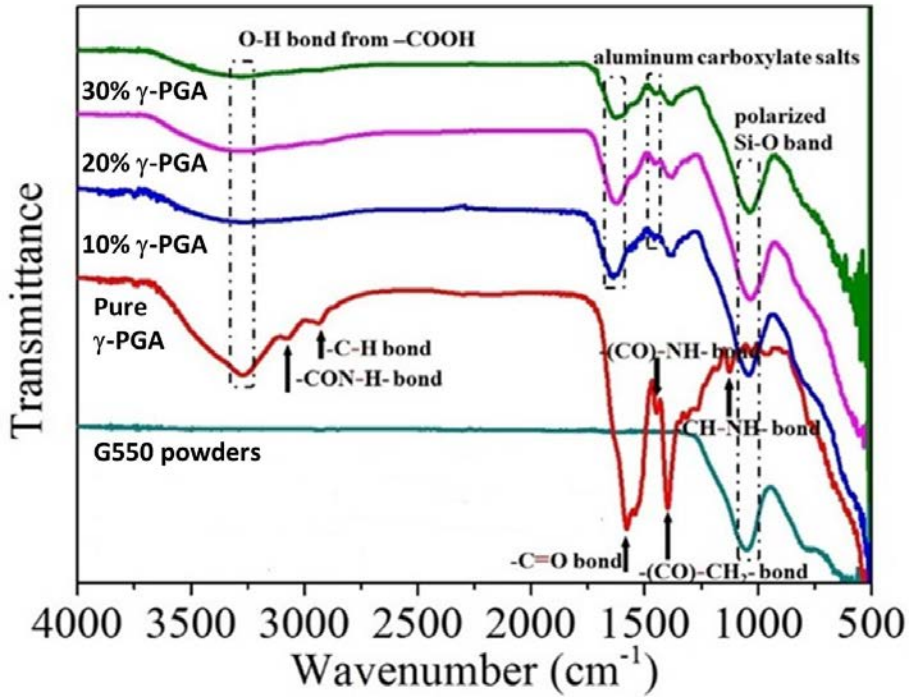

Figure 2-3. FT-IR spectra of G550 powders, pure γ-PGA and the cements prepared by γ-PGA solutions with the concentrations (m/m) of 10 to 30% at P/L ratio of 1: 1.

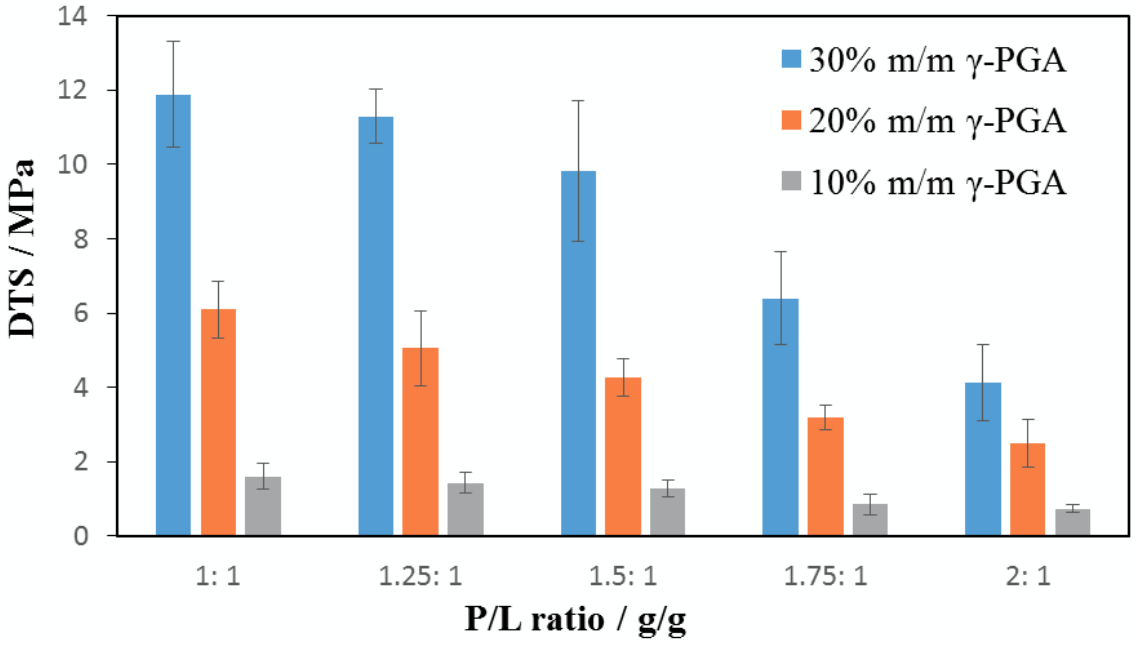

Figure 2-4. Diametral tensile strength as a function of the γ-PGA concentration and mixing P/L ratio.

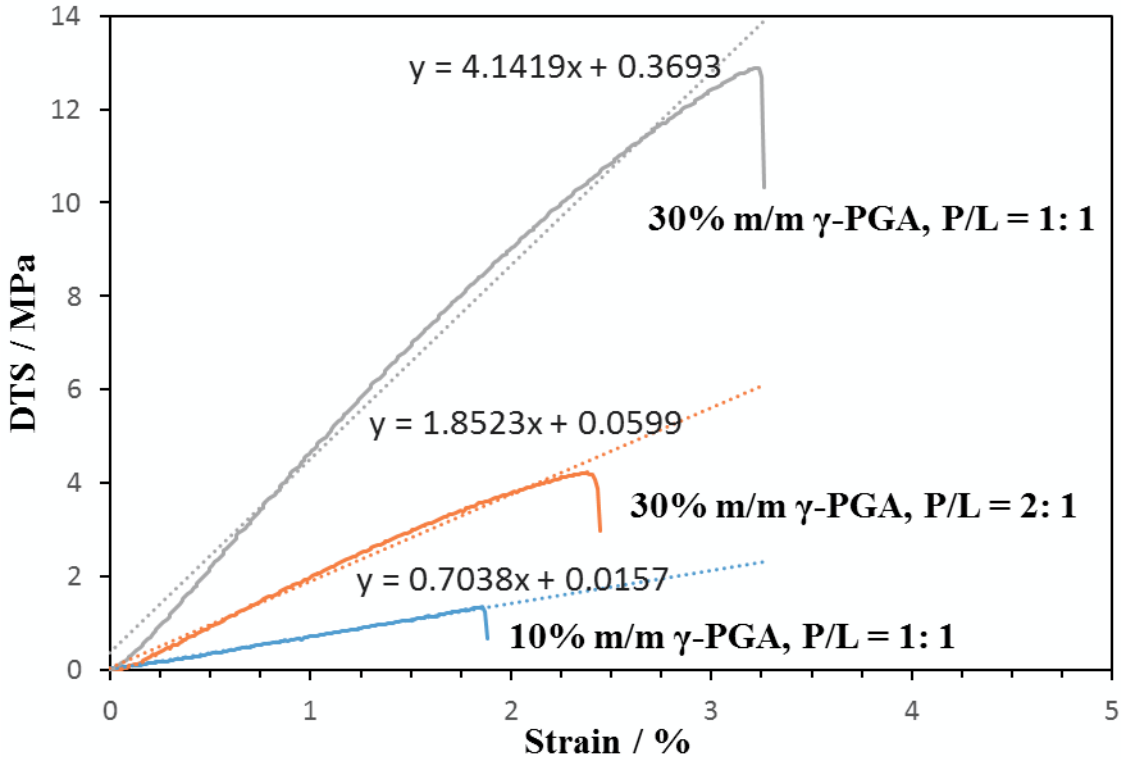

Figure 2-5. Representative DTS-strain curves of glass ionomer cements under various preparation parameters.

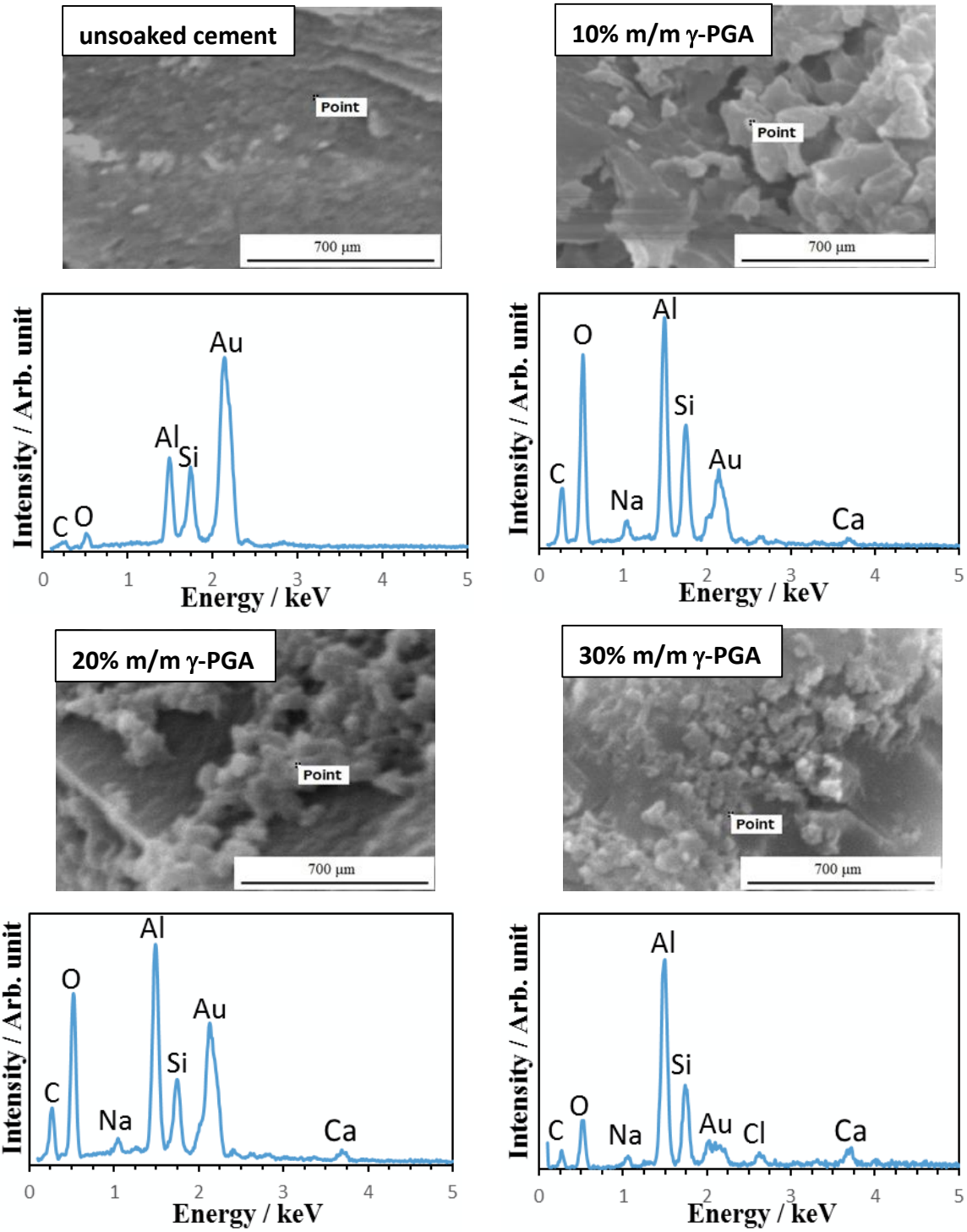

Figure 2-6. SEM micrographs and EDX spectra of SBF-unsoaked cement surface, the deposits precipitating on the surfaces of cements prepared by the P/L ratio of 1: 1 under various concentrations (m/m) of γ-PGA solution, after soaking in SBF for 7 days.

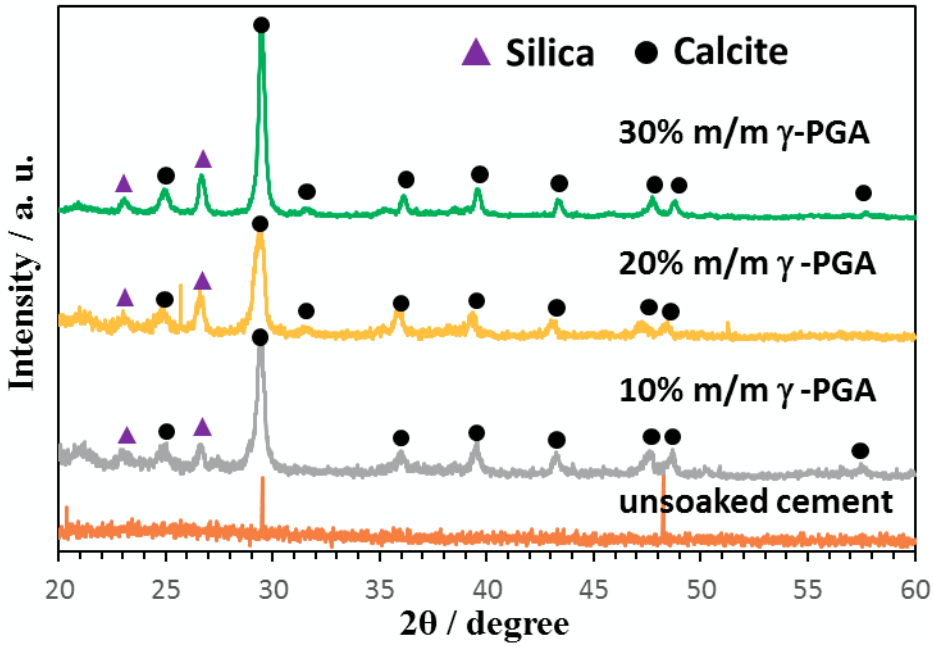

Figure 2-7. TF-XRD patterns of the surfaces of cements prepared by different concentrations (m/m) of γ-PGA using P/L ratio of 1: 1, before and after soaked in SBF.

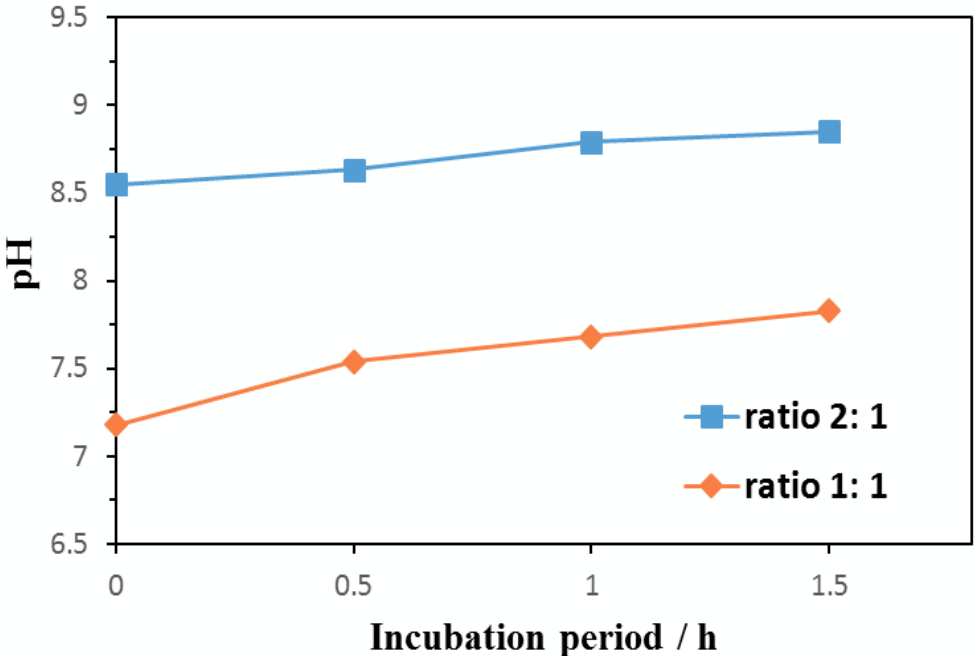

Figure 2-8. pH tendencies in initial periods of the pastes mixed by G532 powders and 10% m/m γ-PGA solution at P/L ratio of 2: 1 and 1: 1, tested in 5 ml pure water.

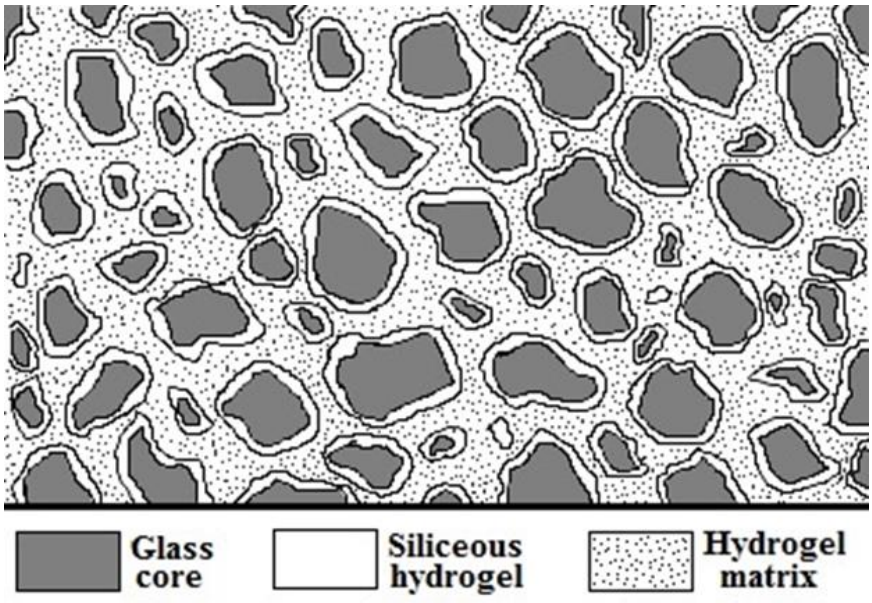

Figure 2-9. Interior structure of glass ionomer cement [24].

Chapter 3

MODIFICATION WITH CALCIUM ACETATE AND PHOSPHORIC ACID 2-HYDROXYETHYL METHACRYLATE ESTER TO PROVIDE PMMA BONE CEMENT WITH BIOACTIVITY IN SIMULATED BODY ENVIRONMENT

1. Introduction

As one kind of clinical material used for anchoring artificial hip joints to contiguous bone, polymethylmethacrylate (PMMA) bone cement has been paid much attention in orthopedic field due to its better performance at early recovery stage [1]. However, one significant problem is that this type bone cement lacks of a chemical bonding ability to bone. Intrinsic mechanical interlocking [2] is insufficient to sustain long-term stable implantation, so loosening between bone cement and the implant is liable to occur [3].

It is essential to develop a biocompatible and adhesive PMMA bone cement for implantation without loosening. Some bioactive materials such as bioglass 45S5 [4, 5] or glass-ceramic A-W [6, 7] can generate a physiological active bone-like substance that creates a tight contact to living bone after implanted into body environment. Incorporating such fillers into PMMA cement by mechanical mixing has also achieved the purpose of improved bone bonding [8]. However, in some cases, this method still faces challenges in its detail: for example, the formation of apatite was restricted to spots where bioactive particles could be exposed to body fluid, and acquiring a better performance on osteoconductivity and affinity required an increase in the content of glass beads to 70 mass% [9]. The addition of massive amounts of bioactive powders may limit the physical properties of PMMA cement. Therefore, an alternative design for the fabrication of bioactive PMMA bone cement needs to be developed.

It has been revealed that simulated body fluid (SBF), whose composition is nearly equal to that of human blood plasma, has a similar ability to body fluid for the production of bone mineral

apatite [10]. Therefore, studies [11] related to the reaction mechanism between bioactive materials and SBF could be viewed as the evidence to understand the formation process of apatite: some functional groups such as Si-OH [12,13], -COOH [14,15] or PO_4H_2 [16] played an important role in attracting apatite nucleation and Ca^{2+} ions released into SBF accelerated the growth of apatite. The finding suggests that utilization of combinations of functional groups and Ca^{2+} ions can possibly equip PMMA bone cement with apatite-forming ability. A previous research [17] recommended calcium acetate as the ideal source of Ca^{2+} ions, due to its appropriate solubility and satisfied performance on setting time and compressive strength among all selected calcium salts. On the other hand, Tanahashi [16] discovered that the potentials of functional groups differed from one another in the aspect of inducing apatite nucleation, as the nucleation rate decreased in the order of PO_4H_2 > -COOH >> $-CONH_2$ ≈ -OH > $-NH_2$, thus phosphate groups (PO_4H_2) were considered as the optimal option.

In this study, phosphoric acid 2-hydroxyethyl methacrylate ester (Pa2hme) was employed to supply phosphate (PO_4H_2) groups, its chemical structure was shown in **Figure 3-1**. The primary target is to develop a bioactive PMMA bone cement by modification with the combinations of various amounts of calcium acetate and Pa2hme. The effects of both additives on other cement properties were also investigated. Bioactivity was estimated by the formation of apatite in an SBF environment, and setting time and compressive strength were examined as the workability and mechanical properties, respectively. The contents of calcium acetate and Pa2hme were also optimized for practical application in clinic.

2. Experimental

All chemical reagents used for the preparation and analysis in our study were of reagent grade without further purification. PMMA powders with a molecular weight about 70,000 and average grain size of 4 um were supplied by Sekisui Plastics Industries, Tokyo, Japan. The calcium

acetate was produced by sintering calcium acetate monohydrate ($Ca(CH_3COO)_2 \cdot H_2O$, Wako Chemical Industries, Osaka, Japan) at 220 ºC for 2 h and sieved to a particle size <44 μm, then stored at 120 ºC before cement preparation.

2.1. Preparation of the modified PMMA cements

The preparation of PMMA cement relies on the mixing of a powder and a liquid phase. The powder phase was composed of a mixture of PMMA beads, pre-heated $Ca(CH_3COO)_2$ and benzoyl peroxide (BPO, Wako Chemical Industries, Osaka, Japan) as a polymerization initiator. The mixing was required at least for 1 min. The liquid phase was prepared by blending MMA monomer (Wako Chemical industries, Osaka, Japan) with Phosphoric acid 2-hydroxyethyl methacrylate ester (Pa2hme, Aldrich, Tokyo, USA) and a polymerization accelerator N,N-dimethyl-p-toluidine (DmpT, Wako Chemical Industries, Osaka, Japan). The contents of additives and detailed composition in the powder and liquid phase are shown in **Table 3-I-a and Table 3-I-b**, and the amounts of BPO and Dmpt remained constant. One sample (viewed as the reference) prepared with P00 + L00 owned the same composition of commercially available PMMA bone cement offered by CMW® 1, Debuy International Ltd., England. Every paste was obtained by mixing the powder with the liquid phase at a powder/liquid (P/L) mass ratio of 1: 0.5 at ambient temperature.

2.2. Measurement of setting time and maximum temperature

Setting times of cements were measured according to the ISO 5833 [18]. Mixed pastes packed into cylindrical poly(meth acrylic) molds were allowed to polymerization under the prescribed conditions of 23 ± 2 ºC and 40~60% relative humidity. The rise in temperature with curing time was sensed by using a thermocouple probe (Plamic 100 Ω) penetrated into the center of each mold, a thermo record (TR-81, T&D corp., Matsumoto-shi, Japan) connected to the probe was in charge of data storage (sampling rate: 1 s) until the temperature reached its peak (maximum). The determination of setting time started from the beginning of mixing, ended with the value

corresponding to the halfway between prescribed and peak temperature on the exothermic temperature/time curve. The measurements for each combination of Pa2hme and $Ca(CH_3COO)_2$ were carried out four times and all setting times and maximum temperatures were expressed as mean ± SD (standard deviation).

2.3. Bioactivity evaluation in simulated body fluid

In our study, cements with bioactivity *in vitro* were assessed by the formation of bone-like apatite on their surfaces in an SBF environment. SBF owns nearly equal constituents compared to those of human blood plasma [19], ion concentrations are 142.0 Na^+, 5.0 K^+, 1.5 Mg^{2+}, 2.5 Ca^{2+}, 147.8 Cl^-, 4.2 HCO_3^-, 1.0 HPO_4^{2-}, 0.5 SO_4^{2-}, in mol/m^3, the preparation of SBF was following the publication proposed by Professor Kokubo [10]. Prepared cements polished by 1000# SiC paper were cut into a rectangular pieces with dimensions of $10 \times 15 \times 1$ mm^3 then stored in the plastic containers filled with 35mL SBF at 37 ºC. After soaking for designed intervals (1, 3, 7 and 14 days), all cements were removed, rinsed and dried at room temperature.

2.4. Compressive strength evaluation

For the compressive strength measurement, mixed pastes were shaped into the cylindrical objects with 6 mm in diameter and 12 mm in height recommended by ISO 5833 [20]. The incubation for all specimens was achieved in SBF, molded cements before completely cured were left in SBF at 37 ºC for 7 days. The compressive load was applied at cross-head speed of 20 mm/min using an Universal Testing Machine (Autograph AG-1, Shimadzu Co., Kyoto, Japan) until fracture occurred. The compressive strength was calculated from fracture load and geometric area of the specimen. 10 specimens were measured for each combination to figure out the averages and standard deviations.

2.5. Characterization

Thin-film X-ray diffractometer (TF-XRD; MXP3V, MAC Science Ltd., Yokohama, Japan), scanning electron microscope (SEM; S-3500N, Hitachi High-Technologies, Tokyo, Japan) combined with energy-dispersive X-ray microanalyzer (EDX; EMAX Energy, Horiba Ltd., Kyoto, Japan) and Fourier-transformed-infrared spectrometer (FT-IR; FT/IR6100, Jasco Analytical Instruments, Tokyo, Japan) were employed to investigate the surface changes in structure and morphology of all cements. TF-XRD patterns were performed by using a step scanning mode at 0.02º steps per second with CuKα radiation, all samples were scanned from 20 to 40º in 2θ (where θ is the Bragg angle). A thin film of carbon was sputter-coated on all specimens for SEM observation and the range of wavenumber in FT-IR measurement was set from 500 to 2000 cm^{-1}. pH meter (F-23IIC, Horiba Ltd., Kyoto, Japan) was introduced to detect pH values of remaining SBF used for bioactivity evaluation under designed periods, the concentrations of Ca and P in the SBF under the same periods were also measured by Inductively Coupled Plasma-optical Emission Spectrometry (ICP-OES; Optima 4300 DV, PerkinElmer, Inc., America).

3. Results

3.1. Setting behavior

It should be note that Pa2hme only beyond 30 mass% could be completely dissolved in MMA liquid. No heating release were detected from the modified cements "P00" (without $Ca(CH_3COO)_2$), "Pa2hme30# + CA5%", "Pa2hme50# + CA5%" and "Pa2hme50# + CA20%", they still remained a dough state after standing for at least 2 h, which made them only suitable for bioactivity examination.

Table 3-II-a and Table 3-II-b lists the setting times and maximum temperatures of all cements prepared by the combinations of $Ca(CH_3COO)_2$ and Pa2hme under various contents,

respectively. The combinations of $Ca(CH_3COO)_2$ and Pa2hme led to an acceleration of setting compared to the reference sample. Comparison among all the modified cements, under the same content of Pa2hme, the shortest setting times were obtained from the samples whose mass ratios of $Ca(CH_3COO)_2$/Pa2hme were close to the mixing ratio (2: 1) of powder/liquid, increasing or decreasing the amounts of $Ca(CH_3COO)_2$ prolonged the setting based on this ratio. The same tendency can be also found from the variations in maximum temperature. Moreover, it could be found that $Ca(CH_3COO)_2$ didn't produce obvious influence on setting time and maximum temperature, but the content of Pa2hme increased to 50 mass% produced drastic decline in maximum temperature.

3.2. Characterization of apatite formation

Figure 3-2 shows the original surface morphologies of reference cement "L00 + P00" and modified sample "Pa2hme30# + P00" observed by SEM, EDX spectra of cements prepared by L00 + P00, Pa2hme30# and Pa2hme50# combined with various contents of $Ca(CH_3COO)_2$ before soaking in SBF (0 day). On SEM photographs, scratches created by the polish of SiC paper were found on reference cement; except scratches, holes brought from the mixing were also detected on modified sample, and the surface features of other modified cements were similar to that of "Pa2hme30# + P00". No redundant elements were detected on pure PMMA cement, while the Ca and P elements detected the surfaces of modified cements indicated that the additives $Ca(CH_3COO)_2$ and Pa2hme had been successfully merged into the cement, and the intensities of Ca were enhanced following the increasing content of $Ca(CH_3COO)_2$.

SEM photographs shown in **Figure 3-3** are the surface morphologies of cements prepared by Pa2hme30# and Pa2hme50# combined with various contents of $Ca(CH_3COO)_2$ after soaking in SBF for 14 days, respectively. Layered deposition composed of individual spherical particles was covering the whole surfaces of Pa2hme30# series cements modified with CA35% and CA50%,

and no deposition was observed on Pa2hme50# series cements regardless of the content of $Ca(CH_3COO)_2$, surface features were almost unchanged compared to initial cements shown in **Figure 3-2**.

Figure 3-4 shows the FT-IR spectra of all cements prepared by the combination of Pa2hme and $Ca(CH_3COO)_2$ with various contents after soaking in SBF for 14 days. The functional groups listed in **Table 3-III** are corresponding to those number-marked peaks appearing on the FT-IR spectra, these groups are considered to be the characteristics of PMMA. While the intrinsic peaks belong to phosphate-containing Pa2hme and $Ca(CH_3COO)_2$ are hard to be confirmed on all modified samples due to the overlapping of peaks. Moreover, the tendency in FT-IR spectra were in accordance with that of SEM observation, the layered deposition on cement surfaces changed the spectra, a new series of peaks appearing at around 600 to 1050 cm^{-1} were ascribed to P–O stretching (550 and 600 cm^{-1}: PO_4^{3-} ν_4 vibration; 950 cm^{-1}: PO_4^{3-} ν_1 vibration; 1020 cm^{-1}: PO_4^{3-} ν_3 vibration), which indicated that the deposited microspheres contained phosphate radical (PO_4^{3-}), might belong to calcium phosphate salt [21].

Figure 3-5-a displays the TF-XRD patterns of cements prepared by (a) Pa2hme30# and (b) Pa2hme50# with different contents of $Ca(CH_3COO)_2$ after soaking in SBF for 14 days, and **Figure 3-5-b** shows the TF-XRD patterns of Pa2hme30# series cements modified with (c) CA35% and (d) CA50% after soaking in SBF for designed periods. No peaks were detected on Pa2hme50# series cements regardless of $Ca(CH_3COO)_2$ contents; these cements still maintained the initial state (0 day) even after soaking in SBF for 14 days, while high contents of $Ca(CH_3COO)_2$ such as 35 mass% and 50 mass% changed the patterns of Pa2hme30# series cements: the peaks with low crystallinity appearing at about 26º, 32º, and 34º in 2θ were assigned to the diffractions of hydroxyapatite on the basis of JCPDS Card No. 09-0432, and the first emergences of apatite peaks for CA35% and CA50% were after 14 days and 3 days of soaking in SBF, respectively, which was

accordance with the SEM observation, the spherical deposits were identified as low-crystalline apatite.

The apatite-forming ability of the cements containing various content of both additives in SBF environment is judged by TF-XRD results, the evaluation is summed up on **Table 3-IV**. The apatite forming period varied from 3 to 14 days depending on the combinations of $Ca(CH_3COO)_2$ and Pa2hme. Namely increases in the amount of $Ca(CH_3COO)_2$ accelerated the formation rate of apatite, while the same change trend on Pa2hme brought an opposite result.

3.3. Variation in compressive strength

The compressive strength of cements modified with various contents of both additives after 7 days soaking in SBF is summarized in **Figure 3-6**. The highest compressive strength was 71.6 ± 1.4 MPa provided by sample "Pa2hme30# + CA20%", just exceeded the lower limit of ISO 5833 [20], and still lower than that (96.9 ± 7.2 MPa) of the SBF-soaked reference. It was clearly seen that all additives produced a decline in compressive strength, the decay was following the increase of both additives.

3.4. Changes in the ionic concentrations of Ca and P and corresponding pH in SBF

Figure 3-7 exhibits the changes of concentrations of Ca and P in remaining SBF and **Figure 3-8** exhibits the corresponding pH values of the same SBF measured at 37 ºC under various intervals after cements soaking. Rapid release of Ca^{2+} ions (represented by Ca in figure 3-7) was finished within 3 days of soaking in Pa2hme30# series cements and within 1 day of soaking in Pa2hme50# series cements. More $Ca(CH_3COO)_2$ added into cements led to enhanced releases of Ca^{2+} ions in SBF irrespective of the deposition of apatite. Rapid release of PO_4H_2 groups (represented by P in figure 3-7) was finished within 1 day of soaking in both cements series. It should be noted that P concentration of SBF soaked by sample "Pa2hme30# + CA35%" started to

drop after 7 days, and the concentration of P in sample "Pa2hme30# + CA50%" soaked SBF showed almost the same as that of initial SBF since the apatite began to deposit, the reduced portion of P was considered as the consumption for apatite formation, supported by XRD results. The pH of remaining SBF decreased with the increase in soaking time and the contents of $Ca(CH_3COO)_2$, its drop became more obvious in Pa2hme50# series samples.

4. Discussions

Setting behavior of all modified cements implied that adding Pa2hme alone may inhibit the radical polymerization, and successful polymerization depended on the combination of $Ca(CH_3COO)_2$ and Pa2hme under a controllable range on amounts. Considering the corresponding relationship between the mass ratio of $Ca(CH_3COO)_2$/monomer and the shortest times, one reasonable explanation was that the efforts from both sides had counteracted with each other on a critical ratio which was close to the mixing ratio (2: 1). Therefore, the initiator/accelerator BPO/DmpT only worked on the rest of PMMA/MMA, which accelerated the setting. Comparison in both additives, Pa2hme was the dominant role in affecting the setting behavior of modified cements. In our research, the acceleration of setting was consistent with the result of the modification of PMMA cement with phosphorylated hydroxyethylmethacrylate (HEMA-P) [22].

Modification with $Ca(CH_3COO)_2$ and phosphate (PO_4H_2) groups containing Pa2hme in a suitable contents provided the PMMA bone cement with bioactivity in terms of the apatite formation, the generation of a bioactive surface consisting of sphere apatite particles was attributed to the coaction of the phosphate (PO_4H_2) groups in the structure of Pa2hme and Ca^{2+} ions. Phosphate (PO_4H_2) groups shared the same role as Si-OH groups [23]. Those incorporated onto the cement surface could initiate the heterogeneous nucleation of apatite, and continuous release of Ca^{2+} ions from water-soluble calcium acetate led to an increase in supersaturation degree with respect to apatite. It was clear to see that increasing in content of $Ca(CH_3COO)_2$ could shorten the

apatite-forming period from **Table 3-IV**, but increasing in content of Pa2hme did not provide cements with apatite-forming ability. The possible reason could be concluded from initial surface changes caused by the changes in pH with soaking periods and concentration variations of Ca and P in SBF (seen in **Figure 3-2**, **Figure 3-7 and Figure 3-8).** High contents of Ca and P detected on cement surface were liable to release into SBF, the dissolution of $Ca(CH_3COO)_2$ brought acetate ions (CH_3COO^-) into SBF, and the increase in P concentration of SBF implied that phosphate (PO_4H_2) groups were also discharged into SBF, both acidic species were attributed to the drop of pH of SBF. The drastic decreases of pH were finished within 1 days due to the rapid release of both additives, and the increase in the both additives contents brought more serious decrease. Low pH environment was not an ideal environment for apatite precipitation, because it led to low supersaturation degree of apatite. Besides that, the increase of P content indicated that cement surface had lost PO_4H_2 functional groups for attracting the nucleation of apatite, the possibility to induce apatite nucleation only relied on the plenty of Ca^{2+} ions on cement surface to rise the supersaturation degree of apatite. For Pa2hme50# series cements, although the amount of $Ca(CH_3COO)_2$ increased to 50 mass%, a sustained declining pH of SBF combined with the ions (Ca^{2+} or PO_4^{3-}) on the surface was no longer suitable for the deposition of apatite. For bioactive PMMA cement, although pH did not offer a satisfied condition, abundant Ca^{2+} ions released into SBF enhanced the supersaturation degree of apatite and further prompted the apatite deposition. The results suggested that apatite-forming ability of the cements modified with calcium acetate and Pa2hme was not only controlled by the contents of both additives, the surface compositions, the changes of pH and concentrations of Ca and P in SBF also showed influences on that.

Unlike bioactive glasses or glass-ceramics [24], $Ca(CH_3COO)_2$ and Pa2hme were soft additives, incorporation of them was incapable to make up the loss of compressive strength from the replaced parts of cements, thus more additives led to greater deterioration in mechanical strengths; the hydrolysis and release of $Ca(CH_3COO)_2$ and Pa2hme (expressed by the way of Ca

and P concentrations shown in **Figure 3-7**) created pores on the surface of modified cements, which made a further loss of strength after exposure to the SBF [25]. Even if the bioactive PMMA cements could induce the deposition of apatite on surfaces, tiny amounts of apatite was unable to enhance the strength of cements.

Consequently, taking apatite-forming ability, setting time and compressive strength into consideration, the optimal content was 30 mass% of Pa2hme in liquid and 35 mass% of $Ca(CH_3COO)_2$ in powder. However the obtained cement still failed to satisfy the practical standard ISO5833 due to its poor mechanical performance (far behind the lower limit: 70MPa). The effective way to enhance the physical properties of modified cements was reducing Pa2hme content in liquid phase based on the tendency shown in **Figure 3-6**, but Pa2hme was separated from MMA matrix at a lower content. So, a better solution is to search a new phosphate-containing monomer which can be mixed with MMA at lower proportion to replace Pa2hme.

5. Conclusions

The combinations of $Ca(CH_3COO)_2$ and phosphate (PO_4H_2) groups containing Pa2hme can equip PMMA bone cement with apatite-forming ability in simulated body environment. Increasing the content of $Ca(CH_3COO)_2$ significantly shortened the formation period of apatite; while high ratios of both additives in modified cements result in the deterioration of compressive strength. Bioactive cements with highest compressive strength still failed to satisfy the practical standard ISO 5833 because of the Pa2hme itself. It is necessary to adopt new monomer to enhance the physical properties for clinic application.

References

[1] K. D. Kühn, Bone cements (Springer, Berlin 2000).

[2] R. Skripitz and P. Aspenberg, “Attachment of PMMA cement to bone: force measurements in rats,” *Biomaterials*, 1999, 20(4): 351–356.

[3] M. Freeman, G. W. Bradley and P. A. Ravell, “Observation upon the interface between bone and polymethylmethacrylate cement,” *J. Bone Joint Surg.*, 1982, 64: 435-462.

[4] L. L. Hench, “The story of Bioglass,” *J. Mater. Sci. Mater. Med.*, 2006, 17(11): 967–978.

[5] M. Plewinski, K. Schickle, M. Lindner, A. Kirsten, M. Weber and H. Fischer, “The effect of crystallization of bioactive bioglass 45S5 on apatite formation and degradation,” *Dent. Mater.*, 2013, 29(12): 1256–1264.

[6] A. Hoppe, N. S. Güldal and A. R. Boccaccini, “A review of the biological response to ionic dissolution products from bioactive glasses and glass-ceramics,” *Biomaterials*, 2011, 32(11): 2757–2774.

[7] T. Kasuga, “Bioactive calcium pyrophosphate glasses and glass-ceramics,” *Acta Biomater.*, 2005, 1(1): 55–64.

[8] M. A. G. Corchón, M. Salvado, B. J. Torre, F. Collía, J. A. Pedro, B. Vázquez and J. S. Román, “Injectable and self-curing composites of acrylic/bioactive glass and drug systems, A histomorphometric analysis of the behaviour in rabbits,” *Biomaterials*, 2006, 27(9): 1778–1787.

[9] S. Shinzato, T. Nakamura, T. Kokubo and Y. Kitamura, “A new bioactive bone cement: Effect of glass bead filler content on mechanical and biological properties,” *J. Biomed. Mater. Res.*, 2001, 54(4): 491–500.

[10] T. Kokubo and H. Takadama, “How useful is SBF in predicting in vivo bone bioactivity?,” *Biomaterials*, 2006, 27(15): 2097–2915.

[11] T. Kokubo, H. M. Kim and M. Kawashita, “Novel bioactive materials with different mechanical properties,” *Biomaterials*, 2003, 24(13): 2161–2175.

[12] P. Li, C. Ohtsuki, T. Kokubo, K. Nakanishi, N. Soga and K. Groot, "The role of hydrated silica, titania, and alumina in inducing apatite on implants," *J. Biomed. Mater. Res. A*, 1994, 24(1): 7–15.

[13] T. Kokubo, "Design of bioactive bone substitutes based on biomineralization process," *Mater. Sci. Eng. C*, 2005, 25(2): 97–104.

[14] T. Miyazaki, C. Ohtsuki, Y. Akioka, M. Tanihara, J. Nakao, Y. Sakaguchi and S. Konagaya, "Apatite Deposition on Polyamide Films Containing Carboxyl Group in a Biomimetic Solution," *J. Mater. Sci. Mater. Med.*, 2003, 14(7): 569–574.

[15] M. Kawashita, M. Nakao, M. Minoda, H. M. Kim, T. Beppu, T. Miyamoto, T. Kokubo and T. Nakamura, "Apatite-forming ability of carboxyl group-containing polymer gels in a simulated body fluid," *Biomaterials*, 2003, 24(14): 2477–2484.

[16] M. Tanahashi and T. Matsuda, "Surface functional group dependence on apatite formation on self-assembled monolayers in a simulated body fluid," *J. Biomed. Mater. Res.*, 1997, 34(3): 305–315.

[17] A. Mori, C. Ohtsuki, A. Sugino, K. Kuramoto, T. Miyazaki, M. Tanihara and A. Osaka, "Bioactive PMMA-Based Bone Cement Modified with Methacryloxypropyltrimethoxysilane and Calcium Salts --Effects of Calcium Salts on Apatite-Forming Ability--," *J. Ceram. Soc. Jpn.*, 2003, 111(10): 739–742.

[18] ISO. "International standard 5833/2: Implants for surgery-acrylic resin cements," orthopaedic application; 1992.

[19] T. Kokubo, S. Ito, Z. T. Huang, T. Hayashi, S. Sakka, T. Kitsugi, and T. Yamamuro, "Ca, P-rich layer formed on high-strength bioactive glass-ceramic A-W," *J. Biomed. Mater. Res. A*, 1990, 24(3): 331–343.

[20] ISO. "International standard 5833/2: Implants for surgery-acrylic resin cements," orthopaedic application; 1992.

[21] L. M. Alonso, J. Á. D. García-Menocal, M. T. Aymerich, J. Á. Á. Guichard, M. García-Vallés, S. M. Manent and M. Ginebra, "Calcium phosphate glasses: Silanation process and effect on the bioactivity behavior of glass-PMMA composites," *J. Biomed. Mater. Res. B*, 2014, 102(2): 205–213.

[22] C. Wolf-Brandstetter, S. Roessler, S. Storch, U. Hempel, U. Gbureck, B. Nies, S. Bierbaum and D. Scharnweber, "Physicochemical and cell biological characterization of PMMA bone cements modified with additives to increase bioactivity," *J. Biomed. Mater. Res. B*, 2013, 101(4): 599–609.

[23] J. Tamura, K. Kawanabe, M. Kobayashi, T. Nakamura, T. Kokubo, S. Yoshihara and T. Shibuya, "Mechanical and biological properties of two types of bioactive bone cements containing MgO-CaO-SiO_2-P_2O_5-CaF_2 glass and glass-ceramic powder," *J. Biomed. Mater. Res. A*, 1996, 30(1): 85–94.

[24] D. Rentería-Zamarrón, D. A. Cortés-Hernández, L. Bretado-Aragón and W. Ortega-Lara, "Mechanical properties and apatite-forming ability of PMMA bone cements," *Mater. Des.*, 2009, 30(8): 3318–3324.

[25] A. Sugino, T. Miyazaki, G. Kawachi, K. Kikuta and C. Ohtsuki, "Relationship between apatite-forming ability and mechanical properties of bioactive PMMA-based bone cement modified with calcium salts and alkoxysilane," *J. Mater. Sci. Mater. Med.*, 2008, 19(3): 1399–1405.

Tables and Figures

Table 3-I-a. Detailed constituents in powder phase

CA	$\frac{\text{CA}}{\text{PMMA + CA}}$	Powder phase (mass ratio)		
		PMMA	CA	BPO
P00	0.00	0.971	0	0.029
5%	0.05	0.922	0.049	0.029
20%	0.20	0.777	0.194	0.029
35%	0.35	0.631	0.340	0.029
50%	0.50	0.486	0.485	0.029

CA: pre-heated calcium acetate $Ca(CH_3COO)_2$;

BPO: benzoyl peroxide;

Table 3-I-b. Detailed constituents in liquid phase

Pa2hme	$\frac{\text{Pa2hme}}{\text{MMA + Pa2hme}}$	Liquid phase (mass ratio)		
		MMA	Pa2hme	DmpT
L00	0.00	0.496	0	0.004
30#	0.30	0.347	0.149	0.004
50#	0.50	0.248	0.248	0.004

Pa2hme: Phosphoric acid 2-hydroxyethyl methacrylate ester;

DmpT: N,N-dimethyl-p-toluidine;

Table 3-II-a. Setting time of the cements containing various contents of Pa2hme and $Ca(CH_3COO)_2$

Cement composition	Setting time (s)				
	P00	CA5%	CA20%	CA35%	CA50%
Pa2hme30#	∞	∞	215 ± 18	183 ± 16	200 ± 7
Pa2hme50#	∞	∞	∞	247 ± 6	192 ± 17

the reference sample "L00 + P00": 361 ± 25 (s);

∞: no heat release can be detected, viewed as an unset cement;

Table 3-II-b. Maximum temperature of the cements containing various contents of Pa2hme and $Ca(CH_3COO)_2$

Cement composition	Max. temperature (ºC)				
	P00	CA5%	CA20%	CA35%	CA50%
Pa2hme30#	✖	✖	75.2 ± 2.3	78.6 ± 2.7	75.6 ± 1.5
Pa2hme50#	✖	✖	✖	58.1 ± 3.0	60.6 ± 4.1

the reference sample "L00 + P00": 82.5 ± 2.4 ºC;

✖: no heat release can be detected from the thermo record;

Table 3-III. Functional groups presented in the spectra shown in Figure 3-4.

	Wavenumber (cm^{-1})	Combination	Functional groups
1	1723	C=O	Carbonyl C=O
2	1483	C-H	α-methyl (CH_3)
3	1280	C-H	α-methyl (CH_3)
4	1244	C-O	-**O**-**C**=O
5	1205	C-H	CH chains
6	1143	C-C	$C(CH_2)_n$ chains
7	1060	C-O	-**O**-**C**H_3
8	984	C=C	R**H**C=**C**H_2
9	843	C=O	R**C**=**O**OCH_3
10	752	C-H	-(CH_2)-

Table 3-IV. Apatite-forming ability of PMMA cements modified with various combinations of Pa2hme and $Ca(CH_3COO)_2$ in SBF environment, based on the XRD results[#] of designed soaking periods.

Cement composition	Apatite-forming period (d)				
	P00	CA5%	CA20%	CA35%	CA50%
Pa2hme30#	–	–		+	++
Pa2hme50#	–	–	–	–	–

[#]–: Apatite was not found after 14 days;

+: apatite was formed within 14 days;

++: apatite was formed within 3 days;

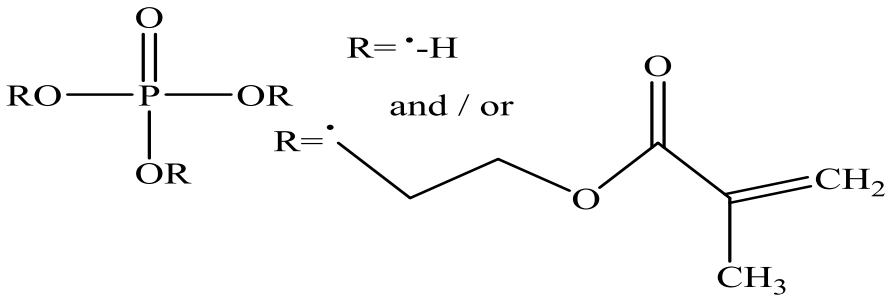

Figure 3-1. Chemical structure of Phosphoric acid 2-hydroxyethyl methacrylate ester (Pa2hme).

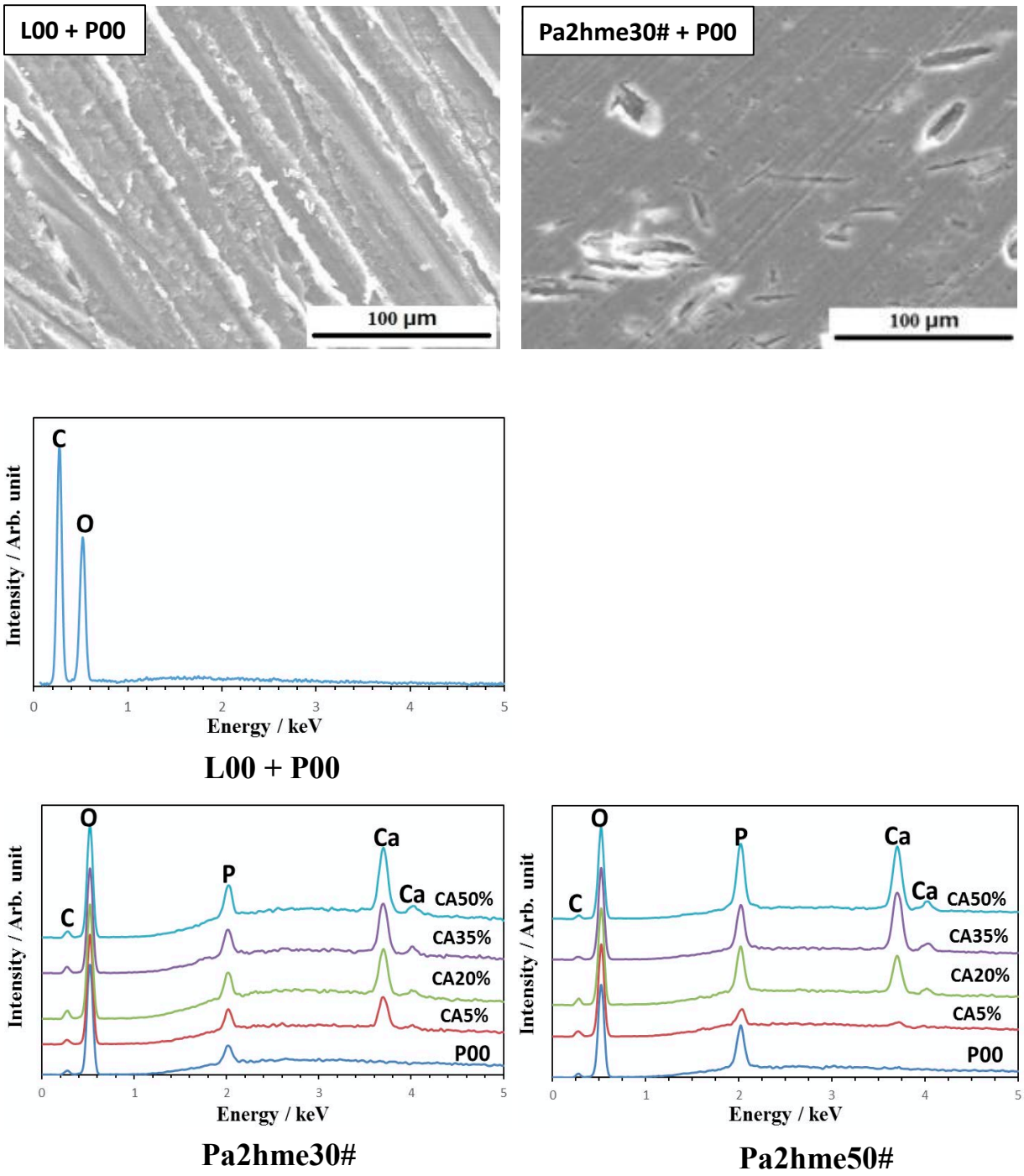

Figure 3-2. Representative SEM images of the sample: L00 + P00 and Pa2hme30# + P00; EDX spectra of the cements prepared by L00 + P00, Pa2hme30# and Pa2hme50# with various contents of $Ca(CH_3COO)_2$ before SBF soaking.

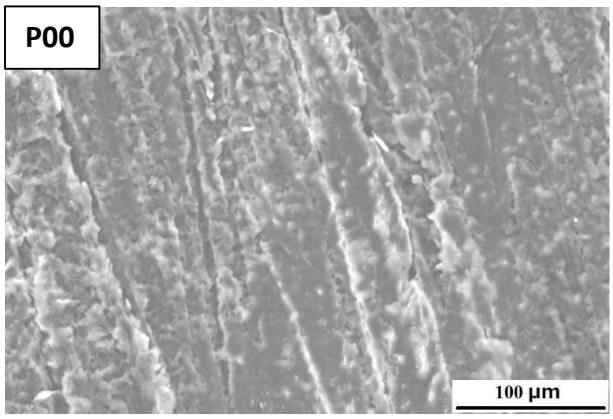

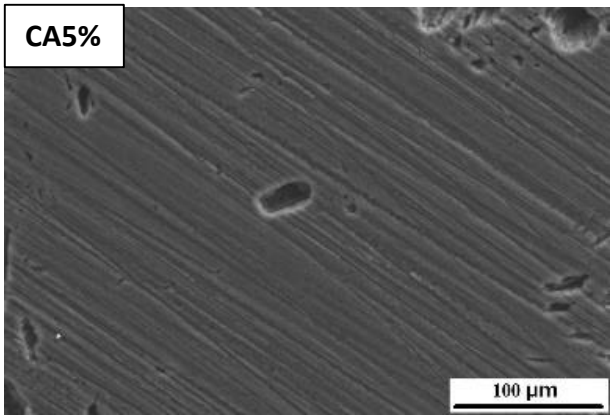

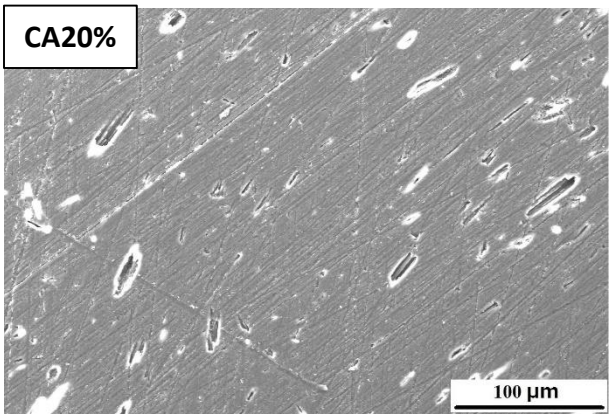

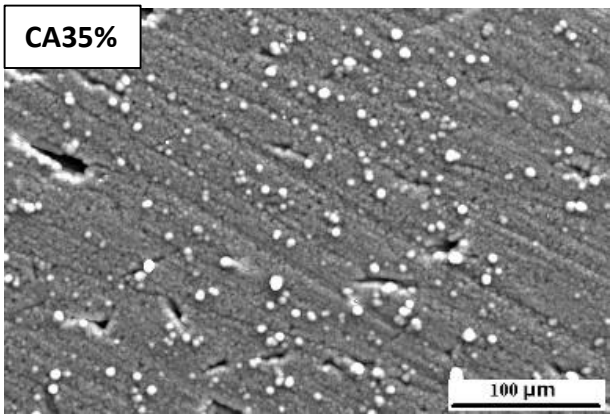

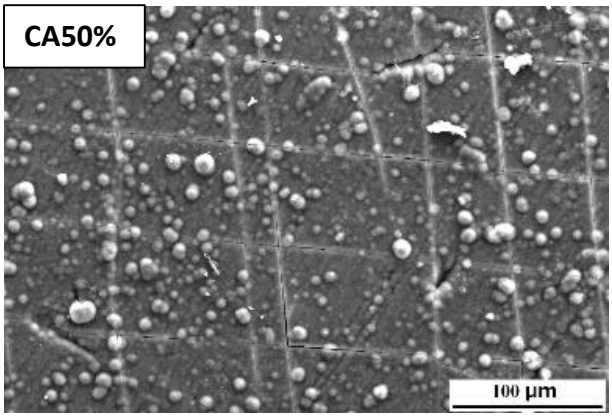

Pa2hme30#

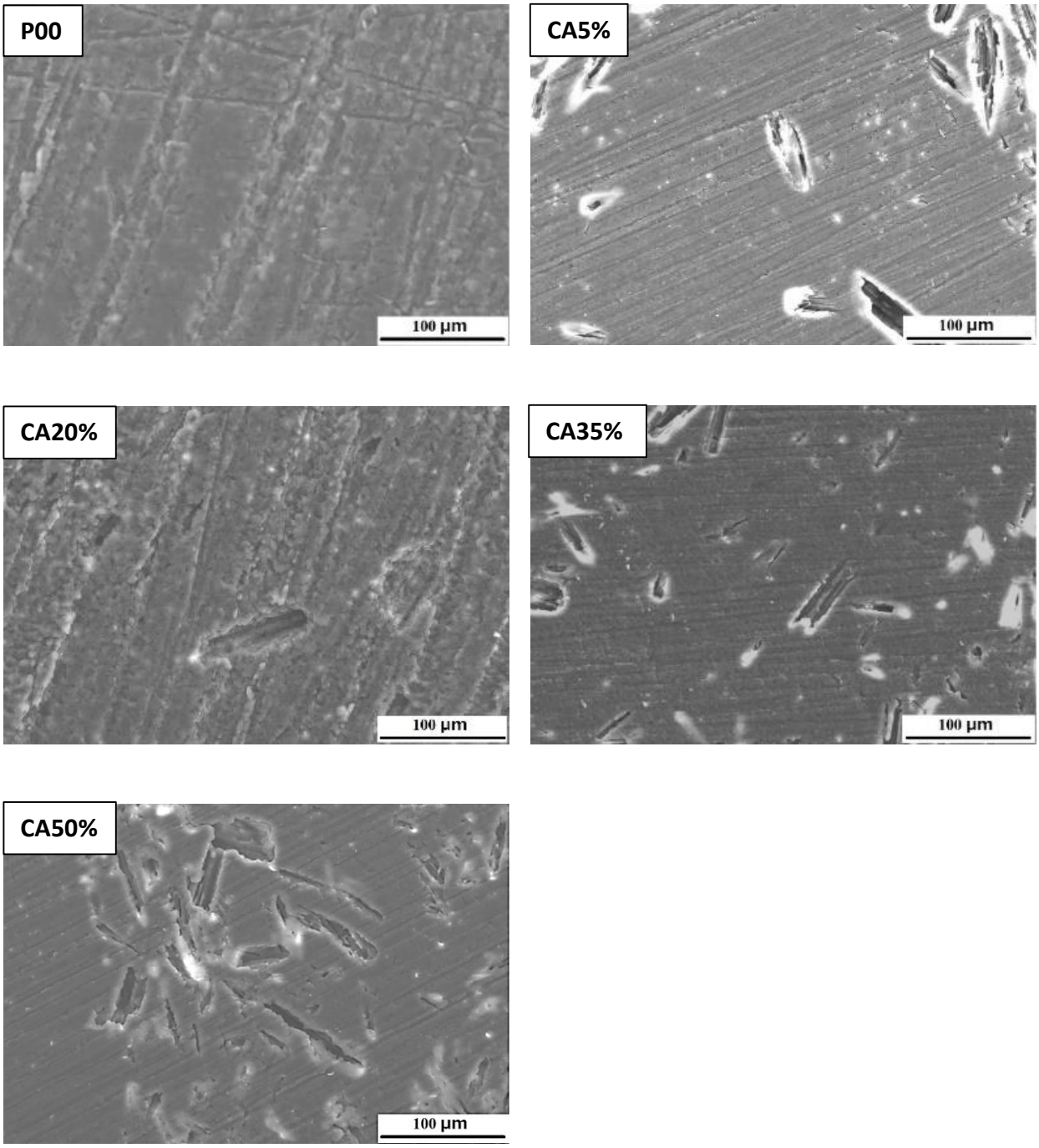

Pa2hme50#

Figure 3-3. Surface SEM images of the cements prepared by Pa2hme30# and Pa2hme50# with various contents of $Ca(CH_3COO)_2$ after soaking in SBF for 14 days.

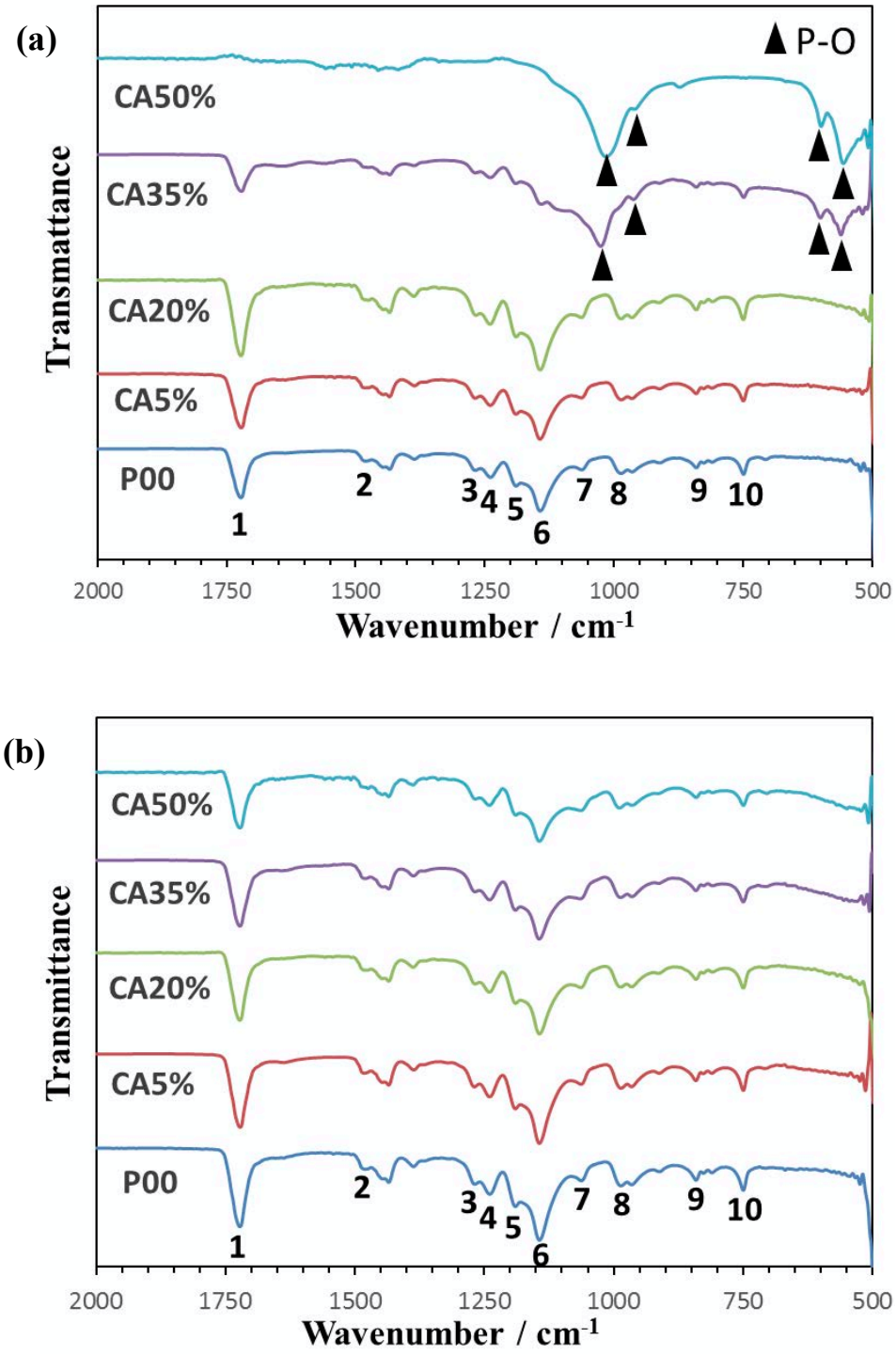

Figure 3-4. FT-IR spectra of the cements prepared by (a) Pa2hme30# and (b) Pa2hme50# with various contents of $Ca(CH_3COO)_2$ after soaking in SBF for 14 days.

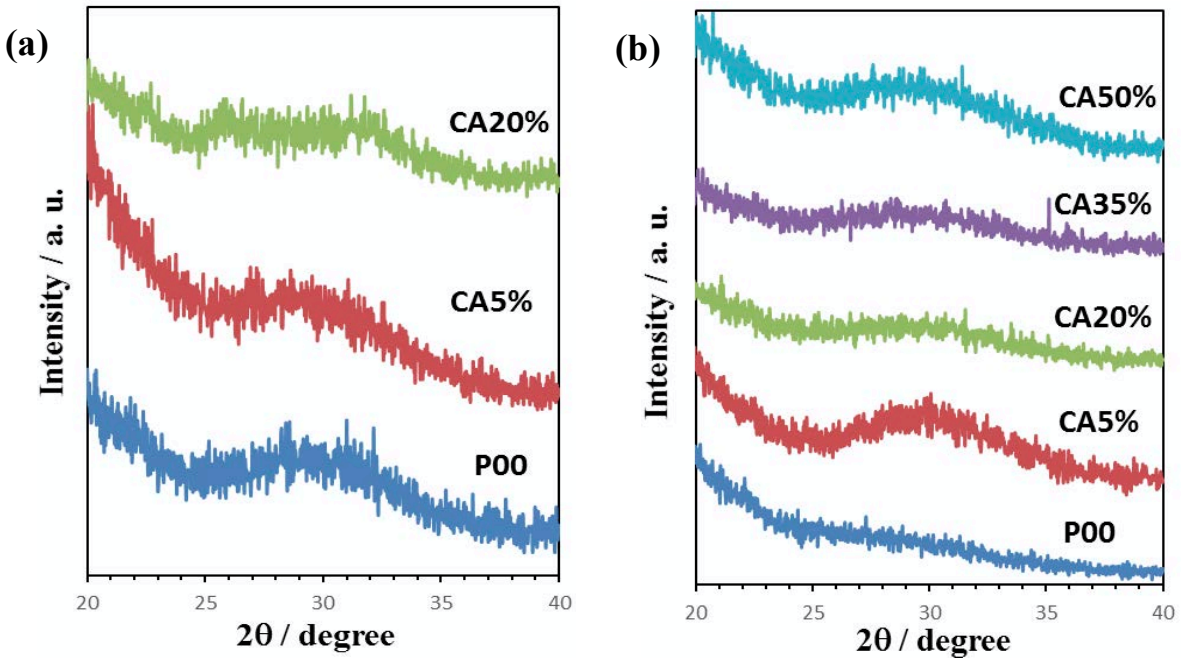

Figure 3-5-a. TF-XRD patterns of the surfaces of the cements prepared by (a) Pa2hme30# and (b) Pa2hme50# with different contents of $Ca(CH_3COO)_2$ after 14 days soaking in SBF.

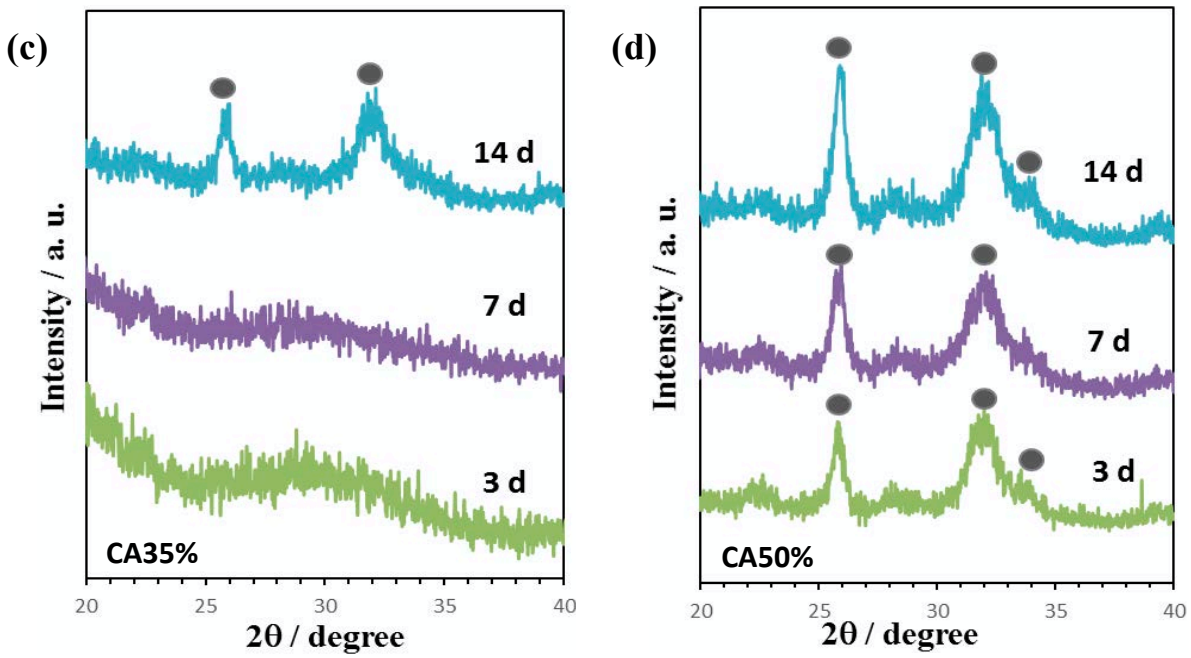

Figure 3-5-b. TF-XRD patterns of the surfaces of Pa2hme30# series cements combined with (c) CA35% and (d) CA50% after soaking in SBF for designed intervals.

Black circle (•): Apatite.

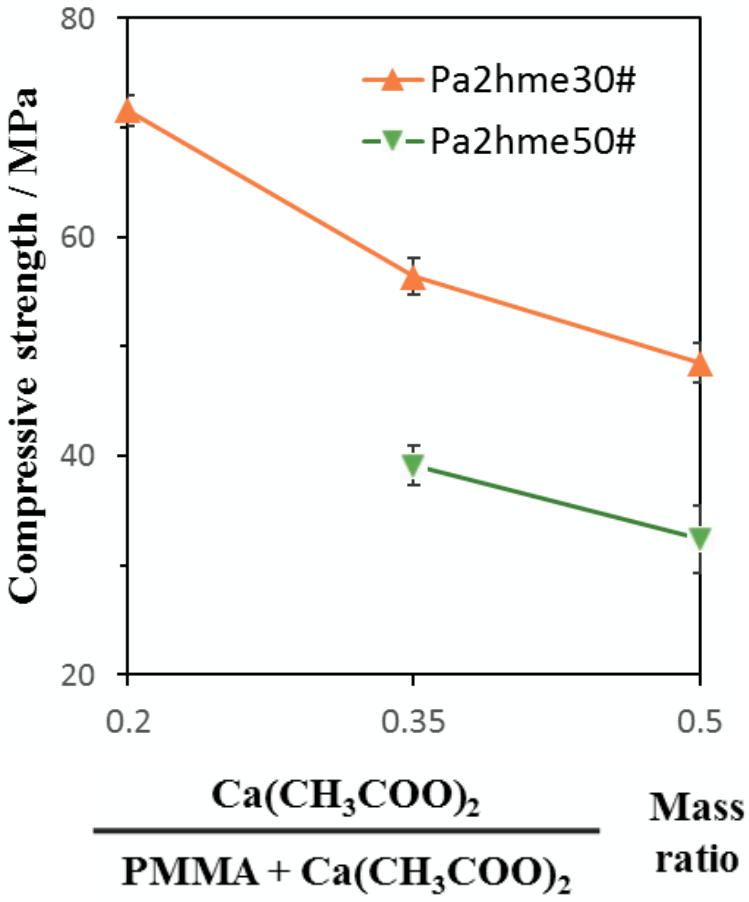

the reference sample “L00 + P00”: 96.9 ± 7.2 MPa;

Figure 3-6. Variations in compressive strength of the cements as a function of the contents of $Ca(CH_3COO)_2$ and Pa2hme after soaking in SBF for 7days.

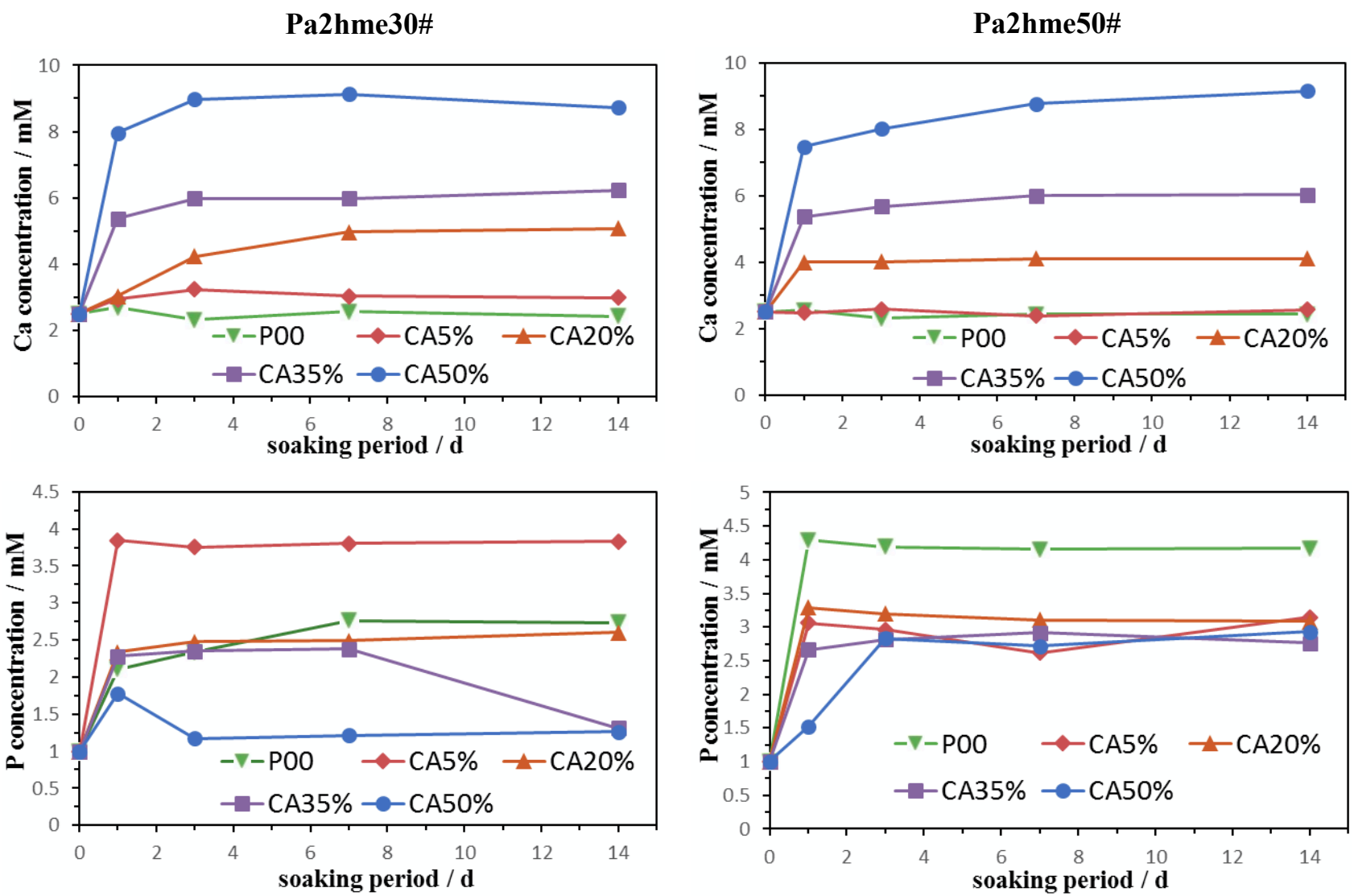

Figure 3-7. Concentrations of Ca and P in remaining SBF after soaking the modified cements over the designed intervals. Left and right parts are Pa2hme30# series cements and Pa2hme50# series cements, respectively.

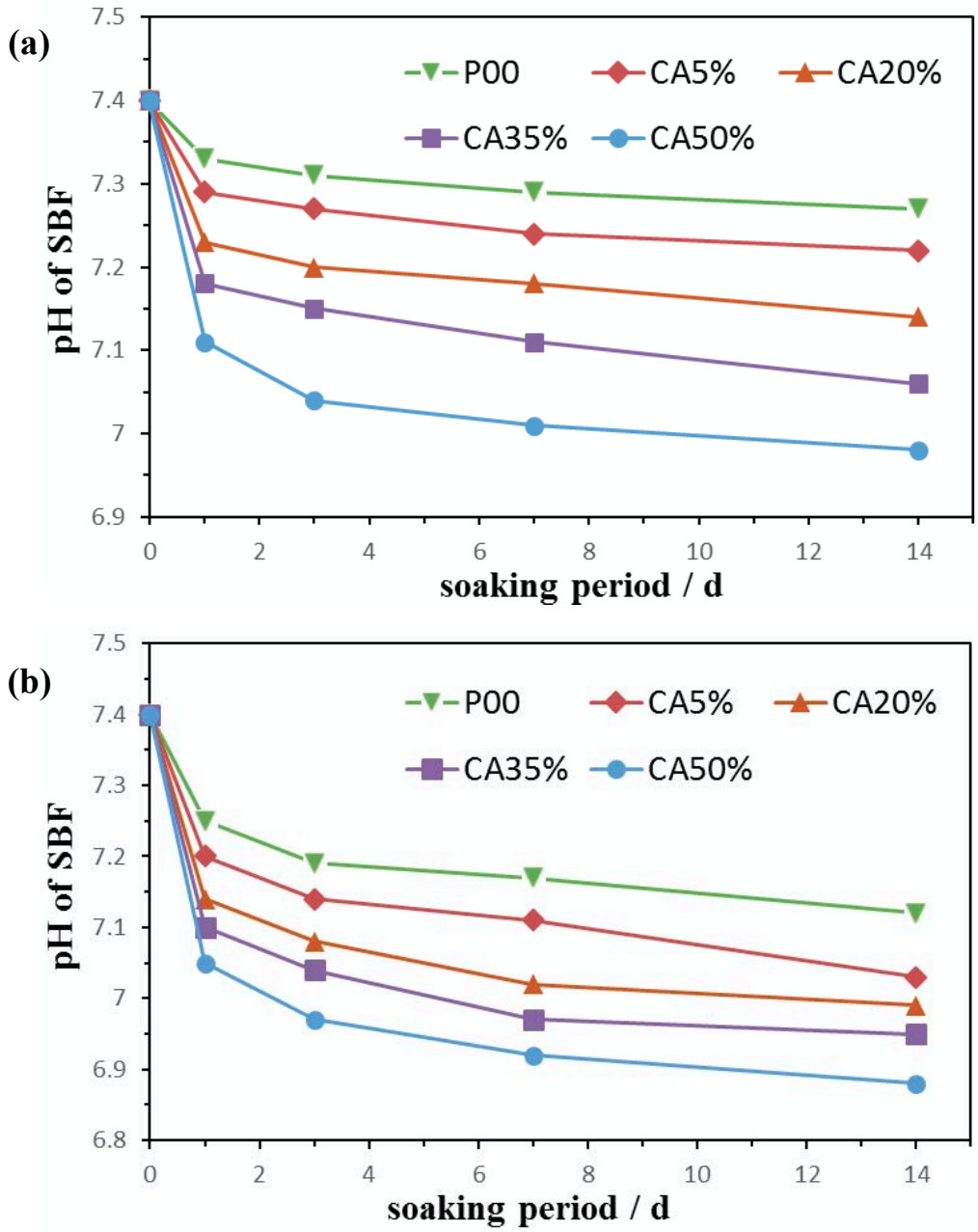

Figure 3-8. pH values of SBF measured at 37 ºC, after soaking the cements prepared by (a) Pa2hme30# and (b) Pa2hme50# combined with various contents of $Ca(CH_3COO)_2$ over the designed intervals.

Chapter 4

MODIFICATION OF CALCIUM ACETATE AND BIS [2-(METHACRYLOYLOXY) ETHYL] PHOSPHATE TO PROVIDE PMMA BONE CEMENT WITH BIOACTIVITY IN SIMULATED BODY ENVIRONMENT

1. Introduction

Bone cement prepared by polymethylmethacrylate (PMMA) powder and methylacrylate (MMA) liquid has been utilized as one kind of artifacts to anchor joint replacements to bone [1]. However, the cement itself lacks the capability of directly bonding to the living bone, once implanted into bone defects, PMMA cement will be encapsulated by fibrous tissue due to the normal physiological reaction to protect human body from foreign substance [2], and the isolation from surrounding bone may make bone cement lose its fixation function after long-term implantation [3]. To overcome this problem, it is necessary to equip PMMA bone cement with bone-bonding ability, i.e. bioactivity [4].

Successful adhesion to bone through generating apatite layer on their surfaces has been found on so-called "bioactive ceramics" [5], so incorporation such biomaterials like Bioglass [6], sintered hydroxyapatite ($Ca_{10}(PO_4)_6(OH)_2$) [7, 8] or wollastonite ($CaSiO_3$) [9] into PMMA cements has gained a fixed connection with bone after implanted into body environment. In addition, apatite nucleation process on bioactive materials in simulated body fluid disclosed that: the functional groups such as Si-OH [10], Ti-OH [11], -COOH [12, 13], and PO_4H_2 [14] plus Ca^{2+} ions could induce the apatite formation. In bone cement case, apatite deposited on cement surface has been realized by the modification of Si-OH groups and calcium chloride [15], now incorporation of phosphate (PO_4H_2) groups and calcium acetate has been under research.

In chapter 3, modification with calcium acetate and phosphoric acid 2-hydroxyethyl methacrylate ester (Pa2hme) has equipped PMMA cement with apatite-forming ability in simulated body fluid (SBF), but the deterioration in compressive strength caused bioactive PMMA cement failed to meet the standard of clinic application, and the strength was unable to be enhanced by reducing the amount of Pa2hme due to its dissolution limitation in MMA.

In this study, formation of a bioactive surface on PMMA cement was attempted by the modification of a new phosphate (PO_4H_2) groups containing additive Bis [2-(methacryloyloxy) ethyl] phosphate (BisP) combined with calcium acetate. BisP could be mixed with MMA at a low proportion, which created a possibility to enhance the properties required by ISO5833, its chemical structure was shown in **Figure 4-1**. Except the same investigations in chapter 3, the role of each additive on apatite formation was examined, the optimization related to the contents of both additives was explored and the performances of BisP and Pa2hme on apatite formation, setting and mechanical strength were compared.

2. Experimental

PMMA powders and pre-treatment to calcium acetate monohydrate ($Ca(CH_3COO)_2 \cdot H_2O$) was the same as described in chapter 3.

2.1. Preparation of PMMA cements

The sources for PMMA cement preparation were divided into two parts: the powder source, PMMA powders were mixed with the pre-treated $Ca(CH_3COO)_2$ powders combined with a polymerization initiator benzoyl peroxide (BPO, Wako Chemical Industries, Osaka, Japan); the liquid source, a mixture consisted of MMA liquid (Wako Chemical industries, Osaka, Japan), the monomer BisP (Aldrich, Tokyo, USA) and N,N-dimethyl-p-toluidine (DmpT, Wako Chemical Industries, Osaka, Japan) as a polymerization accelerator. All details about the powder and liquid

sources were listed in **Table 4-I-a and Table 4-I-b,** respectively. The mixing ratio of powder/liquid (P/L) was 1: 0.5, g/g; and the preparation process was maintained at 23 ± 2 ºC.

2.2. Measurement of setting time and maximum temperature

The mixed paste was used for the determination of setting time and maximum temperature. A thermocouple probe (plamic 100 Ω) connecting to the thermo record (TR-81, T&D corp., Matsumoto-shi, Japan) was installed into the center of the paste to test the curing temperature per second, until the temperature reached its peak. Setting time was defined as the time corresponding to $(T_{max} + T_{start.})/2$ (T_{max}: Maximum temperature, T_{start}: Temperature at starting of mixing) on the temperature/time curve according to ISO 5833. The tests were repeated four times for each combination. All the setting times and maximum temperatures are presented as mean ± SD (Standard Deviation).

2.3. Bioactivity evaluation in simulated body fluid

Bioactivity could be evaluated by the formation of apatite on cement surface in simulated body environment. The cements polished by #1000 SiC paper were cut into a rectangular pieces with dimensions of 10 × 15 × 1 mm^3 then stored in the plastic containers filled with 35mL SBF at 37 ºC. After soaking for designed intervals (1, 3, 7 and 14 days), all cements were removed, rinsed and dried at room temperature.

2.4. Mechanical measurement

Cylindrical samples with 6 mm in diameter and 12 mm in height were utilized for compressive strength measurement. All specimens before completely hardened were immersed in SBF at 37 ºC for 7 days and subsequently compressed by a compressive load with a crosshead speed of 20 mm/min controlled by an Universal Testing Machine (Autograph AG-1, Shimadzu

Co., Kyoto, Japan) until fracture happened. Compressive strength was calculated by the fracture load and sample's cross-sectional area. The averages and their standard deviations were collected from ten specimens for each combination.

2.5. Characterization

Surface morphological changes of cements before and after immersion in SBF were examined by scanning electron microscope (SEM; S-3500N, Hitachi High-Technologies, Tokyo, Japan) combined with energy-dispersive X-ray microanalyzer (EDX; EMAX Energy, Horiba Ltd., Kyoto, Japan) after sputter coating a thin film of carbon on them. Thin-film X-ray diffractometer (TF-XRD; MXP3V, MAC Science Ltd., Yokohama, Japan) and Fourier-transformed-infrared spectrometer (FT-IR; FT/IR6100, Jasco Analytical Instruments, Tokyo, Japan) were employed to examine structural changes on cement surfaces, all samples were scanned from 20 to 40º in 2θ and wavenumber was ranged from 500 to 2000 cm^{-1}. pH meter (F-23IIC, Horiba Ltd., Kyoto, Japan) was introduced to detect pH values of the SBF after soaking cements for designed periods, the concentrations of Ca and P in SBF under the same periods were also measured by Inductively Coupled Plasma-optical Emission Spectrometry (ICP-OES; Optima 4300 DV, PerkinElmer, Inc., America).

3. Results

3.1. Setting behavior

It should be noted that the sample "BisP50 + P00" failed to become a paste state at mixing stage. In the combination of BisP and $Ca(CH_3COO)_2$, samples without heating release were restricted to the ones of "P00" (without $Ca(CH_3COO)_2$), "BisP30# + CA5%" and "BisP50# + CA5%", they were only suitable for bioactivity evaluation.

Table 4-II-a and Table 4-II-b lists setting times and maximum temperatures of all cements modified with both additives under various contents, respectively. It is clear to see that adding $Ca(CH_3COO)_2$ alone delayed the setting, and adding BisP alone delayed the polymerization reaction to the extreme level just like Pa2hme. Except the sample "Bis10# + CA35%" and "Bis10# + CA50%", the combinations of $Ca(CH_3COO)_2$ and BisP led to an accelerated setting compared to the reference "L00 + P00". Once the mass ratios of $Ca(CH_3COO)_2$/BisP were close to the powder/liquid ratio (2: 1), the corresponding cements owned the shortest times, and these shortest setting times decreased with the increase of both additives. Both increases or decreases in the amounts of $Ca(CH_3COO)_2$ prolonged the setting based on this ratio under the same contents of BisP, which was consistent with results obtained from the Pa2hme-modified cements. The combination of $Ca(CH_3COO)_2$ and BisP led to a more complicated results on maximum temperatures, expect Bis30# series, the samples modified with $Ca(CH_3COO)_2$ and BisP whose mass ratios were closed to the mixing ratio (2: 1) still acquired the highest temperatures, the highest temperatures decreased following the increase of both additives.

3.2. Characterization of apatite formation

Figure 4-2 displays the typical morphologies and elements distribution on the surfaces of cements modified with the combination of $Ca(CH_3COO)_2$ and BisP under various contents before soaking in SBF by SEM observation combined with EDX spectra. Except the holes (created by mixing) and scratches, nothing was observed on SEM images. And the element Ca and P detected on EDX spectra indicated that $Ca(CH_3COO)_2$ and BisP had been prosperously incorporated into the cements. Their peak intensities were increased with increase in both additive contents. This tendency was more obviously perceived in element Ca than P.

The SEM photographs shown in **Figure 4-3** are the surface morphologies of cements prepared by (a) L00; (b) BisP10#; (c) BisP20#; (d) BisP30# and (e) BisP50# with various contents

of $Ca(CH_3COO)_2$ after soaking in SBF for 14 days, respectively. The possibility to observe the deposition of spherical particles on cement surfaces was based on the additives in various amounts of combination, only adding BisP without any $Ca(CH_3COO)_2$ had no potential to induce the particles deposited on cement surfaces, increasing BisP contents delayed the precipitation period under the same content of $Ca(CH_3COO)_2$, BisP50# series cements maintained the same morphology features as the original ones even after soaking for 14 days. In contract, although adding $Ca(CH_3COO)_2$ alone could make the particles depositing, the deposits agglomerated into larger particles instead of individual spherical particle due to lacking of the effect of BisP. This was supported by the comparison between samples "L00 + CA20%" and "BisP20# + CA20%". Namely, increases in the content of $Ca(CH_3COO)_2$ shortened the precipitation period under the same content of BisP, and high content such as 50 mass% of $Ca(CH_3COO)_2$ caused an obvious decrease in diameter of these deposited particles.

Figure 4-4 shows the FT-IR spectra of all specimens modified with the combinations of $Ca(CH_3COO)_2$ and BisP under various contents after soaking in SBF for 14 days. The wavenumbers and corresponding functional groups of these characteristic peaks marked with numbers were referred from **Table 3-III** in chapter 3, the overlapping of peaks caused the characteristic peaks of BisP and $Ca(CH_3COO)_2$ were hard to be detected on all modified samples, all number-marked peaks were identified as the characteristics of PMMA. In addition, the peaks marked by triangular symbol at around 550, 600, 950 and 1020 cm^{-1} were determined to P–O stretching in the mode of ν_4, ν_1, and ν_3 vibration, based on the results and findings of FT-IR spectra in chapter 3, phosphate radical (PO_4^{3-}) derived from the deposited microspheres supplied these triangular symbol marked peaks. In BisP case, the FT-IR spectra showed different results compared with the SEM observation, for example: although the deposited particles were found on the surface of cement "BisP10% + CA5%", the FT-TR peaks belonging to these particles weren't

detected on corresponding spectra. Moreover, FT-IR spectra of sample "L00 + CA5%" showed an intermediate state containing both peaks from the original cements (0 day) and the deposition.

Figure 4-5 displays TF-XRD patterns of the cements prepared by (a) L00; (b) BisP10#; (c) BisP20# and (d) BisP30# with various contents of $Ca(CH_3COO)_2$ after soaking in SBF for designed periods (since 3 days), BisP50# series cements after soaking in SBF for 14 days. The peaks with low crystallinity appearing at about 26º, 32º, and 34º in 2θ were attributed to the diffractions of apatite according to the JCPDS Card No. 09-0432, so those spherical particles deposited on cement surface were identified as low-crystalline apatite. While the apatite deposition was failed on BisP50# series cements irrespective of $Ca(CH_3COO)_2$ contents, they still sustained the amorphous state even after soaking in SBF for 14 days.

On the basis of TF-XRD results, the judgment with regard to apatite-forming ability of all cements modified with $Ca(CH_3COO)_2$ and BisP is listed on **Table 4-III**. It could be noted that apatite forming period varied from 1 to 14 days depending on the combinations of $Ca(CH_3COO)_2$ and BisP. Increase in amount of $Ca(CH_3COO)_2$ accelerated the formation rate of apatite. On the other hand, BisP shared the same role as Pa2hme. Namely, increase in its content rather prolonged the induction period of apatite formation.

3.3. Variation in compressive strength

The compressive strengths of cements modified with various contents of BisP and $Ca(CH_3COO)_2$ after soaking in SBF for 7 days is summarized in **Figure 4-6**. Under the same content of $Ca(CH_3COO)_2$, BisP10# series cements owned the highest compressive strengths among all cements. On the other hand, under the same content of BisP, adding 5 mass% of $Ca(CH_3COO)_2$ provided the highest strengths than other additive amounts. The maximum value was 108.5 ± 2.7 MPa (sample "BisP10# + CA5%") exceeded that of SBF-soaked reference. Starting from the highest strengths, any increases in both contents of additives produced a decline

in compressive strength, when the amount of $Ca(CH_3COO)_2$ was increased to 50 mass%, all cements failed to meet the lower limit of ISO 5833.

3.4. Changes in the concentrations of Ca and P and corresponding pH in cement-soaked SBF

Figure 4-7 exhibits the pH of SBF measured at 37 ºC after all modified cements immersion under various intervals. The corresponding changes in the concentrations of Ca and P of the same SBF are shown in **Figure 4-8.** In most cases, extending the soaking period led to the continuous drop of pH, but in the low contents of BisP (0 mass% or 10 mass%), appropriate $Ca(CH_3COO)_2$ (5 mass% or 20 mass%) boosted the pH within 3 days of soaking. It was assumed that hydrolysis of acetate ions (CH_3COO^-) provided OH^-. Higher contents of both additives brought deeper drop of pH in the first soaking period. Among all modified cements, the increase of Ca concentration was continues irrespective of the formation of apatite, and Ca content and released speed were enhanced with the increases in $Ca(CH_3COO)_2$ contents, as seen in the cements prepared by CA35% and CA50%. In L00 series cements, without any addition of phosphate-containing BisP, the concentrations of P decreased with the increase in soaking period. The decline in P content was ascribed to the consumption on apatite deposition, and its drop tendencies were accordance with the formation timing of apatite observed on SEM photographs. Even if apatite was not formed on cement surface after 14 days of soaking, the concentration of P was increased, and the rapid increase was finished within 3 days.

4. Discussions

Setting behavior of all modified cements showed the following tendency. Compared with the reference “P00 + L00”, addition of $Ca(CH_3COO)_2$ without any BisP prolonged the setting, and adding BisP alone also delayed the radical polymerization to an extreme level similar to Pa2hme. On the contrary, it is noted that adding both of them led to the acceleration of setting in most

specimens (except sample “BisP10# + CA35%” and “BisP10# + CA50%”). In particular, the shortest setting time were obtained under each liquid phase when the mass ratios of $Ca(CH_3COO)_2$/BisP were close to the powder/liquid mixing ratio (2: 1).

Based on the results summarized above, one possible explanation was that the delay effort brought by both sides had counteracted with each other on this critical mass ratio, the initiator/accelerator BPO/DmpT only worked on the rest of PMMA/MMA. Therefore the setting times of the cements prepared under this critical mass ratio of $Ca(CH_3COO)_2$/BisP became more and more shorter when the contents of both additives were increased. Comparison between both additives, no heating release could be captured from the modification combination of BisP with high content (50#) and $Ca(CH_3COO)_2$ with low content (5 mass% or 20 mass%). This implied that BisP showed deeper influence than $Ca(CH_3COO)_2$ in affecting the setting behavior of modified cements.

PMMA bone cement modified with $Ca(CH_3COO)_2$ and phosphate group-containing BisP owned the apatite-forming ability in simulated body environment. Incorporation of $Ca(CH_3COO)_2$ alone could induce the apatite nucleation on cement surface, but the nucleation were restricted to sites where $Ca(CH_3COO)_2$ could be exposed to SBF, meanwhile, the apatite deposits agglomerated into larger particles and grew along the longitudinal direction, while apatite deposits appeared on the surface of cement modified with BisP were individual spherical particles. So the generation of a bioactive layer consisting of individual spherical apatite relied on the coaction of the phosphate (PO_4H_2) groups in the structure of BisP and calcium acetate. The function of phosphate (PO_4H_2) groups was the same as that of Si-OH groups described in chapter 3. The incorporated functional groups on cement surface were beneficial to initiate heterogeneous nucleation of apatite, and the increase in BisP content might prompt more phosphate groups (PO_4H_2) exposed to the cement surface. Continuous hydrolysis of $Ca(CH_3COO)_2$ boosted the amounts of Ca^{2+} ions upon cement surface, leading to an increased supersaturation degree with respect to apatite, which resulted in

the apatite precipitation. Therefore, more Ca^{2+} ions released from modified cement shortened the apatite-forming period, which could be confirmed from **Table 4-III**. In contrast, more BisP incorporated into cements didn't improve the apatite-forming ability.

Based on the surface composition of initial cement (0 day), pH values and the concentrations of Ca and P in SBF environment under designed periods, the possible reason to discuss the variation of apatite-forming period based on various contents of combinations of $Ca(CH_3COO)_2$ and BisP could be concluded as follows: $Ca(CH_3COO)_2$ or BisP incorporated into the cement evoked a damage to the dense structure of PMMA cement, both additives were liable to release into SBF, but their release rate varied. Taking BisP10# series cements as the example, the rapid increase of Ca concentration was finished within 7 days even in the samples with 35 mass% or 50 mass% of $Ca(CH_3COO)_2$, while the rapid increase of P concentration was finished within 1 day (seen the sample prepared by P00 or CA5%). The rapid rising of P content meant that plenty of PO_4H_2 groups stepped into SBF, cement surface without functional groups was hard to attract Ca^{2+} ions from SBF, only relied on the Ca^{2+} ions released from the dissolution of $Ca(CH_3COO)_2$ to achieve the formation of apatite in terms of increasing the supersaturation of apatite. Therefore, at low contents of BisP (10#), apatite could be deposited on the specimen modified with low contents (5 mass%) of $Ca(CH_3COO)_2$, but when BisP contents were increased to 30 mass% or 50 mass%, increased amount of PO_4^{3-} created more difficult situation to attract Ca^{2+} ions, therefore low release amount of Ca^{2+} ions from CA5% failed to induce the precipitation of apatite. In addition, except the issue of BisP leaking, the drop of pH was also responsible for the failure in inducing apatite formation.

Based on the relationship of the variation in the concentrations of Ca and P and pH values, the rapid release stage of both ions was in accordance with the period of drastic decrease in pH. It is speculated that the drop of pH rooted from acetate ions (CH_3COO^-) and phosphate (PO_4H_2) groups discharging into SBF, and increasing the contents of BisP and $Ca(CH_3COO)_2$ brought more

serious decrease in pH especially in 1 day of soaking. For BisP50# series cements, the possibility to obtain apatite deposition relied on high contents of $Ca(CH_3COO)_2$ such as 35 mass% or 50 mass%, but abundant release of both additives produced a low pH environment, and a sustained decline of pH further lowered the condition for apatite precipitation. For example, in the cement "BisP50# + CA35%", the concentration of P showed almost the same as the initial SBF, and no apatite was found on cement surface even after 14 days soaking. One possibility for this phenomenon is that although the release of PO_4H_2 groups in BisP structure was balanced with the consumption part on apatite formation, apatite was deposited on the inner wall instead of the cement surface.

The tendency of apatite-forming ability in the combination of BisP and $Ca(CH_3COO)_2$ suggested that: the extension in BisP content delayed the apatite-forming period. And the SEM micrographs manifested that phosphate-containing BisP distributed on cement surface were beneficial to initiate heterogeneous nucleation of apatite. A better bonding to living bone required apatite grew into a layer without redundant invalid space. In my research, incorporating BisP into PMMA cement could obtain apatite layer consisting of individual spherical particles, but its contents should be adjusted to a lower range (10 mass% or 20 mass%) to shorten the apatite-forming period.

The decline law on compressive strength could be also found from the cement modified with BisP and $Ca(CH_3COO)_2$. In view of the discussion in chapter 3, one method to improve the mechanical strength is decreasing the contents of both additives, low contents modification not only reduced the strength loss from the replaced part of PMMA, but also decreased the release from both additives during soaking period. Unlike Pa2hme, BisP could be successfully mixed with MMA at the low contents (10# or 20#), and combining with low contents (5 mass% or 20 mass%) of $Ca(CH_3COO)_2$ didn't interrupt the setting process, therefore, the loss on compressive strength was improved, even the compressive strength of some specimens, for example "BisP10# and

CA5%" or "BisP10# and CA20%" exceeded that of the reference (P00 and L00), the enhancement were attributed to utilization rate of BPO/Dmpt to rest of PMMA/MMA and the decrease of bubbles generated at the mixing stage.

Consequently, when the tendency on apatite-forming period, the variations in compressive strength and the law in setting times were taken into consideration, the optimized modification plan in the combination of BisP and $Ca(CH_3COO)_2$ for PMMA bone cement was 10 mass% of BisP in liquid combined with 20 mass% of $Ca(CH_3COO)_2$ in powder, under this condition, the modified cement owned 314 ± 4 s of setting time and 99.1 ± 3.5 MPa of compressive strength, both exceeded the lower limit of ISO 5833, and the deposition of apatite on cement surface could be observed within 3 days soaking in SBF.

5. Conclusions

Modification with phosphate-containing BisP and $Ca(CH_3COO)_2$ can equip PMMA bone cement with bioactivity via the deposition of apatite on the cement surface in a simulated body environment: adding $Ca(CH_3COO)_2$ alone could prompt the formation of apatite, phosphate (PO_4H_2) groups distributed on cement surface were beneficial to the heterogeneous nucleation of apatite. Increasing the content of $Ca(CH_3COO)_2$ shortened the formation period of apatite, increasing the content of BisP led to an opposite result. Because fast setting was achieved at a ratio close to the mixing ratio of the powder/liquid (2: 1), prolonging the setting time could be realized by reducing the contents of both additives and avoiding this ratio mentioned above. The cement prepared by Bis10# and CA5% owned the top compressive strengths (108.5 ± 2.7 MPa), and the strength declined from this top value with the increase of both additives. In view of balancing apatite-forming period and other properties required by ISO 5833, the optimal modification is a combination of 10 mass% of BisP and 20 mass% of $Ca(CH_3COO)_2$.

References

[1] S. M. Kenny and M. Buggy, "Bone cements and fillers: A review," *J. Mater. Sci. Mater. Med.*, 2003, 14(11): 923–938.

[2] S. B. Goodman, J. Schatzker, G. Sumner-Smith, V. L. Fornasier, N. Goften and C. Hunt, "The effect of polymethylmethacrylate on bone: an experimental study," *Arch. Orthop. Trauma. Surg.*, 1985, 104(3): 150–154.

[3] S. L. Evans, C. M. Hunt and S. Ahuja, "Bone cement or bone substitute augmentation of pedicle screws improves pullout strength in posterior spinal fixation," *J. Mater. Sci. Mater. Med.*, 2002, 13(12): 1143–1145.

[4] C. Ohtsuki, T. Miyazaki and M. Tanihara, "Development of bioactive organic–inorganic hybrid for bone substitutes," *Mater. Sci. Eng. C*, 2002, 22(1): 27–34.

[5] W. P. Cao and L. L. Hench, "Bioactive materials," *Ceram. Int.*, 1996, 22(6): 493–507.

[6] K. Goto, J. Tamura, S. Shinzato, S. Fujibayashi, M. Hashimoto, M. Kawashita, T. Kokubo and T. Nakamura, "Bioactive bone cements containing nano-sized titania particles for use as bone substitutes," *Biomaterials*, 2005, 26(33): 6496–6505.

[7] G. X. Ni, K. Y. Chiu, W. W. Lu, Y. Wang, Y. G. Zhang, L. B. Hao, Z. Y. Li, W. M. Lam, S. B. Lu and K. D. K. Luk, "Strontium-containing hydroxyapatite bioactive bone cement in revision hip arthroplasty," *Biomaterials*, 2006, 27(24): 4348–4355.

[8] K. Ishihara, J. Arai, N. Nakabayashi, S. Morita and K. Furuya, "Adhesive bone cement containing hydroxyapatite particle as bone compatible filler," *J. Biomed. Mater. Res. A*, 1992, 26(7): 937-945.

[9] S. Shinzato, M. Kobayashi, W. F. Mousa, M. Kamimura, M. Neo, Y. Kitamura, T. Kokubo and T. Nakamura, "Bioactive polymethyl methacrylate-based bone cement: Comparison of glass beads, apatite- and wollastonite-containing glass-ceramic, and hydroxyapatite fillers on mechanical and biological properties," *J. Biomed. Mater. Res. A*, 2000, 51(2): 258–272.

[10] K. Tsuru, C. Ohtsuki, A. Osaka, T. Iwamoto and J. D. Mackenzie, “Bioactivity of sol–gel derived organically modified silicates: Part I: In vitro examination,” *J. Mater. Sci. Mater. Med.*, 1997, 8(3): 157–161.

[11] T. Kokubo, “Design of bioactive bone substitutes based on biomineralization process,” *Mater. Sci. Eng. C*, 2005, 25(2): 97–104.

[12] T. Miyazaki, C. Ohtsuki, Y. Akioka, M. Tanihara, J. Nakao, Y. Sakaguchi and S. Konagaya, “Apatite deposition on polyamide films containing carboxyl group in a biomimetic solution,” *J. Mater. Sci. Mater. Med.*, 2003, 14(7): 569–574.

[13] M. Y. Koh, C. Ohtsuki and T. Miyazaki, “Modification of Polyglutamic Acid with Silanol Groups and Calcium Salts to Induce Calcification in a Simulated Body Fluid,” *J. Biomater. Appl.*, 2011, 25(6): 581–594.

[14] M. Tanahashi and T. Matsuda, “Surface functional group dependence on apatite formation on self-assembled monolayers in a simulated body fluid,” *J. Biomed. Mater. Res.*, 1997, 34(3): 305–315.

[15] T. Miyazaki, C. Ohtsuki, M. Kyomoto, M. Tanihara, A. Mori and K. Kuramoto, “Bioactive PMMA bone cement prepared by modification with methacryloxypropyltrimethoxysilane and calcium chloride,” *J. Biomed. Mater. Res. A*, 67(4): 1417–1423.

Tables and Figures

Table 4-I-a. Detailed in powder components

CA	$\frac{CA}{PMMA + CA}$	Powder components (mass ratio)		
		PMMA	BPO	CA
P00	0.00	0.971	0.029	0
5%	0.05	0.922	0.029	0.049
20%	0.20	0.777	0.029	0.194
35%	0.35	0.631	0.029	0.340
50%	0.50	0.486	0.029	0.485

CA: pre-heated calcium acetate $Ca(CH_3COO)_2$;

BPO: benzoyl peroxide;

Table 4-I-a. Details in liquid components

BisP	$\frac{BisP}{MMA + BisP}$	Liquid components (mass ratio)		
		MMA	DmpT	BisP
L00	0.00	0.496	0.004	0
10#	0.10	0.446	0.004	0.050
20#	0.20	0.397	0.004	0.099
30#	0.30	0.347	0.004	0.149
50#	0.50	0.248	0.004	0.248

BisP: Bis [2-(methacryloyloxy) ethyl] phosphate;

DmpT: N, N-dimethyl-p-toluidine;

Table 4-II-a. Setting time of the cements prepared by various combinations of $Ca(CH_3COO)_2$ and BisP under various contents

Cement composition	Setting time (s)				
	P00	CA5%	CA20%	CA35%	CA50%
L00	361 ± 25	386 ± 30	431 ± 29	631 ± 25	826 ± 35
BisP10#	∞	294 ± 7	314 ± 4	365 ± 14	453 ± 5
BisP20#	∞	308 ± 10	194 ± 3	226 ± 8	287 ± 7
BisP30#	∞	∞	185 ± 8	159 ± 3	168 ± 3
BisP50#	✕	∞	210 ± 10	135 ± 7	120 ± 10

Supplementary sample "Bis10# + CA10%": 266 ± 14 s;

∞**:** no heat release can be detected, viewed as an unset cement;

✕: not tested, failed in the mixing stage;

Table 4-II-b. Maximum temperature of the cements prepared by various combinations of $Ca(CH_3COO)_2$ and BisP under various contents

Cement composition	Max. temperature (ºC)				
	P00	CA5%	CA20%	CA35%	CA50%
L00	82.5 ± 2.4	79.2 ± 2.7	76.5 ± 1.8	67.8 ± 2.2	56.0 ± 6.6
BisP10#	∞	79.3 ± 2.0	79.9 ± 1.4	76.9 ± 1.3	68.0 ± 1.7
BisP20#	∞	71.6 ± 2.1	80.6 ± 1.5	69.6 ± 2.1	56.7 ± 3.0
BisP30#	∞	∞	78.4 ± 2.8	77.2 ± 4.4	75.0 ± 1.8
BisP50#	✕	∞	61.0 ± 2.9	65.9 ± 1.9	71.4 ± 2.5

Supplementary sample "Bis10# + CA10%": 81.8 ± 2.0 ºC;

∞: no heat release can be captured from the thermo record;

✕: not tested, failed in the mixing stage;

Table 4-III. Apatite-forming ability of PMMA cements modified with the combinations of various amounts of $Ca(CH_3COO)_2$ and Pa2hme in SBF environment, based on the XRD results# of designed soaking periods

Cement composition	Apatite-forming period (d)				
	P00	CA5%	CA20%	CA35%	CA50%
L00	–	+	+++	++++	++++
BisP10#	–	–	+++	++++	++++
BisP20#	–	–	++	++++	++++
BisP30#	–	–	+	+++	++++
BisP50#	–	–	–	–	–

#–; Apatite was not found after 14 days;

+; apatite was formed within 14 days;

++; apatite was formed within 7 days;

+++; apatite was formed within 3 days

++++; apatite was formed within 1 days

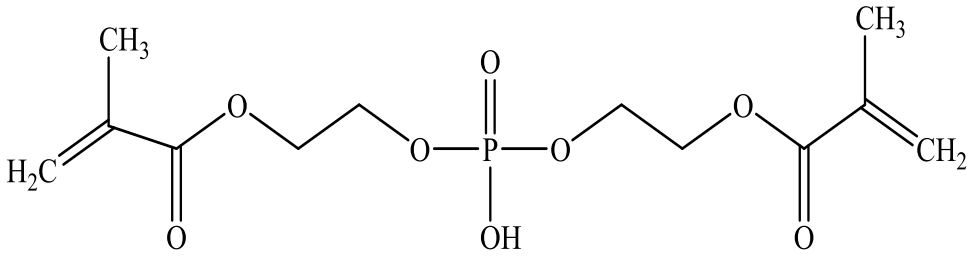

Figure 4-1. Chemical structure of Bis [2-(methacryloyloxy) ethyl] phosphate (BisP)

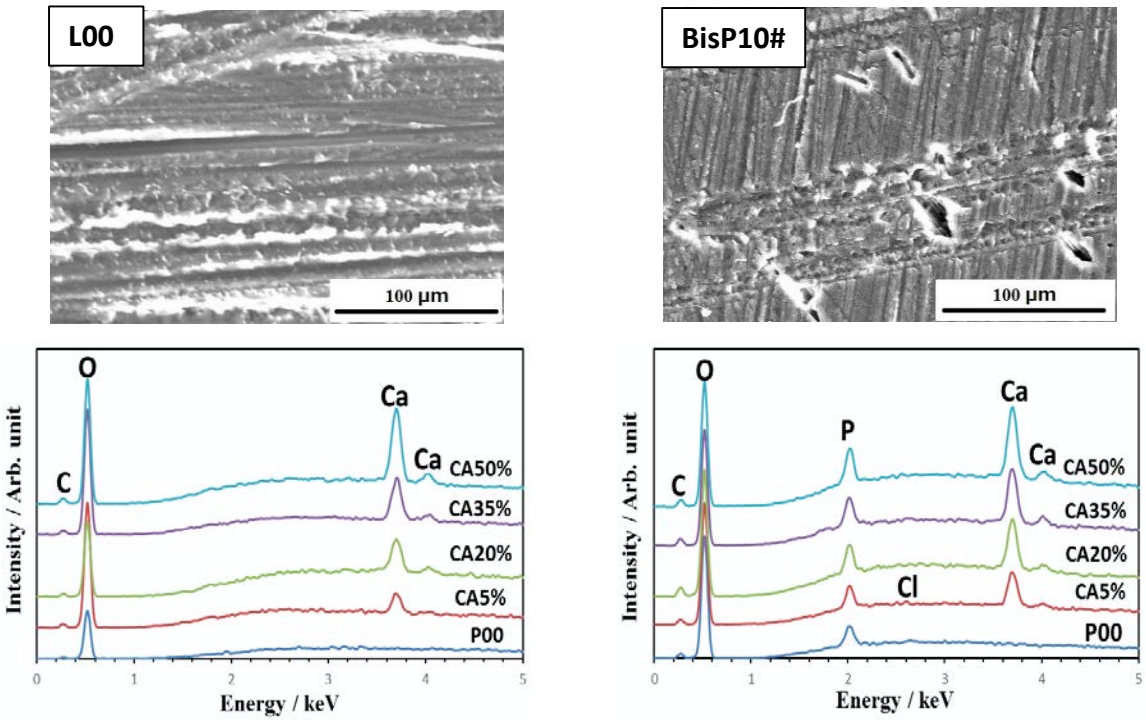
L00
100 µm
BisP10#
100 µm
O
Ca
C
Ca
CA50%
CA35%
CA20%
CA5%
P00
Intensity / Arb. unit
Energy / keV
O
Ca
P
C
Ca
CA50%
CA35%
CA20%
Cl
CA5%
P00
Intensity / Arb. unit
Energy / keV

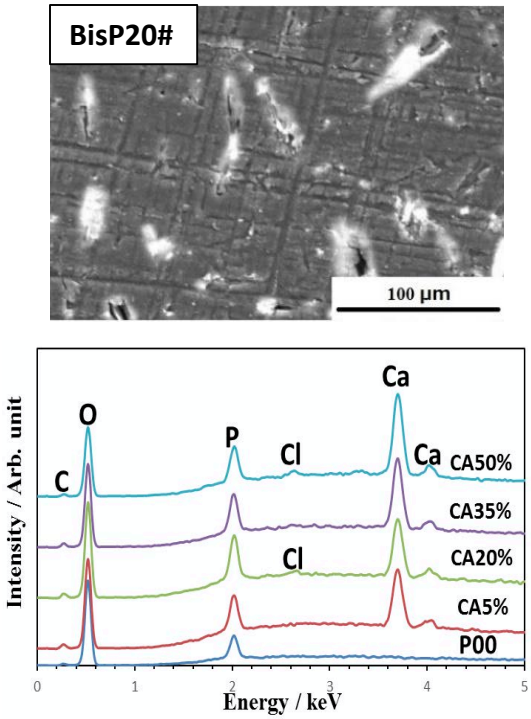
BisP20#
100 µm
Ca
O
P
Cl
C
Ca
CA50%
CA35%
Cl
CA20%
CA5%
P00
Intensity / Arb. unit
Energy / keV

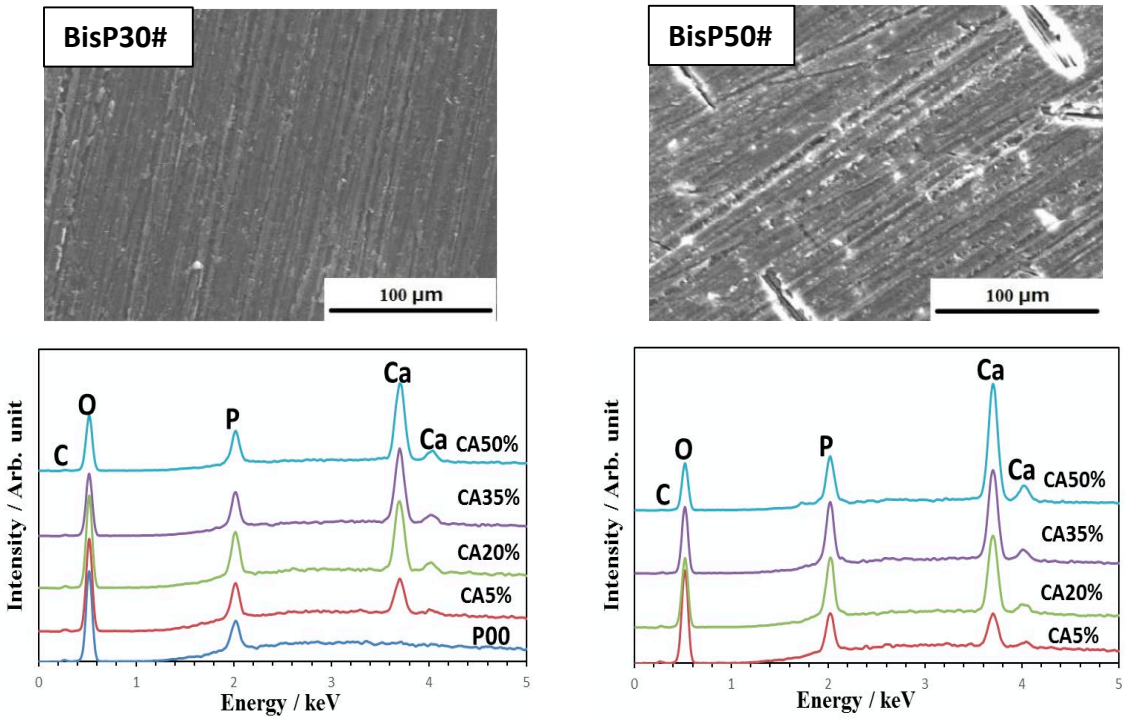

Figure 4-2. Typical SEM images and EDX spectra of original cements modified with the combinations of BisP and $Ca(CH_3COO)_2$ under various contents before SBF soaking.

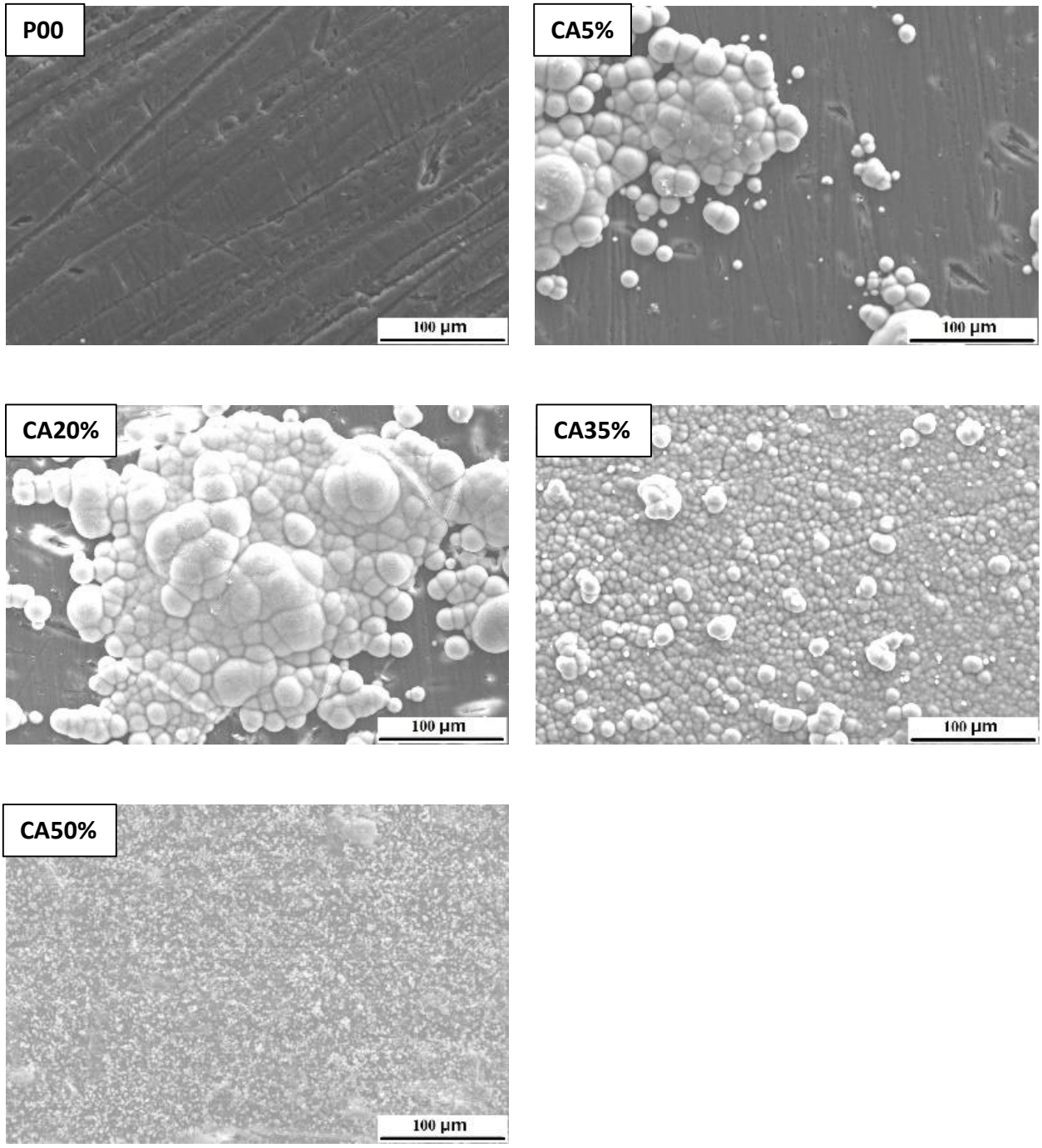

(a) L00

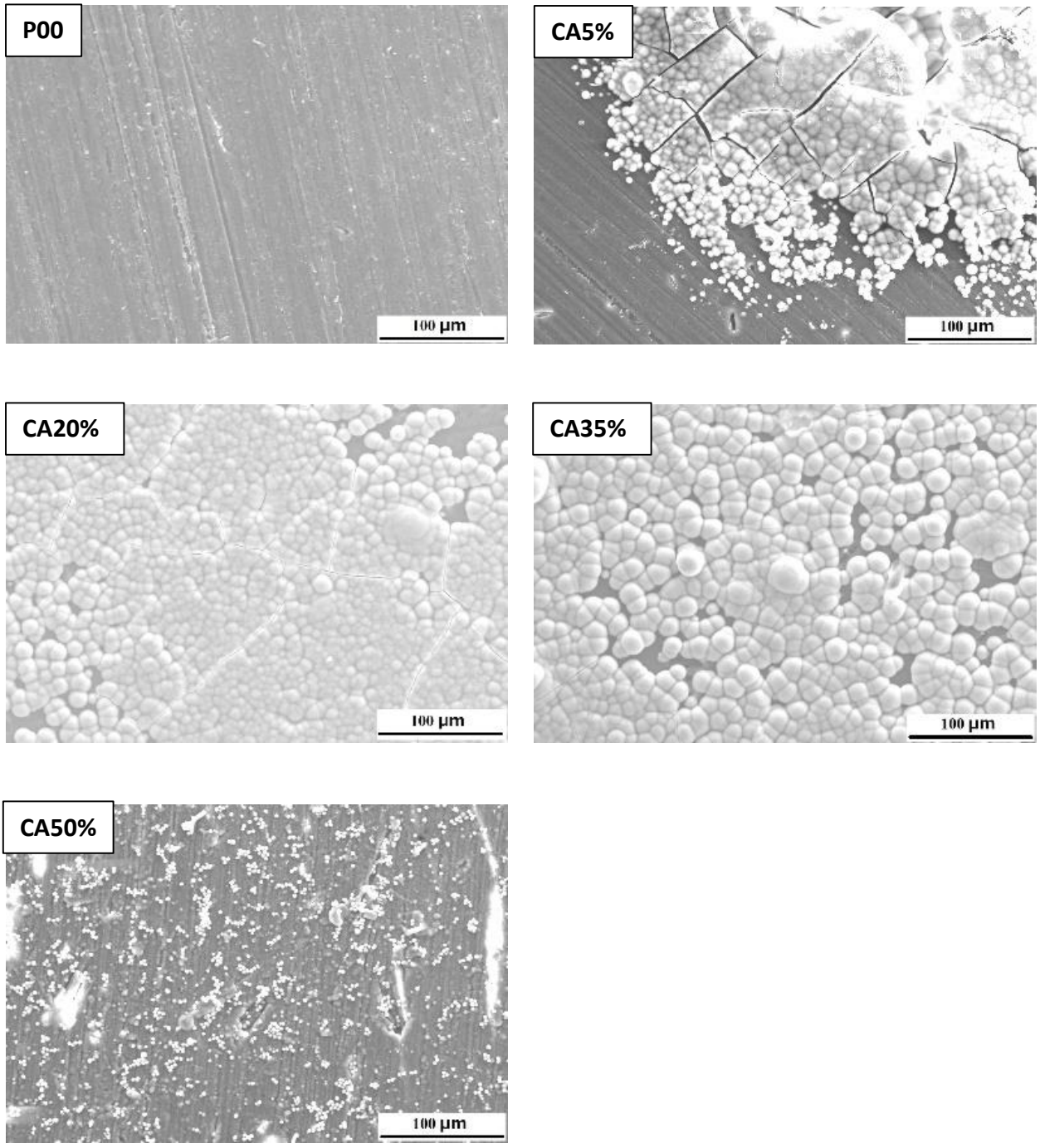

(b) BisP10#

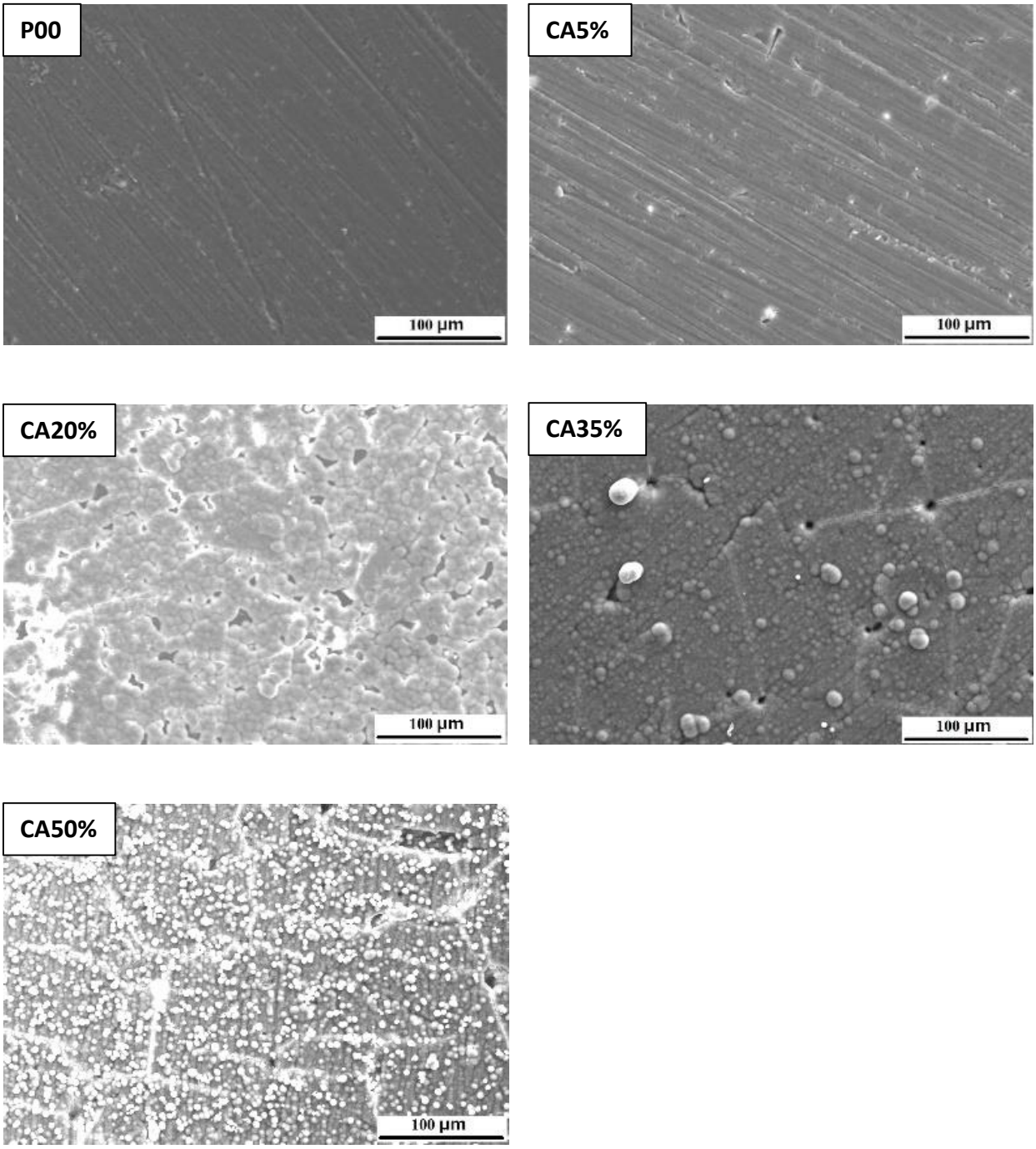

(c) BisP20#

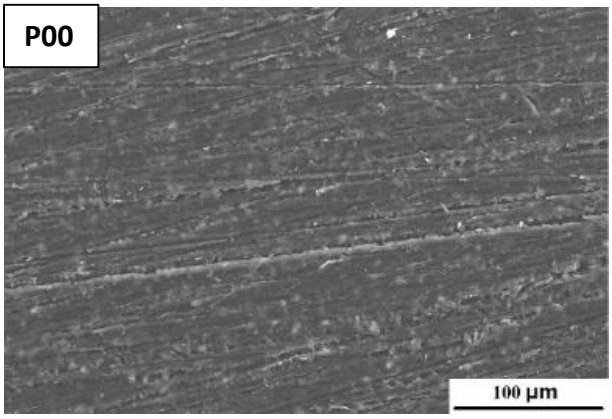

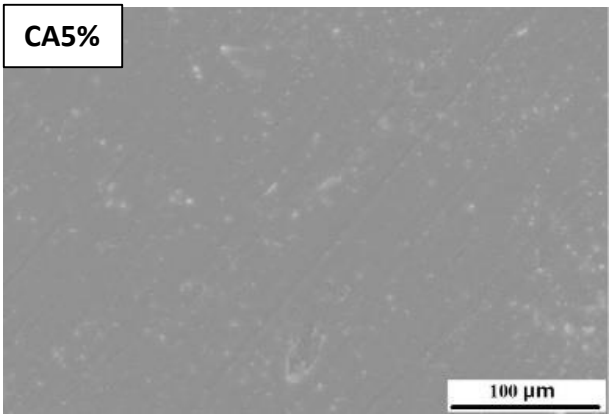

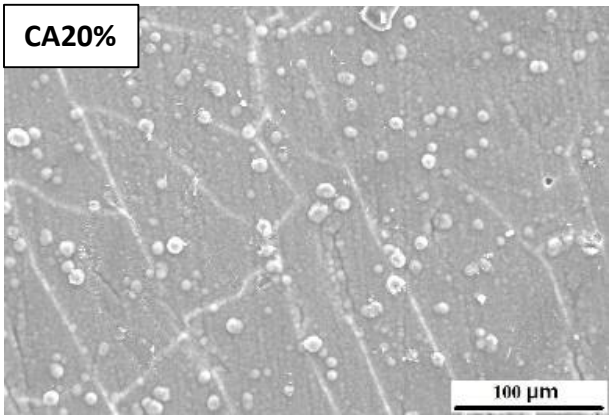

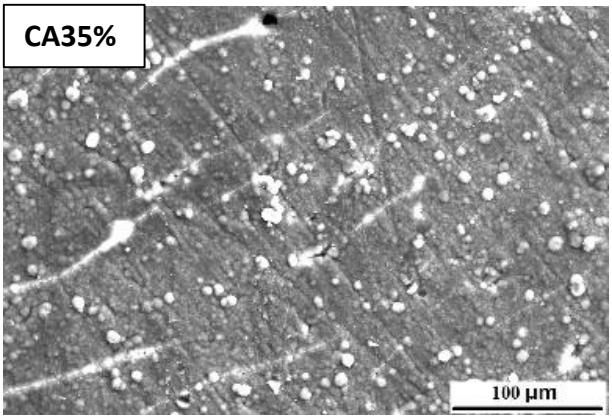

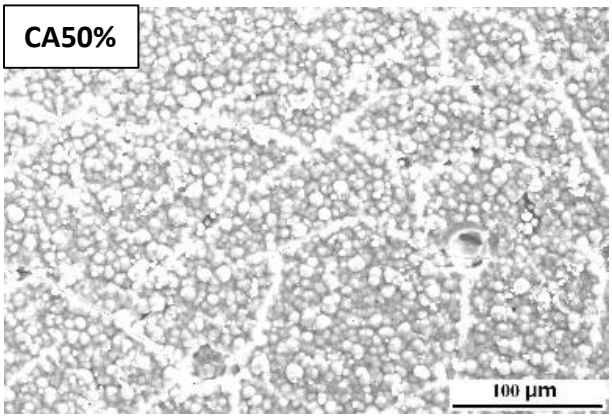

(d) BisP30#

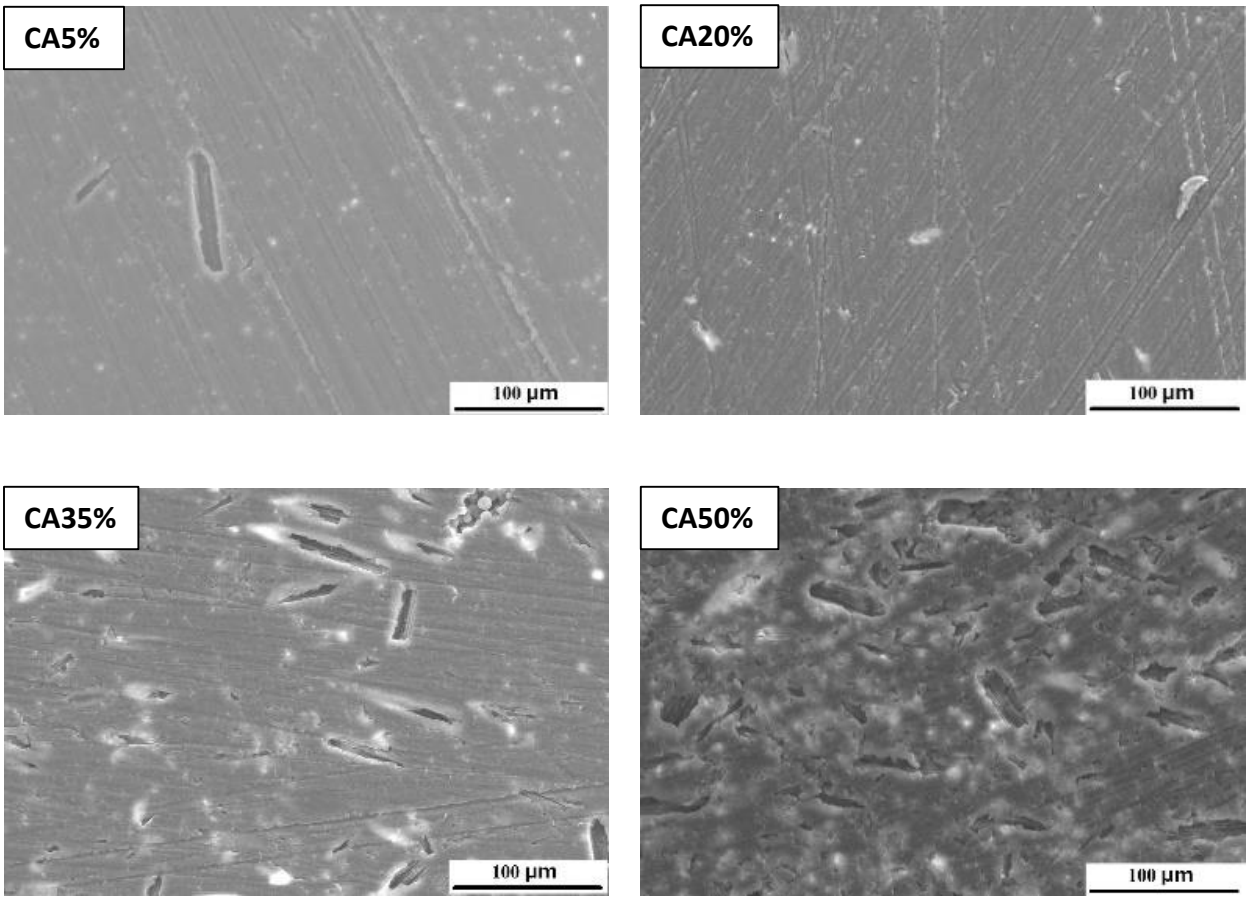

(e) BisP50#

Figure 4-3. SEM photographs of the surfaces of cements prepared by (a) L00; (b) BisP10#; (c) BisP20#; (d) BisP30# and (e) BisP50# with various amounts of $Ca(CH_3COO)_2$ after soaking in SBF for 14 days.

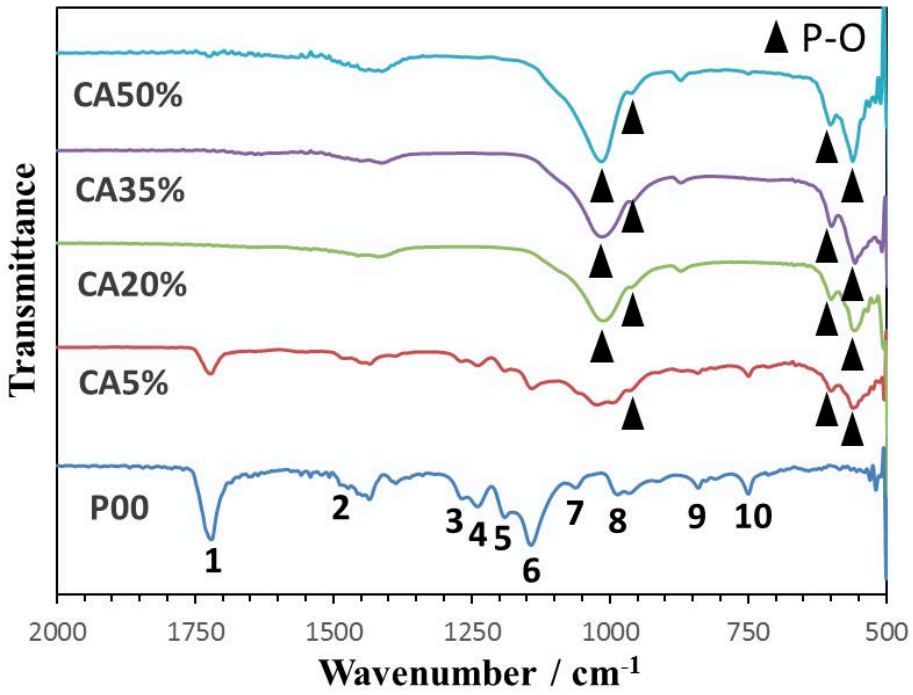

(a) L00

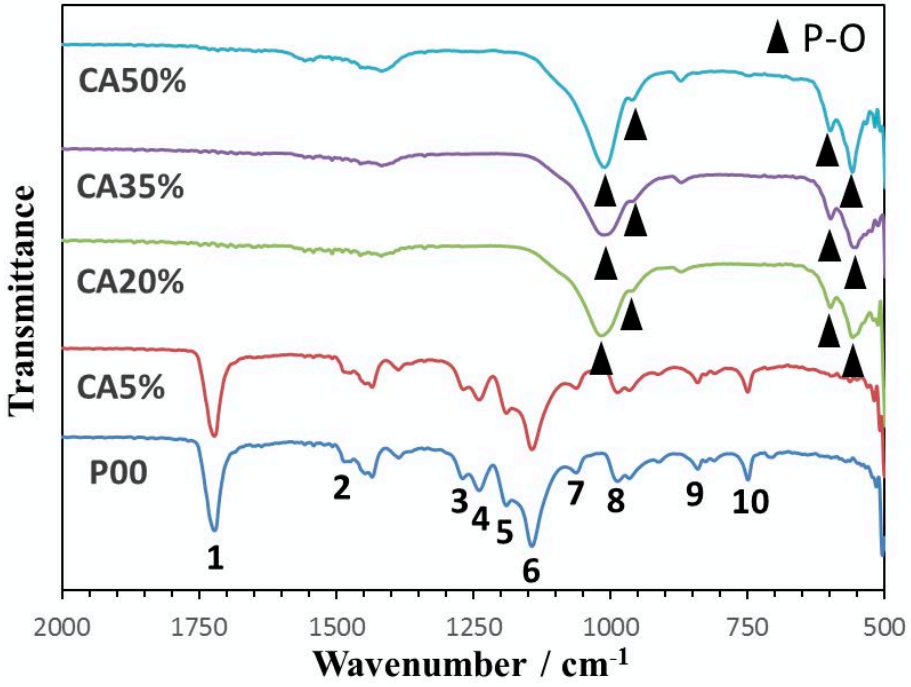

(b) BisP10#

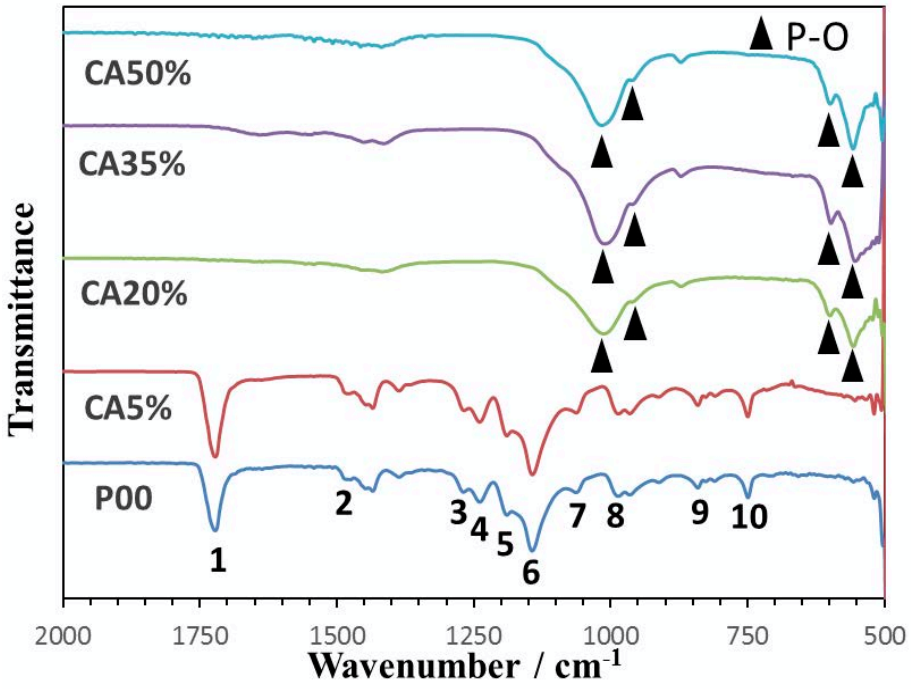

(c) BisP20#

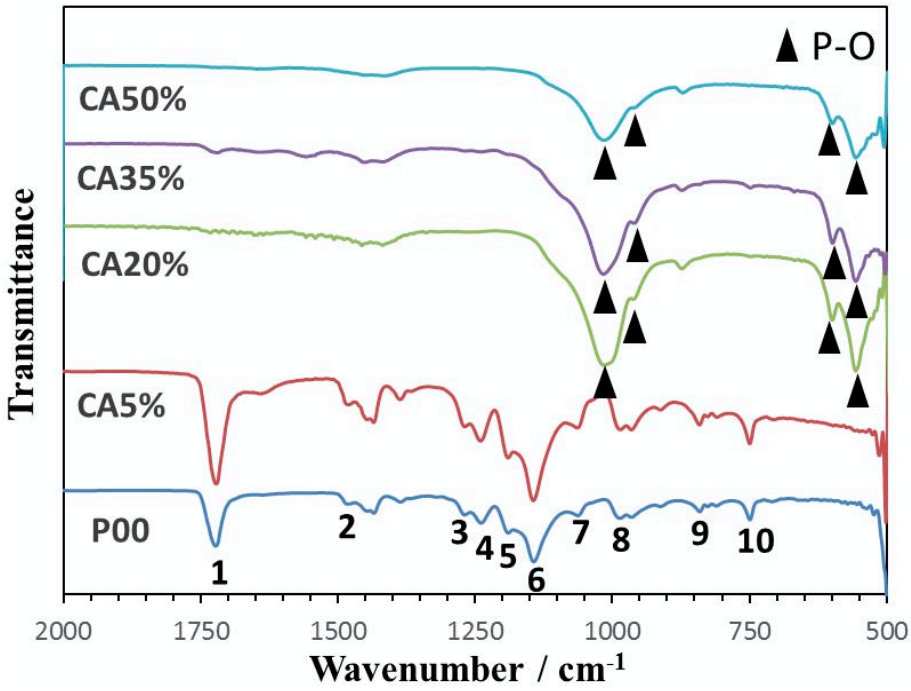

(d) BisP30#

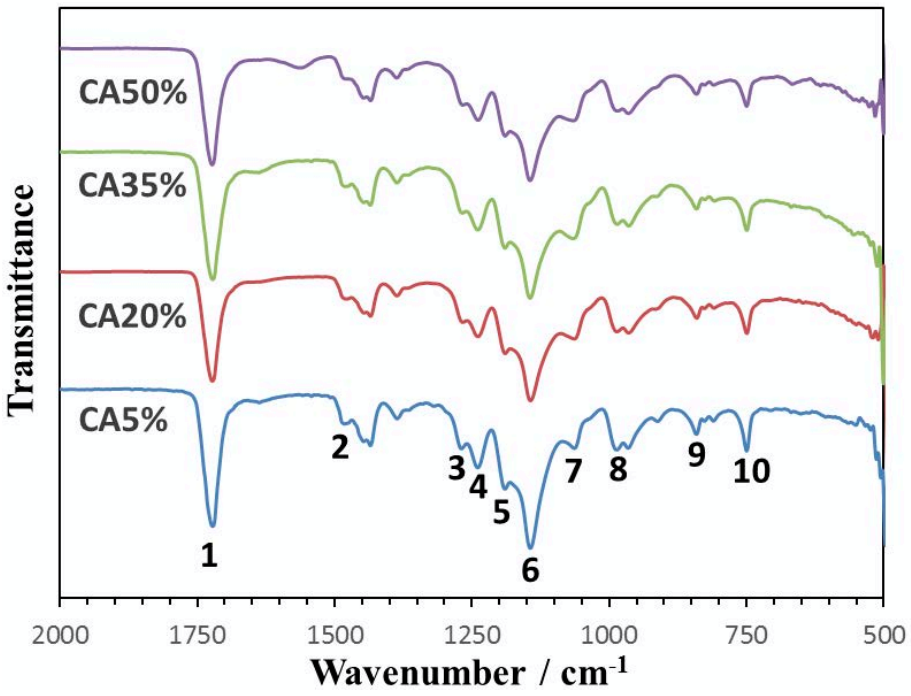

(e) BisP50#

Figure 4-4. FT-IR spectra of the cements prepared by (a) L00; (b) BisP10#; (c) BisP20#; (d) BisP30# and (e) BisP50# with various contents of $Ca(CH_3COO)_2$ after 14 days soaking in SBF.

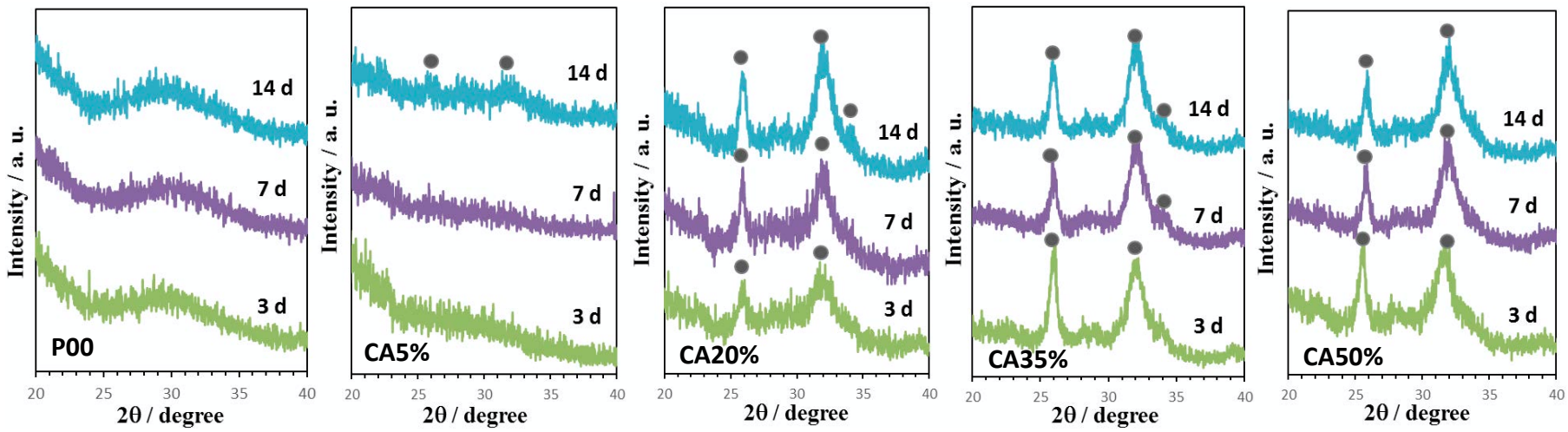

(a) L00

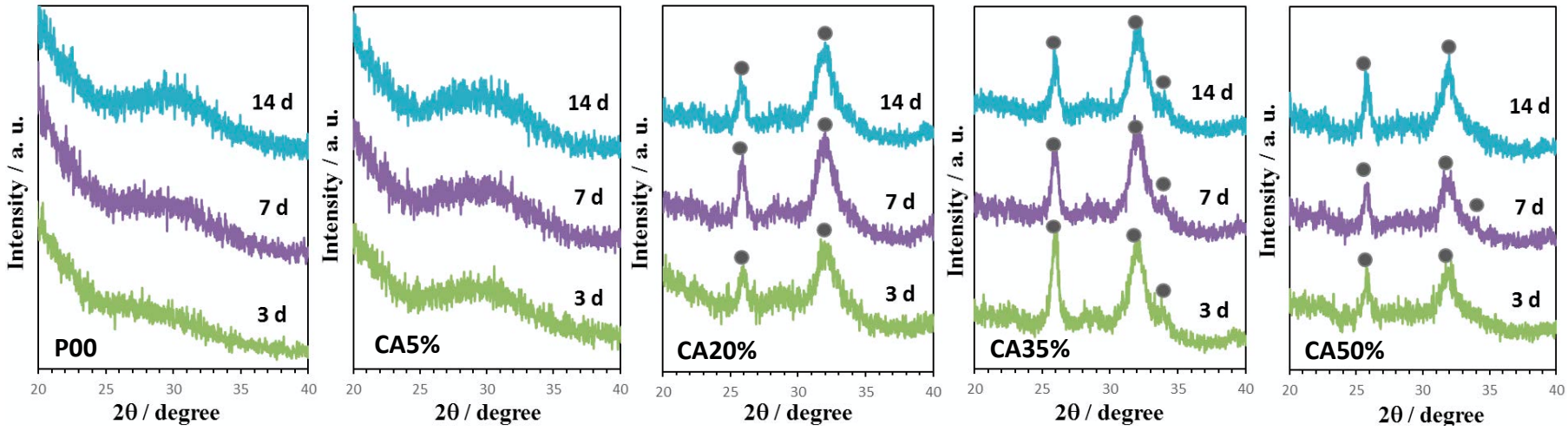

(b) BisP10#

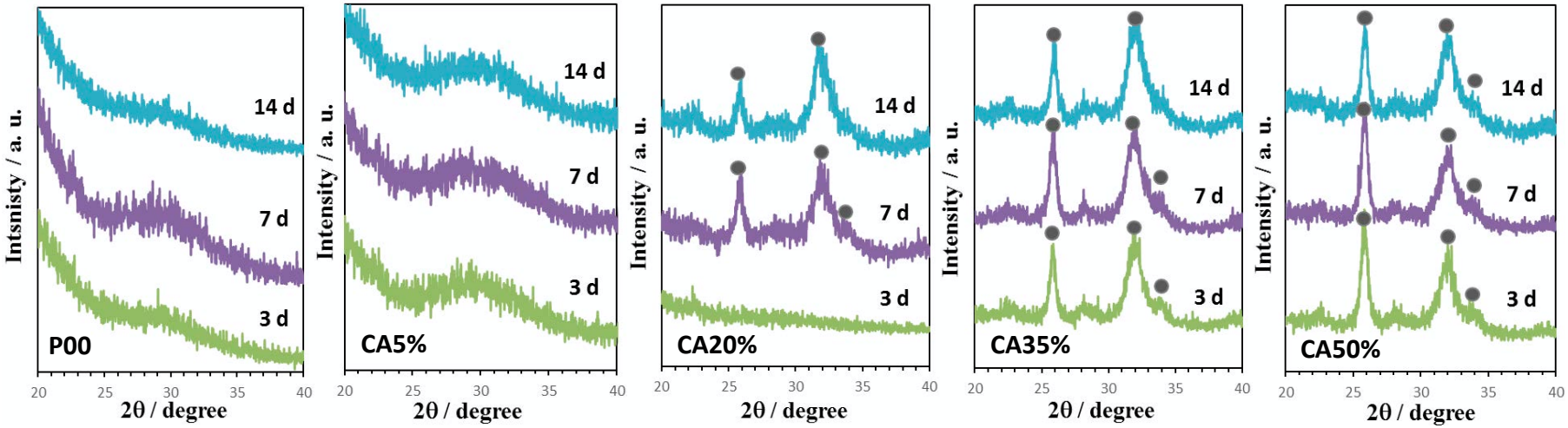

(c) BisP20#

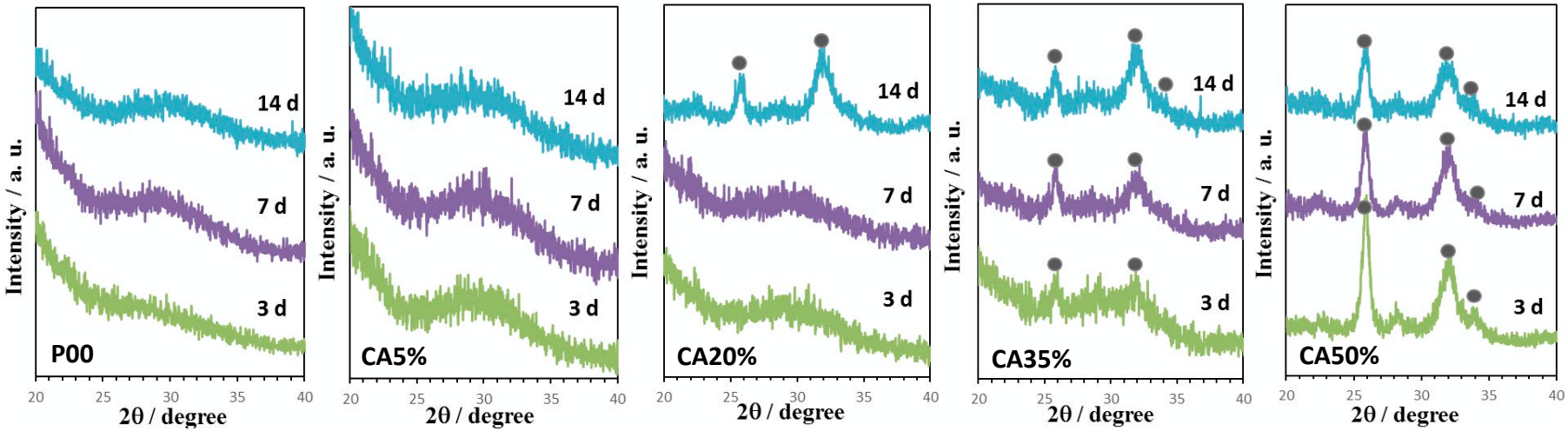

(d) BisP30#

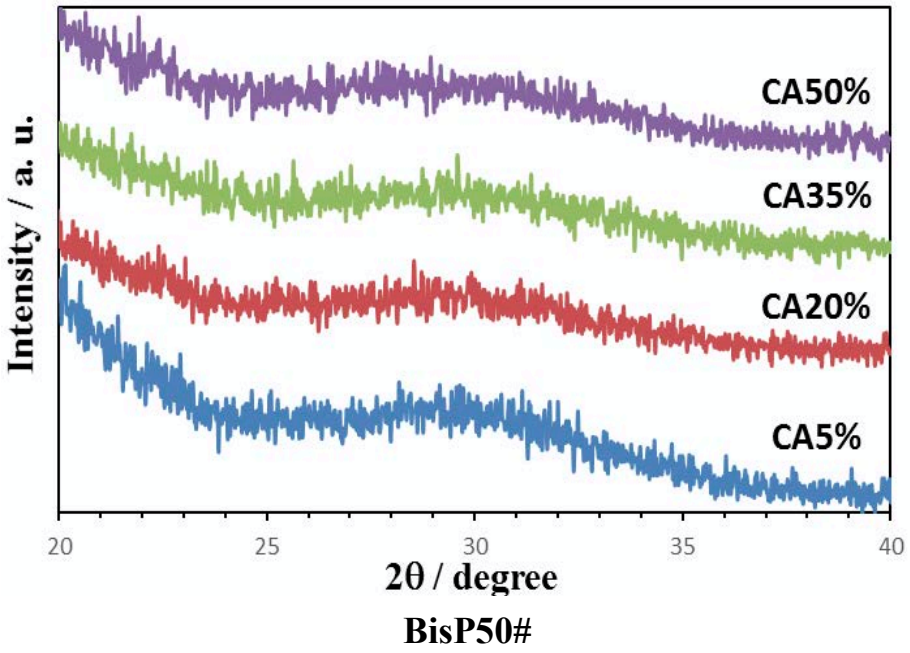

Figure 4-5. TF-XRD patterns of the surfaces of cements prepared by (a) L00; (b) BisP10#; (c) BisP20# and (d) BisP30# with various contents of $Ca(CH_3COO)_2$ after soaking in SBF for designed periods, BisP50# series cements after soaking in SBF for 14 days. Black circle (●): Apatite.

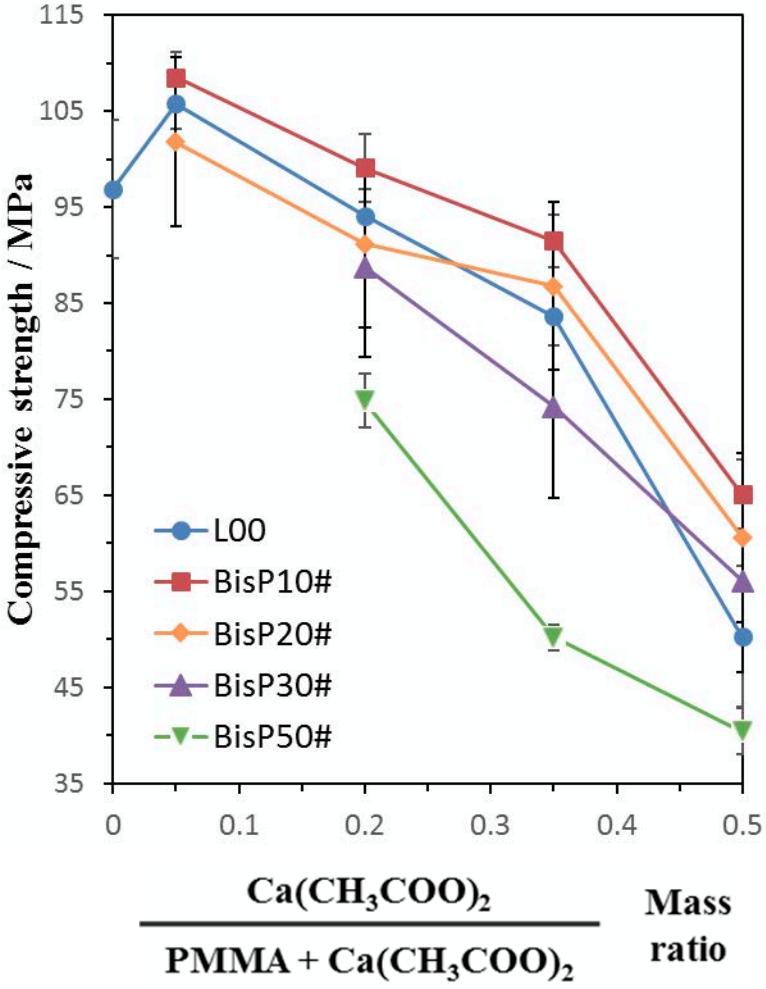

Figure 4-6. Variations in compressive strength of the cements as a function of the contents of $Ca(CH_3COO)_2$ and BisP after 7days soaking in SBF.

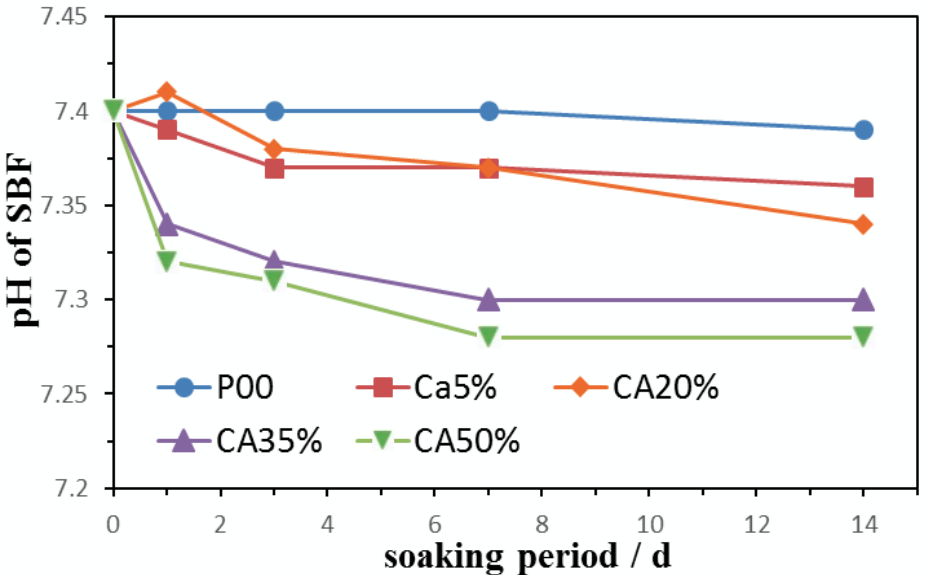

(a) L00

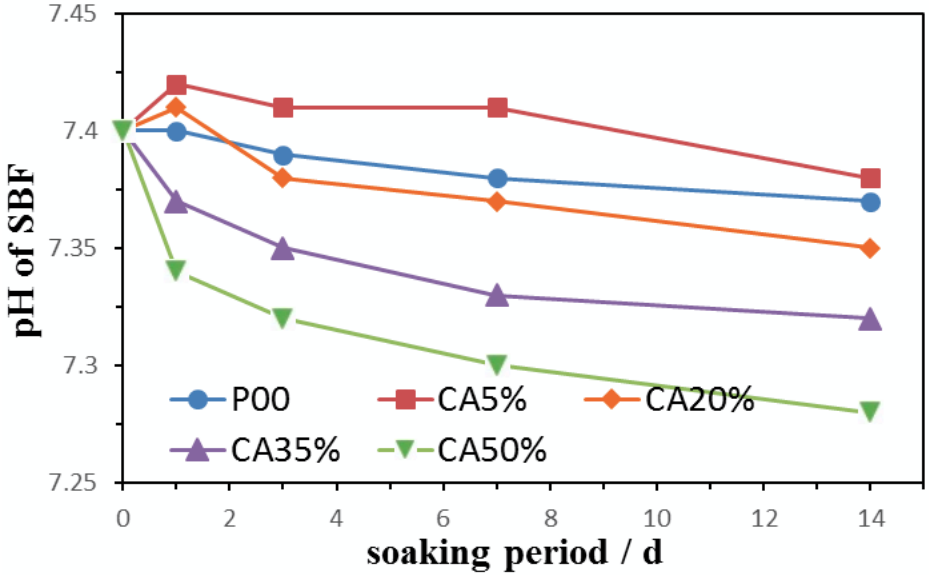

(b) BisP10#

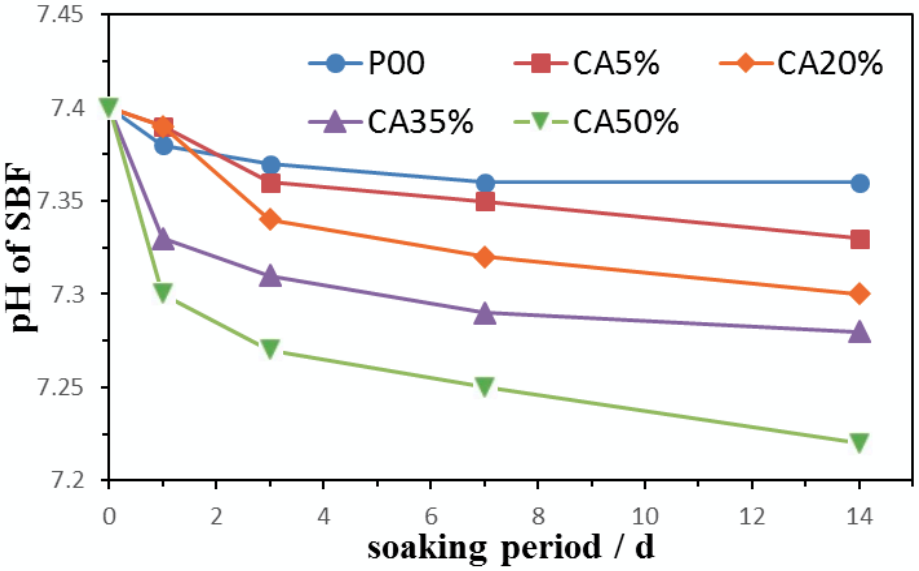

(c) BisP20#

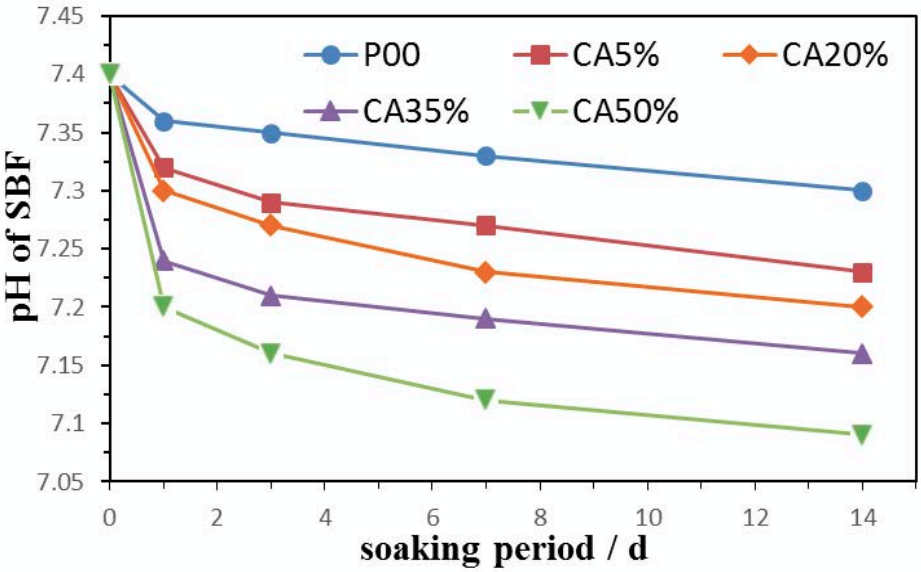

(d) BisP30#

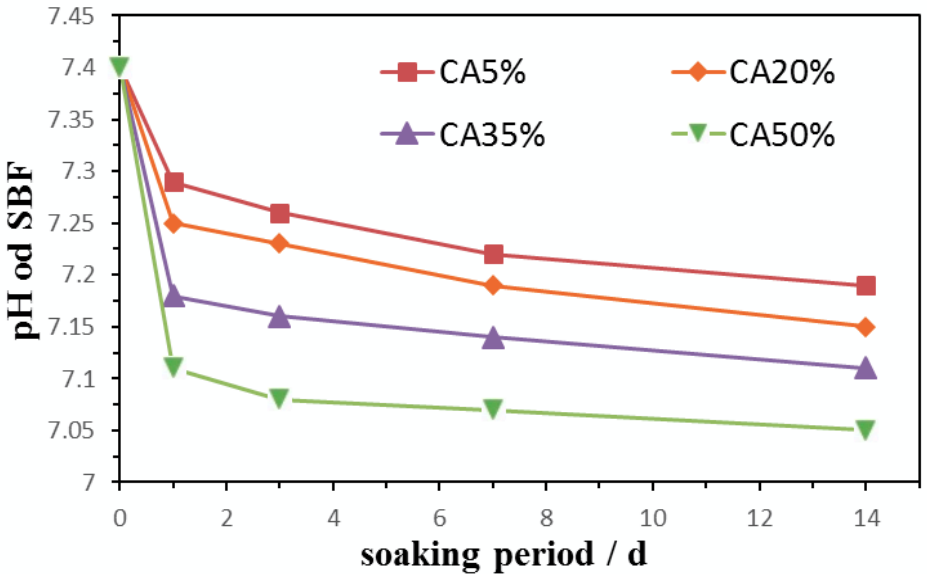

(e) BisP50#

Figure 4-7. pH values of SBF measured at 37 ºC, after soaking the cements prepared by (a) L00; (b) BisP10#; (c) BisP20#; (d) BisP30# and (e) BisP50# combined with various contents of $Ca(CH_3COO)_2$ over the designed intervals.

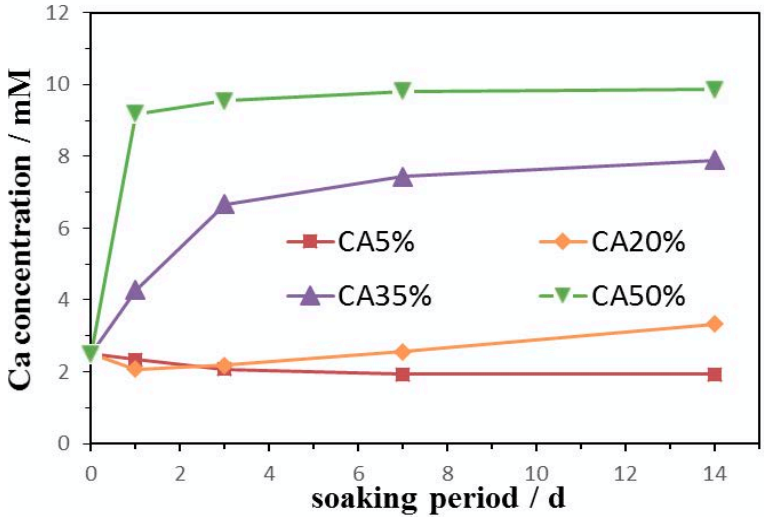

(a) L00

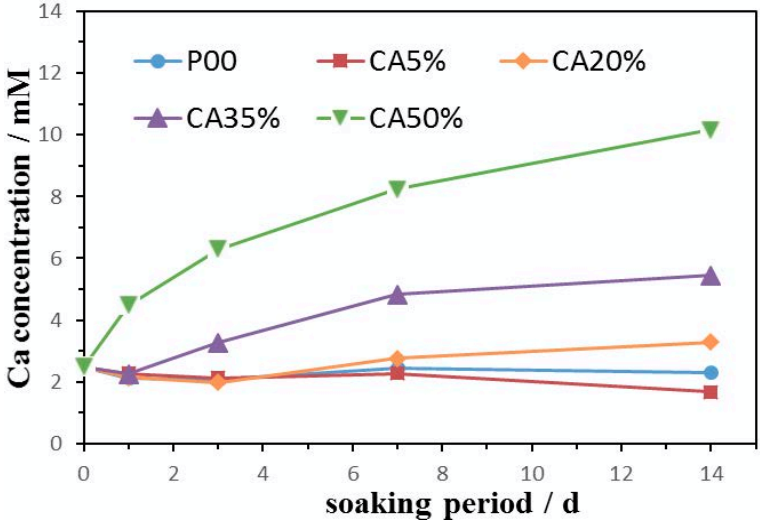

(b) BisP10#

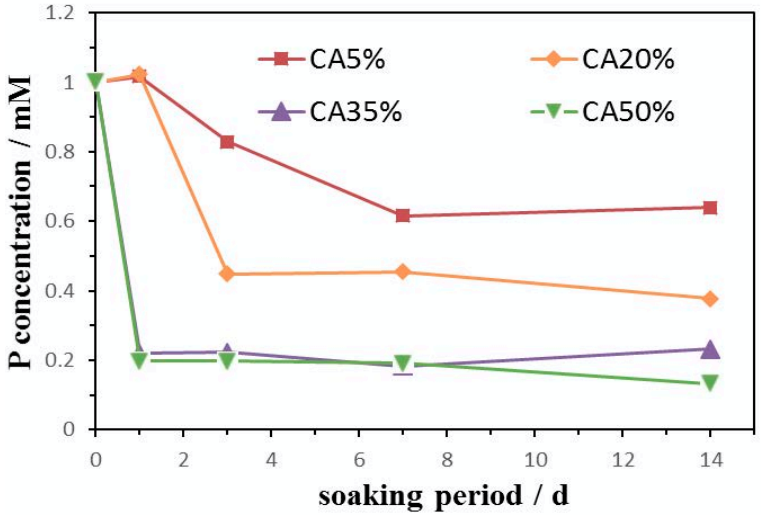

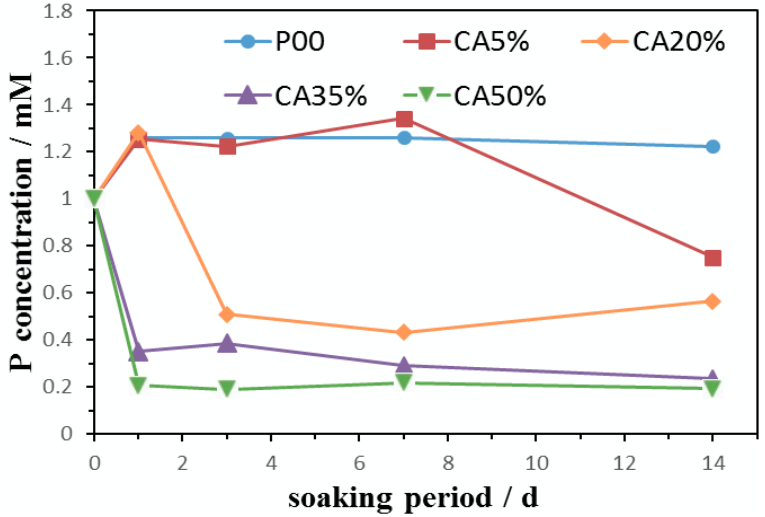

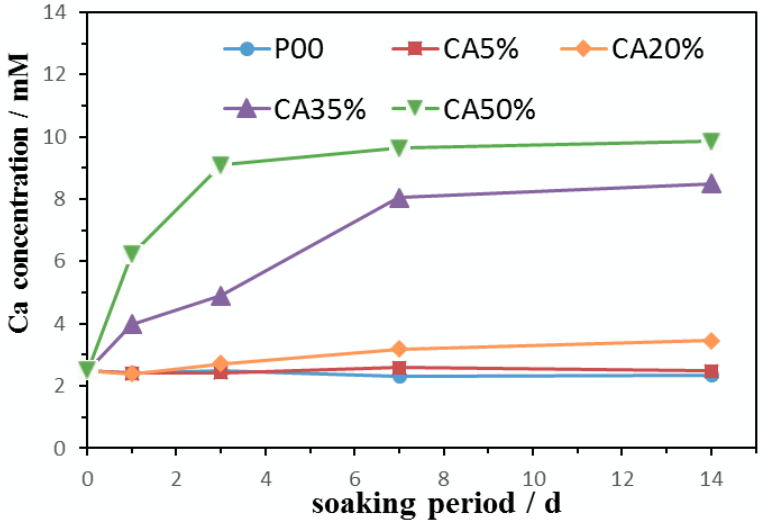

(c) BisP20#

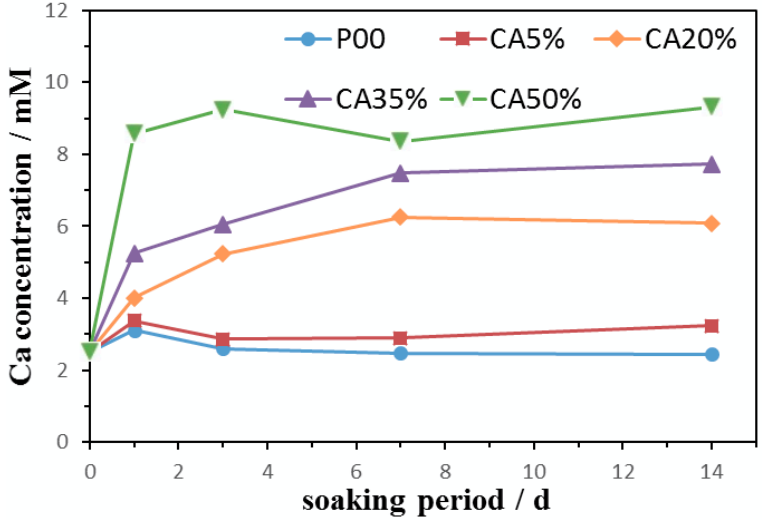

(d) BisP30#

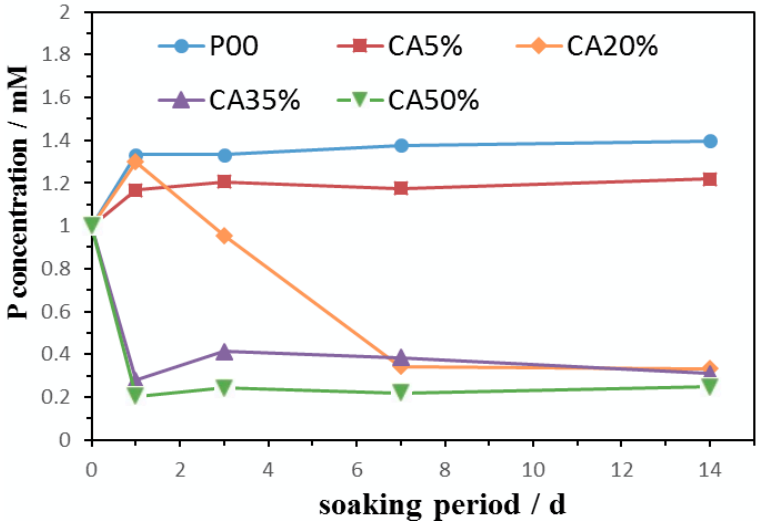

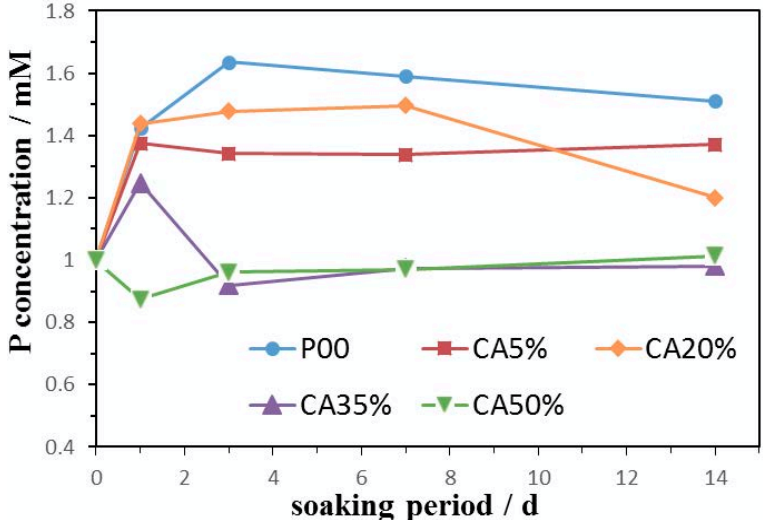

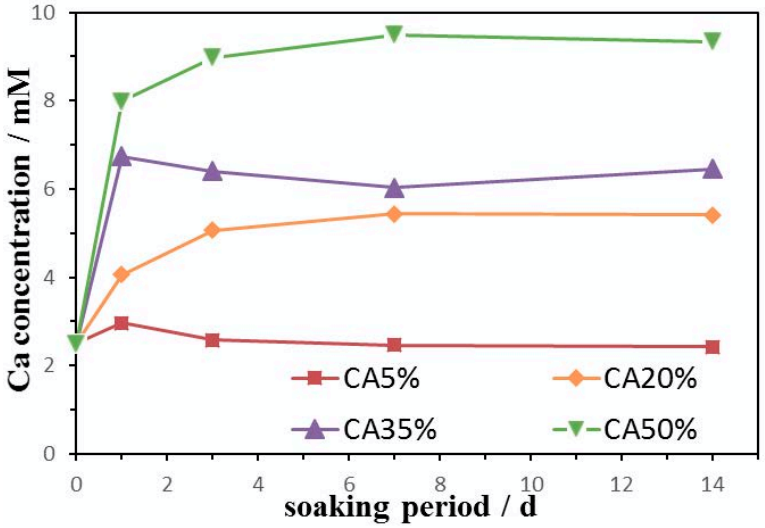

(e) BisP50#

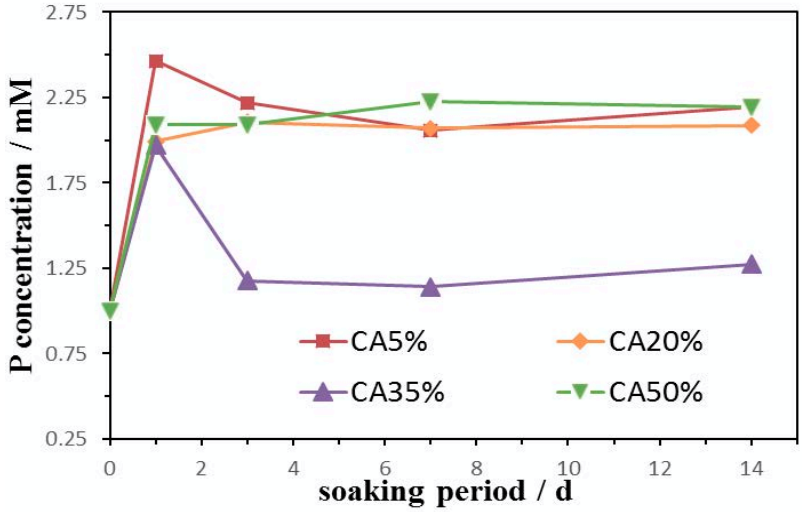

Figure 4-8. Concentration of Ca and P in remaining SBF after soaking the modified cements prepared by (a) L00; (b) BisP10#; (c) BisP20#; (d) BisP30#; (e) BisP50# combined with various contents of $Ca(CH_3COO)_2$ over the designed soaking intervals, respectively.

Chapter 5

GENERAL CONCLUSIONS

This thesis has studied the possibility of equipping various cement-type materials such as dental glass ionomer cements and orthopedic PMMA cements with the bioactivity in terms of inducing bioactive minerals depositing on surfaces in simulated body fluid via incorporation of modifiers with special functions and has investigated the influences of the contents of modifiers on other properties of cements.

In chapter 2, the mixture of γ-PGA solution containing 10% m/m (+) tartaric acid and sol-gel synthesized glass powders G550 (50 SiO_2, 50 Al_2O_3, in mass%) or glass 532 (50 SiO_2, 30 Al_2O_3, 20 CaO, in mass%) were used to prepare glass ionomer cements. FT-IR spectra indicated that GIC was successfully obtained by glass G550 combined with the mixture. Increase in γ-PGA concentration or decrease in powder/liquid mixing ratio improved the diametral tensile strength by increasing the cross linking degree of acidic polymers and the proportion of aluminum polymer salts in cements. The cement prepared by the P/L ratio (g/g) of 1: 1 and the γ-PGA concentration (m/m) of 30% exhibited the highest strength (11.88 ± 1.43 MPa) after 3 days of aging. Calcite phase was deposited on the surface after 7 days immersion in SBF, meaning that this SiO_2-Al_2O_3 glass/γ-PGA cement might own the bioactivity.

In chapter 3, phosphate (PO_4H_2) groups containing phosphoric acid 2-hydroxyethyl methacrylate ester (Pa2hme) was added in liquid phase, and $Ca(CH_3COO)_2$ was incorporated into powder phase. The combination of Pa2hme and $Ca(CH_3COO)_2$ has induced the deposition of apatite layer on PMMA cement surface in simulated body environment. Increases in the content of $Ca(CH_3COO)_2$ shortened apatite forming period, while no apatite was detected when Pa2hme content was increased to 50 mass% regardless of the contents of calcium acetate. One possible reason was low pH environment created by the release of $Ca(CH_3COO)_2$ and Pa2hme. The shorter setting times were found when the mass ratios of $Ca(CH_3COO)_2$/Pa2hme were

close to the powder/liquid ratio (2: 1), while increase or decrease in the amounts of $Ca(CH_3COO)_2$ prolonged the setting based on this. High contents of both additives caused the deterioration in compressive strength. The cement with apatite-forming ability failed to meet the compressive strength requirement of ISO 5833, which was ascribed to the limitation of Pa2hme dissolved in MMA.

In chapter 4, modification with Bis [2-(methacryloyloxy) ethyl] phosphate (BisP) and $Ca(CH_3COO)_2$ also prompted apatite formed on the surface of PMMA cement in simulated body environment. Increasing the content of $Ca(CH_3COO)_2$ shortened apatite formation period, and phosphate (PO_4H_2) groups distributed on the cement surface were beneficial to the heterogeneous nucleation of apatite. The addition of $Ca(CH_3COO)_2$ or BisP alone prolonged the setting. On the other hand, the combination of $Ca(CH_3COO)_2$ and BisP generated a faster setting when their mass ratios were close to the powder/liquid (2: 1). Additionally, the faster setting was further accelerated with increase in both additives under this ratio. Lower contents of additives (CA5%, L00 or BisP10#) enhanced the strength, and the top compressive strengths (108.5 ± 2.7 MPa) declined following the increase of both additives. In view of balancing apatite-forming period and other properties required by ISO 5833, it is concluded that the optimal modification is a combination of 10 mass% of BisP and 20 mass% of $Ca(CH_3COO)_2$, the modified PMMA cement owned 314 ± 4 s of setting time and 99.1 ± 3.5 MPa of compressive strength, the formation of apatite was finished within 3 days soaking in SBF.

Under the same contents in all additives, BisP showed a better performance than Pa2hme on mechanical strength and apatite-forming ability of PMMA bone cement.

On the basis of these results, essential designs and optimization for developing bioactive cement-type materials with practical potentials have been achieved in terms of cement composition. These cement biomaterials should be further improved in future in order to be utilized in dental and orthopedic fields.

ACHIEVEMENTS

(A) Journal Publication

1. J. Liu, Y. Kuwahara, Y. Shirosaki and T. Miyazaki, "The investigation of bioactivity and mechanical properties of glass ionomer cements prepared from Al_2O_3-SiO_2 glass and poly(γ-glutamic acid)", *J. Nanomater*., Article ID 168409, 6 pages (2013).

2. J. Liu, Y. Shirosaki and T. Miyazaki, "Bioactive PMMA bone cement modified with combinations of phosphate group-containing monomers and calcium acetate", *J. Biomater. Appl.*, Jan. 7, 2015, doi: 10.1177/0885328214562436.

(B) Conferences

1. Oral: J. Liu, Y. Kuwahara, Y. Shirosaki and T. Miyazaki, "Bioactivity and mechanical properties of glass ionomer cements containing Al_2O_3-SiO_2 glass and poly(γ-glutamic acid)", *The 13th Asian BioCeramics Symposium*, Dec. 4-6, 2013, Kyoto, Japan.

2. Poster: J. Liu, Y. Shirosaki and T. Miyazaki, "Bioactive PMMA Bone Cement Modified with Bis [2-(methacryloyloxy) ethyl] Phosphate and Calcium Acetate", *The 15th IUMRS International Conference in Asia*, Aug. 24-30, Fukuoka, Japan.

3. Oral: J. Liu, Y. Shirosaki and T. Miyazaki, "Formation of bioactive surface on PMMA bone cement via modification with calcium acetate and phosphate group-containing monomers", *The 14th Asian BioCeramics Symposium*, Oct. 28-30, 2014, Shanghai, China

ACKNOWLEDGEMENT

The research in this thesis was carried out at Graduate School of Life Science and System Engineering, Kyushu Institute of Technology.

I would like to thank Associate Professor Toshiki Miyazaki, for providing me a chance to study on biofunctional materials. His wealthy technical knowledge and insights have enriched my understanding in this field, and his pragmatic attitude and rigorous atmosphere on science deeply inspired me, leaving me a best model on how to perform the researches with a true passion and how to pass through all the setbacks with enthusiasm and belief.

I would like to thank Associate Professor Yuki Shirosaki, for sharing me the details of characterization methods and presenting constructive comments and suggestions on my research. I gained affluent experiences and valuable opinions in regard to the professional learning and dedicated attitude on scientific research from you. I acknowledge Professors Nobuya Shinozaki, Masamichi Naitoh and Hidenori Era for fruitful suggestion and discussion.

I would like to thank my tutor Mr. Kuwahara and all other members in Miyazaki laboratory. Without your permanent patient and warm assistance, I could not quickly adapt to the life in Japan and swimmingly devote myself to the research.

My sincere gratitude are also expressed to all staffs in Wakamatsu campus and Kyushu Institute of Technology for all kinds of supports and activities such as house renting, academic conference, Japanese language lectures and annual travelling, which helped me not only save more time to do experiments but also better understand the Japanese culture.

I am also grateful to the China Scholarship Council for offering me the scholarship to study in Japan. Financial aid created a stable learning environment and brought a wonderful life experience for me.

Moreover, I felt appreciated to everything my parents done for me. Their love and encouragement are constant sources of motivation to support the successful completion of my studies. Beyond that, I also expressed my gratitude to the persons who once made a contribution to the realization of this thesis, as well as my apology to them I could not mention one by one.

2014

Liu Jinkun